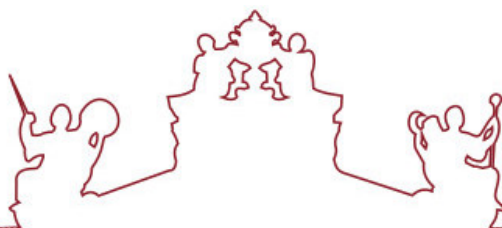




SAPIENZA
UNIVERSITÀ DI ROMA



ARISTOTLE
UNIVERSITY OF
THESSALONIKI



**Universidade de Évora - Instituto de Investigação e Formação Avançada
Università degli Studi di Roma "La Sapienza" Aristotle University of
Thessaloniki**

Mestrado em Ciência dos Materiais Arqueológicos (ARCHMAT)

Dissertação

A Deep Insight into the Green Deteriorated Paint Layers at the Maritime Station of Alcântara: An Archeometric Study

Andrea Acevedo Mejía

Orientador(es) | Milene Gil

Ana Manhita

Mafalda Barrocas Dias Teixeira da Costa

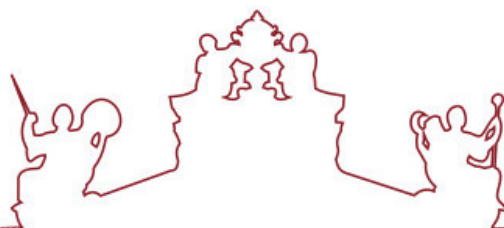
Évora 2022



SAPIENZA
UNIVERSITÀ DI ROMA



ARISTOTLE
UNIVERSITY OF
THESSALONIKI



**Universidade de Évora - Instituto de Investigação e Formação Avançada
Università degli Studi di Roma "La Sapienza" Aristotle University of
Thessaloniki**

Mestrado em Ciência dos Materiais Arqueológicos (ARCHMAT)

Dissertação

A Deep Insight into the Green Deteriorated Paint Layers at the Maritime Station of Alcântara: An Archeometric Study

Andrea Acevedo Mejía

Orientador(es) | Milene Gil
Ana Manhita
Mafalda Barrocas Dias Teixeira da Costa

Évora 2022

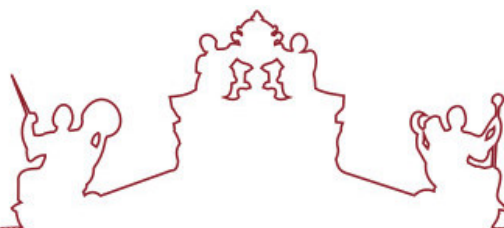




SAPIENZA
UNIVERSITÀ DI ROMA



ARISTOTLE
UNIVERSITY OF
THESSALONIKI



A dissertação foi objeto de apreciação e discussão pública pelo seguinte júri nomeado pelo Diretor do Instituto de Investigação e Formação Avançada:

Presidente | Nicola Schiavon (Universidade de Évora)

Vogais | Agnes Le Gac () (Arguente)
Alessandra Celant (Università degli Studi di Roma "La Sapienza")
Luca Malatesta ()
Mafalda Barrocas Dias Teixeira da Costa ()
Yiannis Karapanagiotis (Aristotle University of Thessaloniki)



Co-funded by the
Erasmus+ Programme
of the European Union

UNIVERSITY OF ÉVORA

ARCHMAT

ERASMUS MUNDUS MASTER IN ARCHaeological
MATerials Science

A Deep Insight into the Green Deteriorated Paint
Layers at the Maritime Station of Alcântara: An
Archeometric Study

Andrea Acevedo Mejía

47337

Évora, Portugal, November 2022



ARISTOTLE
UNIVERSITY
OF THESSALONIKI



UNIVERSIDADE
DE ÉVORA



SAPIENZA
UNIVERSITÀ DI ROMA

(this page was intentionally left blank)

Table of contents

Acknowledgements	6
Abstract	9
Chapter 1: Introduction	12
1.1 Contextualization, aims and objectives of the research	12
1.2 Methodological approach	12
1.3 Structure of the thesis	14
1.4 List of references	14
Chapter 2: Historical and artistic background	15
2.1 The mural painting movement in the 20 th century: from Mexico to Portugal	15
2.2 <i>Almada Negreiros</i> : biography and mural painting artwork	18
2.3. The mural paintings of the Maritime Station of Alcântara	21
2.4 Historical overview of natural and synthetic pigments used until the 20 th century	23
2.4.1 Prehistory	23
2.4.3 Medieval period	25
2.4.4 Post-industrial revolution and modern pigments	25
2.5 List of the green pigments available for artists in the 20th century	30
2.6 Properties and main causes of deterioration of pigments on mural paint layers	36
2.6.1. Pigment properties	36
2.6.2. Main causes of deterioration of mural paintings (topics)	37
2.7 List of references	39
Chapter 3: Case Study and Methodology	49
3.1. Introduction to the Maritime station of Alcântara: geographic location and some notes about the history of the construction and of the surrounding environmental conditions	49
3.2. Identification of the mural paintings and criterium of selection for in loco and laboratory analysis	51
3.3. Identification of powdered green pigments	53
3.4. Experimental conditions	55
3.4.1 In loco non-invasive analyses	55
3.4.2. Laboratorial analysis of microsamples	59
3.5 List of references	63
Chapter 4: Results and discussion	67
4.1. Identification and characterization of the green paint layers	67
4.1.1. Green colour palette and identification of pigments	67
4.1.2. Painting technique	77
4.1.3. Decay mechanisms	81
4.2. Characterization of green pigments in powder: a complementary study	83

4.3. List of references _____	87
Chapter 5: Conclusions and future perspectives _____	90
Appendix _____	93
Appendix I: State of conservation of the green paint layers _____	93
Appendix II: Punctual area location of the colorimetry/ spectrophotometry analysis _____	102
Appendix III: Punctual area location of the h-EDXRF analysis _____	105
Appendix IV: Correlation colorimetry-spectrophotometry/h-EDXRF measurements _____	108
Appendix V: Microsampling location _____	109
Appendix VI: Compendium of results from the samples by colorimetry, h-EDXRF, μ -XRD, and micro-Raman spectroscopy _____	113
Appendix VII: μ -XRD diffractograms of the microfragments analyzed _____	114
Appendix VIII: XRPD diffractograms of selected reference pigments _____	116

(this page was intentionally left blank)

Acknowledgements

First, I would like to express my deepest gratitude to my academic supervisors Dra. Milene Gil, Dra. Mafalda Costa and Dra. Ana Manhita for their guidance and support along these months. I can say that I learned so many different and interesting topics thanks to this project, and I enjoyed to explore Almada Negreiros' artwork, which is such an interesting artist.

I want to thank my main supervisor, Milene Gil for her motivation and the time she spent on me during the whole process, as well as the passion in which she works; that was an inspiration to continue with my project. I want to thank Mafalda Costa for her supervision and help during the analysis, as well as the time she spend on me.

I would like to thank to the Hercules Laboratory for allowing us to use the equipment and the installations for the analysis of this project. I also want show my deepest gratitude to the Administração do Porto de Lisboa, S.A. (APL) that let us carry out the in loco analysis for the mural paintings of the Maritime Station of Alcântara. I want to thank the project *O Desvendar da Arte da Pintura Mural de Almada Negreiros (1938-1956)*, which is the main project this study belongs to.

I really want to thank the Erasmus Mundus ArchMat program, that gave me the opportunity to experience such a peculiar, interesting, and exciting program, to the coordinator of the ArchMat programme, Dr Nicola Schiavon, and the partners and staff from Évora, Thessaloniki, and Rome. I want to thank to the professors from the University of Évora, the Aristotle University of Thessaloniki and Sapienza University, that put all the effort during their classes and inspired us with their enthusiasm during these two years.

Now, I want to thank to all the people that I met and were with me during this long journey. Angélica, you encouraged me to start exploring the world by myself, that was the best lesson ever, muchísimas gracias. I want to thank Blanca, Yael, and Juan, who were with me during the hard situations of the first semester. And I want to thank Milica, who were there in the hardest situations and supported me (and fed me) all the time, you are an amazing person and an amazing friend. I also want to thank Janée, for all the nice experiences, trips, and funny conversations we had, as well as the nice cookies and boardgames.

Thank you to all the people I met in Thessaloniki. Dani, Beatraki and Nathan, you are the craziest people ever and I had amazing experiences with you, all I want to say to you is τίποτα. I also want to thank Olga, Paraskevi and Vaggelis, who always looked for a way to enjoy our time in Thessaloniki; and Hugo, which I always had the most interesting conversations. I specially want to thank four beautiful people: Emma, Lilla, Coline and Teresa; with you I grew as a person and learned that life is a risk. With you I had the most adventurous experiences of these years, thank you so much for this amazing friendship, all I want to say is mexikói vagyok.

For Kabya, Sneha, and Sayan, thank you for making me laugh so bad and thank you Sayan for the super nice food. I cannot forget Ehsan for the infinite support you gave me during bedbug times, and the support you gave me since then, besides the

amazing tea and the amazing conversations. You are the best wife ever. I want to thank Amira, for being a wonderful person. And Maddy... Maddy Maddy, thank you for being such a mysterious colleague, such an interesting friend and such a lovely and supportive boyfriend. Nanna olave σε περιμένω.

I want to thank all my friends from Mexico who were with me since the beginning of the times: Diana, Yael, Karla, Valebria, Karen, Guty, Ricardo Almada, Juan, Efrén, Moy, Kenia, Toño, Karla (from the folkloric dance class), Quique, and Bryan.

Finally, I want to thank to the people who made this experience possible: my family. Thank you for always trust me and support the decisions I have taken during 25 years. Thank you for your motivation and inspiration, for the laughs and for all the love. You are and will always be my wind rose wherever I am, I love you so much.

As a nutshell, muchas gracias a todos.

(this page was intentionally left blank)

Abstract

The present case study addresses one of the most emblematic mural paintings set painted in 1945 by the Portuguese artist Almada Negreiros at the Maritime Station of Alcântara, Lisbon. In total, they are eight monumental murals depicting Portuguese culture and history. The paintings were made with a bright chromatic palette which today display different states of conservation. The green paint layers are particularly damaged, showing visible severe flaking and powdering in the lightest shades. The goal of this research is to understand the decay phenomenon by identifying the pigments, the painting technique, and the external deterioration factors for the future safeguard of these mural paintings. In addition to the main study, green pigments in powder were analyzed to have a deeper understanding of the green pigments available in Portugal during the 20th centuries, looking for any relation between the pigments and the paint layers from the case study. The analytical setup comprises in-loco technical photography in the visible, ultraviolet (UVF) and infrared radiation (NIR), h-OM, h-EDXRF, colorimetry and spectrophotometry. Microsamples of selected paint layers were also collected for laboratory analyses (OM, SEM-EDS, μ -XRD, and micro-Raman spectroscopy). The pigments in powder were studied by colorimetry and spectrophotometry, h-EDXRF, and XRPD. Almada Negreiros' green painting palette consisted of green-yellow hues. Green earth pigments, the synthetic pigments PG 8 and PG 1, as well as the presence of chrome-based pigments were detected. In addition, other chromophores like the synthetic pigment PY 1 were detected as a pigment used by the artist. The degree of disruption of the samples did not enable to evaluate the painting technique. Analysis like Py-GC/MS and FTIR are required to define the presence of organic binders. About causes of deterioration, the flaking and powdering of the green paint layers can be explained by the presence of salts neoformations, in addition to the signs of bio colonization. Related with the pigments in powder, green chromophores like eskolaite, clinocllore, and phthalocyanine green were detected, as well as the presence of a possible chromium-oxide green pigment, from Almada Negreiros' studio, that the artist might have used for the murals of the Maritime Station of Alcântara.

Resumo

Visão aprofundada das camadas cromáticas verdes deterioradas na Estação Marítima de Alcântara: um estudo arqueométrico

O presente estudo de caso aborda um dos mais emblemáticos conjuntos de pintura mural pintado em 1945 pelo artista português Almada Negreiros na Estação Marítima de Alcântara, Lisboa. No total, são oito murais monumentais que representam a cultura e a história portuguesas. As pinturas foram feitas com uma paleta cromática brilhante que hoje em dia apresentam diferentes estados de conservação. As camadas de tinta verde são particularmente danificadas, mostrando visíveis graves flacidez e pó nas tonalidades mais claras. O objectivo desta investigação é compreender o fenómeno de decomposição, identificando os pigmentos, a técnica de pintura, e os factores externos de deterioração para a salvaguarda futura destas pinturas murais. Além do estudo principal, foram analisados os pigmentos verdes em pó para se ter uma compreensão mais profunda dos pigmentos verdes disponíveis

em Portugal durante os séculos XX, procurando qualquer relação entre os pigmentos e as camadas de tinta a partir do estudo de caso. O esquema analítico inclui fotografia técnica in-loco no visível, ultravioleta (UVF) e radiação infravermelha (NIR), h-OM, h-EDXRF, colorimetria e espectrofotometria. Foram também recolhidas microamostras de camadas de tinta seleccionadas para análises laboratoriais (OM, SEM-EDS, μ -XRD, e espectroscopia micro-Raman). Os pigmentos em pó foram estudados por colorimetria e espectrofotometria, h-EDXRF, e XRPD. A paleta de pintura verde de Almada Negreiros consistia em tonalidades verde-amarelas. Foram detectados pigmentos verdes de terra, os pigmentos sintéticos PG 8 e PG 1, bem como a presença de pigmentos à base de cromo. Além disso, outros cromóforos como o pigmento sintético PY 1 foram detectados como um pigmento utilizado pelo artista. O grau de perturbação das amostras não permitiu avaliar a técnica de pintura. Análises como Py-GC/MS e FTIR são necessárias para definir a presença de aglutinantes orgânicos. Sobre as causas de deterioração, a descamação e o pó das camadas de tinta verde podem ser explicados pela presença de neoformações de sais, para além dos sinais de bio-colonização. Relacionados com os pigmentos em pó, foram detectados cromóforos verdes como o eskolaite, clinoclóro e verde ftalocianina, bem como a presença de um possível pigmento verde de óxido de crómio, do atelier de Almada Negreiros, que o artista poderia ter utilizado para os murais da Estação Marítima de Alcântara.

(this page was intentionally left blank)

Chapter 1: Introduction

1.1 Contextualization, aims and objectives of the research

The current research is focused on the green paint layers of the eight monumental mural paintings located in the Maritime Station of Alcântara, Lisbon, Portugal. This stunning artwork was made in 1945 by Almada Negreiros, one of the most important Portuguese artists of the 20th century, and one of the pioneers of the art modern movement in Portugal [1,2].

On this set of eight mural paintings, Almada Negreiros has depicted fantastic and historical aspects of the culture and traditions in Portugal between the 19th and 20th centuries, playing with different artistic styles and colors [3]. The paintings were made with a bright chromatic palette which today displays different states of conservation. The green paint layers are particularly damaged, showing visible severe flaking and powdering in the lightest shades [4]. The main goal of this research is to understand this decay phenomenon by identifying the pigments, the painting technique, and the external deterioration factors. These data will form the basis for the future safeguarding of these mural paintings.

Taking these aspects into consideration, the main research questions to be answered are:

1. Which green pigments were used? Which is their nature (inorganic or organic)? Were they used alone or with a mix of pigments?
2. What was the painting technique used?
3. What are the reasons these paint layers are severely flaking?

Parallel to this research, seven green pigments in powder, from external sources, were also analyzed for a deeper understanding about the type of green artists' pigments available in Portugal during the 20th century. In addition, it helped to compare and identify if there is any kind of relation with the pigments from the paint layers under study.

This study was carried out in the framework of the project ALMADA – *Unveiling the Mural Painting Art of Almada Negreiros (1938-1956)* [5] between the in-loco analysis carried out in July 2021 and the laboratory analysis carried out from March to October 2022. The research represents a challenge for the analysis of pictorial layers and as stated above, it will set the guidelines for future conservation works. In addition, the results will enable a deeper insight into the painting palette of the artist and will contribute to the knowledge of natural and synthetic pigments used on Portuguese modern mural paintings during the first half of the 20th century.

1.2 Methodological approach

The research was carried out in three main phases:

The first phase consisted in literature review of the art history background of the case study, the biography and artwork of Almada Negreiros, the history of use of pigments

in mural paintings (with emphasis on the green hues), and the generic properties of pigments and causes of deterioration of paint layers.

The second phase was the in-loco survey, accompanied by photographic and graphic documentation, to evaluate and map the state of conservation of the green paint layers, and to select the most relevant areas to be studied in more detail by technical photography and analytical techniques. In what concerns technical photography, the setup comprised imaging in the visible (Vis), visible-raking (Vis-RAK), near-infrared (NIR) and in ultraviolet radiation (UV). Ultraviolet induced fluorescence in the visible range (UVF) was particularly important to detect and map organic material related with past interventions (ex. of adhesives and retouches). Selected stable and deteriorated green paint layers were analyzed by handheld optical microscopy (h-OM), colorimetry and spectrophotometry in the visible range, and finally by handheld energy dispersive X-Ray fluorescence (h-EDXRF) for a first insight into color evaluation, pigment identification and elemental characterization. The obtained data were the basis of the micro sampling carried out as the last stage of the in-loco work.

The third phase of the work consisted of the laboratory analysis of the green paint layers collected from stable and deteriorated areas of five out of the eight murals from the Maritime station of Alcântara.

The new set of microanalyses was carried out at HERCULES Laboratory, located in Évora, Portugal. The microsamples were analyzed by optical microscopy in visible and ultraviolet mode (OM-UV-Vis), variable pressure scanning electron microscopy coupled with energy dispersive spectrometry (VP-SEM-EDS) and micro-X-ray diffraction (μ -XRD). Micro-Raman spectroscopy was carried out by Sylvia Lycke and Peter Vandenabeele in the Raman Research Group of Ghent University, Belgium.

The goal was to get a deeper insight of:

- Surface and stratigraphy of the paint layers;
- Painting technique;
- Chemical and mineralogical composition of pigments, binders, and salts;
- Presence of organic matter (originally used and from past intervention materials).

In addition to this data collection, analyzes were also carried out on a set of seven natural and synthetic green powder pigments coming from *LeFranc-Paris*, *Kremer Pigmente*, old drugstores in the Alentejo region or used as colors on Tijomel ceramic manufacture (1941-1992).

The pigments in powder were analyzed by X-ray powder diffraction (XRPD), colorimetry and spectrophotometry in the visible range, and h-EDXRF. The results were compared with the ones obtained from three pigments in powder from *LeFranc-Paris* and *Osaka* found in Almada Negreiros' studio. The analysis of these pigments provided a better understanding of the type of green pigments available in Portugal during the 20th century for artistic purposes. Besides, it helped to match up and see if there is any kind of relation with the pigments of the green paint layers under study.

1.3 Structure of the thesis

The thesis is structured in five chapters:

- Chapter 1 introduces the case study and its importance. In addition, it provides an outline of the methodology and the structure of the thesis.
- Chapter 2 presents the historical and artistic background of the research. It starts with an overview of the mural painting movement during the 20th century abroad and in Portugal, including the biography of the artist Almada Negreiros. The chapter continues with a brief overview about the main pigments available for artists until the 20th century, with an emphasis on the green hues, and finally, it provides a summary of the pigment properties and the main deterioration factors that affect mural painting paint layers.
- Chapter 3 concerns the description of the case study itself. It gives the paintings' location within the building, the geographic location of the maritime station, and the environmental conditions to which each of the paintings has been exposed. Moreover, it describes in detail the methodology used, the experimental conditions and the principles of the analysis undertaken in-loco and in the laboratory.
- Chapter 4 presents the results and their discussion considering the stated research questions.
- Chapter 5 describes the main conclusions taken from the results, states hypothesis, and presents the main points to be evaluated in future studies and/or conservation processes.

1.4 List of references

- [1] Lobo, P. R. (2014). Almada and the Maritime Stations: The portrait of Portugal that the dictatorship wanted to erase. *Revista de História da Arte – série W*, 2, 342-352.
- [2] França, J. A. (2009). A Arte em Portugal no Século XX (1911-1961) (4 Ed). *Livros Horizonte*, 10-100.
- [3] Ferreira, A. Q. (1994). Análise e recepção da modernidade em Almada Negreiros: painéis das Gares Marítimas de Lisboa. Lisboa: *Fundação Engenheiro António de Almeida*, 175-211.
- [4] Gil, M., Costa, M., Cvetkovic, M., Bottaini, C., Cardoso, A., Manhita, A. Dias, C. & Candeias, A. (2021). Unveiling the mural painting art of Almada Negreiros at the Maritime Stations of Alcântara (Lisbon): diagnosis research of paint layers as a guide for its future conservation. *Ge-conservación*, 20, 105-117.
- [5] Projeto. O desvendar da arte mural de Almada Negreiros (1938-1956) (n.d.) Almada Negreiros. <https://almadanegreiros.uevora.pt/>

Chapter 2: Historical and artistic background

2.1 The mural painting movement in the 20th century: from Mexico to Portugal

One of the biggest muralist movements in the history of art was born in Mexico, in 1921 [1]. It spread at an international scale, shaping it in every country with its own social, political, and economic situation [1]. It is not possible to define how long the movement lasted, every country was influenced at different periods and adapted it to its own circumstances. During a century of social and international conflicts, political tensions, and economic crises, the artists felt the need to make what was called *social art* to promote political action, and national pride through authentic artwork [2,3], and to make art an historical heritage open to the public [3]. Portugal for sure was not an exception. Being from Mexico, I would like to emphasize this aspect and provide a deeper vision of this intriguing movement in the following paragraphs.

After the civil war in 1910-1920, Mexico was under a big economic, political, and social instability [4]. The inhabitants fought against a 35-year dictatorship ruled by Porfirio Díaz; the church was out of any political power after the promulgation of the current constitution in 1917 [4], and around 80% of the peasant and indigenous population were illiterate [5]. All these events triggered the urgency to build a reform to promote education, national identity, and freedom of expression [2,4]. Since 1910, the writer and painter Gerardo Murillo Cornado, known as *Dr. Atl*, inspired his students to look for their own national art and break the dependence on the European art school [1,6]. Many of his students, like David Alfaro Siqueiros, were involved in the army during the Mexican civil war; the aftermath transformed their artistic and social concepts [6].

The Mexican Muralism Movement, also called Mexican Mural Renaissance, was born in 1921 with a three-year campaign led by José Vasconcelos Calderón, the secretary of public education of Mexico [1]. At that time, the current government viewed mural painting as an instrument for public awareness [4], hence Vasconcelos recruited the most renowned Mexican painters to work in the campaign [1]. Among all the artists that participated during the campaign, three of them, David Alfaro Siqueiros, Diego Rivera and José Clemente Orozco, were the most representatives of the movement due to their innovative artwork and connections between Latin America, the United States, and Europe [1]. They were popularly called *The Big Three*, that in conjunction with their professor, Dr. Atl, and José Vasconcelos, they started and promoted the Mexican Muralism movement (Figure 1) [1].



Figure 1. From the upper part, from left to right: Gerardo Murillo Coronado and José Vasconcelos (Images retrieved from [1]). The big three, from left to right: Diego Rivera (Image retrieved from [7]), David Alfaro Siqueiros (Image retrieved from [1]) and José Clemente Orozco (Image retrieved from [8]).

According to Malott (2019), the Mexican muralist movement was influenced by a mixture of national and international factors that looked for the awakening of society [1]. The Russian Bolshevik Revolution, which started in 1917, inspired many countries, including Mexico and their artists, to look for communist societies [4]. Two of the Big Three, David Alfaro Siqueiros and Diego Rivera, had total admiration for the Soviet Union [2]. Additionally, they lived and studied abroad, mainly in Europe, and got inspired by the current European movements like

Novecento and futurism in Italy as well as the older mural artwork of Michelangelo and Giotto [3].

Through authentic artwork and styles, the Big Three looked to encourage political action and exhibit the pre-Columbian heritage and the history of Mexico, showing the national and international conflicts until the current period [2]. People, as a collective and as an individual, were the main character in their work, making awareness of the role of man in the world (Figure 2) [10]. Rivera's purposes were to eliminate the way ancient Indian civilizations were denigrated, and to fight against the anti-mestizo and anti-Indian attitudes cemented during Porfirio Díaz's dictatorship [2].

Once it appeared, the mural movement expanded like a chain reaction, starting with the neighboring countries and regions: the United States of America and Latin America [2]. The United States suffered an economic crisis, *The Great Depression*, between 1920 and 1921 [4]. Inspired by Mexican muralism, the United States made a project as part of the recovery plan to promote and make mural art in the cities [1,11]; they invited the Big



Figure 2. José Clemente Orozco (1939). *El hombre de fuego* (The man of fire). Mural for the Cabañas' Museum. Image retrieved from [9].



Figure 3. Diego Rivera, *The Making of a Fresco Showing the Building of a City* (1936). Mural for the San Francisco Art Institute. Image retrieved from: [1]

Three to make mural art in their country, like the one in the San Francisco Art Institute (Figure 3).

Between the artists influenced by the Big three, Bernard Zakheim and Charles Alston worked with Diego Rivera and made mural paintings about the historical context of medicine as a profession [11]; Reuben Kadish and Philip Guston worked with David Alfaro Siqueiros [1], and the renowned artist Jackson Pollock was an admirer of José Clemente

Orozco's work [1].

Compared with Mexico and the United States, Latin America did not have a proper movement [2]. However, the artists still wanted to express their political, social, and cultural concerns through muralism [3]. Many Latin artists looked to meet and invite Mexican artists to learn from the Mexican School in mural painting (Figure 4) [3]. Some outstanding Latin artists that belonged to the movement are Cândido Portinari, from Brazil; Antonio Berni, from Argentina; Teodoro Núñez, from Perú; and César Rengifo from Venezuela [2].

The Mexican Muralism Movement reached Europe few years later. In 1937, Pablo Picasso presented a mural-scale painting called *La Guernica*, representative of the dreadful experience during the Spanish Civil War and the insights of the beginning of the Second World War [12]. In the post-war period, Mexican artwork was officially presented in Italy during the art exhibition called *XXV Biennale di Venezia*, in 1950 [3]. Portugal is not excluded from this movement. According to the art historian José Augusto França (2009), Portuguese artists started to look for authentic national art, out of the standards from the French school [14]. In 1911 they made the first free style exhibition called *Exposição dos Livres*, where they

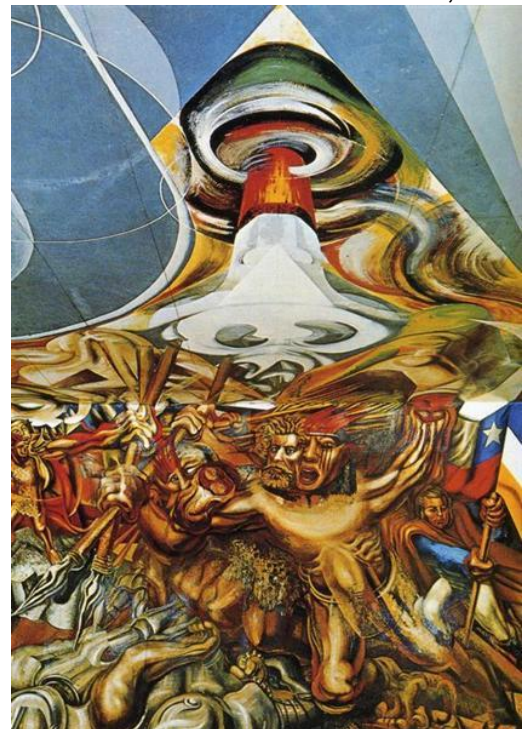


Figure 4. David Alfaro Siqueiros (1941-1942). *Death to the Invader*. Mural of the Library of the School of Mexico in Chile. Image retrieved from: [13].

showed an aesthetic and conceptual breaking from the classic style [14].

It was January 1915 when a quarterly magazine called *Orpheu* was released. The purpose of this project was to propose a new kind of art, staying away from the traditional rules, and “to find in exile the hidden beauty” [15]. The publication of this work was considered the beginning of the first modern movement in Portugal [15]. The main artists responsible for *Orpheu* were: Fernando Pessoa (1888-1935), Mário de Sá-Carneiro (1890-1916), José de Almada Negreiros (1893-1970), Amadeo de Souza-Cardoso (1887-1918), Armando Côrtes-Rodrigues (1891-1971), and Santa-Rita Pintor (1889-1918) [16].

In 1926, a military dictatorship was imposed in Portugal, and the *New State Regime* was established under the control of António de Oliveira Salazar in 1933 [17]. In addition, Portugal was immersed in a back-breaking economic crisis [18], and between 1920 and 1940, only 35% to 48% of the population, aged from 10-14 to 60-64 years, were literate [19].

The dictatorship in Portugal was also a period of expansion, industrialization, and development [20], which provoked a change in the socio-cultural life [21]. França (2009) mentioned common life in Portugal was filled with political passions, trying to bring the republic back to the nation, and fighting against fear and repression [14]. To show the decadent situation of the country, artists started to think about art as a political act [22].

2.2 Almada Negreiros: biography and mural painting artwork

Almada Negreiros, who was a painter, but also a dancer, choreographer, fashion designer, playwright, writer and poet; was born in São Tomé e Príncipe in 1893 [23]. His mother passed away when he was three years old. Because his father moved to Paris, Almada Negreiros and his brother were enrolled in the Campolide Jesuit college



Figure 5. Almada Negreiros painting the Murals of the Maritime Station of Alcântara. Photographic credits: Modernism.pt® All rights reserved.

and moved to Lisbon in 1900. [24]. After the Campolide Jesuit College closed, Almada studied in the Liceu of Coimbra and after that in the International School of Lisbon, where he published his first drawing in 1911 [24]. At just 20 years old, he participated as a cartoonist in the first *Exposição dos Humoristas*, which was one of the starting movements toward modernism [14]. From 1914 to 1916, Almada's interests were more focused on literature and poetry with a political ideology, publishing his work in the magazine *Orpheu* in 1915 [14]. Other renowned works made by Almada during this period of time are the novel *A Engomadeira*, in 1917; the poems *A Cena*

do Ódio and *Mima Fataxa*; and the narrative *K4 o Quadrado Azul*, published in the same year [14].

According to António Quadros Ferreira, full professor in the Faculty of Fine Arts from the University of Porto, Almada decided to find his own artistic style, taking Futurism, the Italian artistic movement, and simultaneism, inspired by the Delaunay, as a basis to start making its own art full of color, light and movement [25]. In addition, Almada got inspired by the Russian ballet of Diaghilev in 1918 [26], turning again his mind towards dance and performances.

França (2009) stated that the death of Amadeo Sousa Cardoso and Santa Rita, as well as the suicide of Sá-Carneiro, members of the magazine *Orpheu* and Almada's close friends, were events that marked Almada and made him look for new opportunities outside Portugal [14]. In 1919, Almada decided to move to Paris, doing different activities like dancing and working in a candle factory to finance his stay in France, avoiding any kind of art academy and developing his own art [14]. According to França, Almada got in touch with the French artist Max Jacob and other renowned artists like Pablo Picasso and Erté (Romain de Tirtoff), who were of huge importance for his future career [14].

The work of França (2006), as well as the work of Manuel Mendes Madeira (2018), mentioned that the year Almada lived in Paris made him reflect on the lack and need for "intellectual artists", as well as the interconnection between art and the artist's homeland [14,26]. The artist manifested this when he wrote in France one of his most famous poems called *Historie du Portugal par Coeur* [26]. He came back to Portugal one year later, in 1920.

During the next years, Almada returned to the exploration of the art of painting. He worked on the decorations of a coffee bar called *A Brasileira do Chiado* in 1920, and participated in some other exhibitions like the *Salão de Outono* in 1925 [14]. In the same year, he wrote one of his most important novels called *Nome de Guerra* [14]. França (2009), states the critical moment that built up Almada's painting style was when, in 1926, Almada saw for the first time S. Vicente de Fora's polyptych, painted in the 15th century [27]. Almada admired how the artist played with the perspective points in the painting [14]. Simão Palmeirim Costa and Pedro J. Freitas stated in 2015 that Almada made use of geometry and different perspective points, from the 1920s until he died [28].

Almada moved to Spain in 1927 and stayed there until 1932 [14]. During that period, he started experimenting with mural painting. Mendes-Madeira (2018) mentioned that, in Madrid, Almada made some mural paintings in the cinemas *Munez Seca*, *Barceló* and *San Carlos* [26]. Almada got in touch with the members of the art movement in Madrid, called *Generación de 1925*, mainly comprised by architects [26]. He left Spain after the political tensions prior to the Spanish Civil War [14]. In Mariana Pintos dos Santos's (2016) and Yara Frateschi Vieira's (2012) works, they affirmed that this last journey, in conjunction with the political, social and economic situation in Portugal and the world, triggered an evolution in the inspirations and ideas of Almada Negreiros: he defended the idea of creating without restraints [22], release from the load of the past

and unlearn what it is not useful for the future [29]. His way of thinking was reflected in future works after he moved permanently back to Portugal in 1932.

Once in Lisbon, Almada Negreiros exploited the art of making mural paintings and big-scale artwork. According to Ellen W. Sapega, between 1929 and 1957, Almada



Figure 6. Almada Negreiros (1936-1938). Vítal for the church Nossa Senhora de Fátima, Lisbon. Image retrieved from: [31].

As stated by Paula Ribeiro Lobo (2014), the maritime stations were part of the plans for modernization and industrialization of Lisbon during the dictatorship of Salazar, under the guidance of the minister Duarte Pacheco [20]. He left the construction of the maritime stations in the hands of the modernist architect Porfírio Pardal Monteiro, Pedro Pardal Monteiro and Eduardo Rodrigues de Carvalho [33]. Almada Negreiros, who had worked with Pardal Monteiro in other public buildings, was responsible for the eight mural paintings in the waiting room of the maritime station of Alcântara, as well as the six mural paintings at the station of Rocha do Conde de Óbidos [20].

The artwork in both Maritime Stations consist of sets of monumental mural

Negreiros collaborated in the pictorial decoration of the indoors and/or outdoors of seven buildings in Lisbon designed by Porfírio Pardal Monteiro, one of the most renowned Portuguese architects of the time [30]. The buildings in which they collaborated are the church of *Nossa Senhora da Fatima* (Figure 6), the building for the journal *Diário de Notícias*, the maritime stations of *Alcântara* (Figure 10) and *Rocha do Conde de Óbidos* (Figure 7), the Faculty of Law and the Faculty of Humanities of the University of Lisbon [32], and the *Ritz Hotel* [30].



Figure 7. Almada Negreiros (1949). Murals of the Maritime Station of Rocha do Conde de Óbidos. Images taken by Guta Carvalho (6-7th of June 2020 © all rights reserved)

paintings designed and painted between 1943 and 1949 [25]. Due to the high charge of critical, historical, and cultural context, as well as the innovation of the artistic style, these artworks are considered one of the most impressive of the artist [25].

Costa and Freitas (2015) mentioned that, during and after the commission in the maritime station of Rocha Conde dos Óbidos, Almada Negreiros started to make high use of geometry and geometrical shapes in his artwork [28]. The mural paintings in the school *Patrício Prazeres* (1956), in Lisbon [34], and the two mural paintings located in the Department of Mathematics of the University of Coimbra (1969) (Figure 8) are examples of the aforementioned [35]. From 1950 onwards, inspired by Le Corbusier and Mondrian, Almada Negreiros was devoted until the end of his life to the study of geometry in paintings by trial and error [28]. Almada Negreiros stated geometry was the initial primitive and universal art [22], one of the main reasons why his last artwork, full of geometric shapes, is called *Começar* (Beginning) (Figure 6) [30]. Almada Negreiros died in Lisbon on the 15th of June, 1970 [23].



Figure 8. Almada Negreiros (1969). *Mathematics since Chaldea and Egypt until our time*. Mural painting for the Department of Mathematics in the University of Coimbra. Image retrieved from: [35].

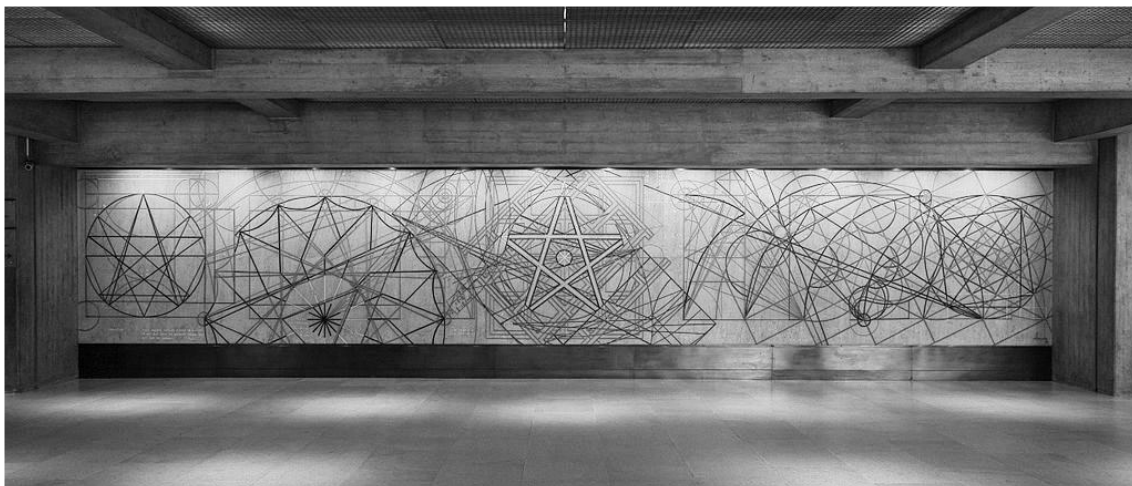


Figure 9. Almada Negreiros (1968-69). *Começar*. Entrance hall for the Calouste Gulbenkian Museum in Lisbon. Retrieved from: [30].

2.3.The mural paintings of the Maritime Station of Alcântara

The case study of this project is comprised of eight mural paintings (Figure 8): two individual panels called “D. Fuas Roupinho, 1º Almirante da Esquadra do Tejo” and “Ó Terra Onde Nasci”, and two triptychs called “Lá vem a Nau Catrineta que tem muito que contar” and “Quem não viu Lisboa não viu coisa boa”; showing in a naturalistic way, the imaginary (cultural) and the real life of Lisbon [25]. The first triptych “Lá vem

a Nau Catrineta que tem muito que contar” represents the popular legend of Nau Catrineta, and evokes Portuguese sailors adrift, being related to the fight between good and evil and homesickness [23].

On the other side, the second triptych represents the riverside of Lisbon from different viewpoints, showing emblematic places like the aqueduct (Aquaduto das Águas Livres), the Cathedral and St. George’s castle, where some women are collecting coal and fish, inspired by the poem of Cesário Verde called “O sentimento dum ocidental” [23]. The first individual painting, “D. Fuas Roupinho, 1º Almirante da Esquadra do Tejo”, represents the miracle of Nazaré, where the courageous Portuguese soldier D. Fuas Roupinho, while he was hunting a deer, was saved by Maria from falling off the cliff. The last individual painting, “Ô Terra Onde Nasci” shows some rustic scenes during times of pilgrimage, showing the courtship between a sailor and a lady next to the chapel, an old lady selling food and a picnic on the upper part [23].



Figure 10. Almada Negreiros (1945). Murals of the Maritime Station of Alcântara. Images taken by Guta Carvalho (June 2020 © all rights reserved).

2.4 Historical overview of natural and synthetic pigments used until the 20th century

Many color materials have been used over time in painting artworks. The most common colorants found in mural paintings, particularly in the fresco technique, are pigments. They can be defined as a colored, fluorescent, white, or black solid, usually insoluble in the vehicle or substrate in which it is incorporated [36]; that is applied to alter the appearance of a material by the absorption/reflection and/or by scattering of light [37]. The following section shows a brief compendium of pigments that were used for mural paintings in Prehistory, Classical antiquity and Pre-Columbian period, Medieval period, and Modern ages.

2.4.1 Prehistory

The first pigments used by our ancestors, during Prehistoric times, were mainly from natural and mineral sources mixed with water, saliva, urine and/or blood as binders [38,39]. According to Inés Domingo and Annalisa Chieli (2021), the natural and mineral sources of colored materials during prehistory were charcoal, soot, minerals, and ochres, with ochres being natural deposits of clays mixed with iron-based oxides and hydroxides, and other impurities [40]. Some of the most important pigments found in Prehistoric studies are gypsum (CaSO_4) and calcite (CaCO_3) in the white colors [41], red and yellow ochres, whose hue depends on the concentration of iron-based minerals, mainly hematite (Fe_2O_3) and goethite, ($\text{FeO}[\text{OH}] \cdot n\text{H}_2\text{O}$) [40]; charcoal (C), soot, manganite ($\text{MnO}(\text{OH})$), pyrolusite (MnO_2) and magnetite (Fe_3O_4) for the black hues [40,41].

There are other minerals used as pigments in Prehistory, but they are less common. Jarosite ($\text{KFe}_3(\text{SO}_4)_2(\text{OH})_6$), a rare yellow mineral, was found in Prehistoric figures from Latin America [40]. Cinnabar (HgS) was found mixed with red ochre in the Neolithic cave paintings of Çatalhöyük (Turkey), however, compared with ochres, it was not widely used for cave painting [40]. It was until the 1st century CE when cinnabar was commonly used by the romans for fresco painting [42]. This pigment was also found in the mural paintings of Teotihuacan (Mexico), dated from 350-500 CE, during the pre-Hispanic period [43].

2.4.2 Classical antiquity and Pre-Columbian period

Over time, the diversity of pigments and hues increased and were used along with the prehistoric pigments. The following paragraphs describe the main pigments used for mural painting by the Egyptian, Chinese, Greek, Roman and pre-Columbian civilizations.

Egyptian blue ($\text{CaCuSi}_4\text{O}_{10}$) was one of the first synthetic pigments in history. It was produced during the first Egyptian Dynasties around 3100 BCE [44], and its earliest use was present in sarcophagi and painted limestone sculptures [44]. According to Rieder (1997), the use and production of Egyptian blue was spread along Greece (around 2500 BCE) and the Roman territory (around 6th century BCE), mainly applied on wall paintings [44]. Han blue ($\text{BaCuSi}_4\text{O}_{10}$) was a similar synthetic pigment of Chinese origins that, according to Berke (2007), was identified in paint layers from the

late Western Zhou period (1207-771 BCE) to the Han dynasty (2nd century BCE-2nd century CE) [45].

Synthetic pigments were also produced in the American continent. Maya blue ($x \cdot \text{indigo} \cdot (\text{Mg}, \text{Al})_4 \text{Si}_8 (\text{O}, \text{OH}, \text{H}_2\text{O})_{24}$) an innovative pigment of Mesoamerican origins, was synthesized since 400 CE by mixing indigo with a clay matrix of palygorskite or sepiolite at 150-200°C [38, 45]. Maya blue was commonly applied in mural paintings, being the wall paintings of Chichén Itzá, Mexico, an example of its use [38].

About natural blue pigments, azurite ($2\text{CuCO}_3 \cdot \text{Cu}(\text{OH})_2$) was first used in Egyptian tomb paintings from the 4th dynasty (2900–2750 BCE), but it was not as used as Egyptian blue [46, 47]. The exploitation of azurite as a pigment started during the medieval period in Europe due to its lower price, comparing with ultramarine blue [46], with the beginning of copper ore mining activities [48]. Azurite was mostly used in easel painting and fresco technique by artists like Giotto and Luca Signorelli [46]. Outside Europe, azurite was used in the far east for wall paintings, which was the case of China during the Sung and Ming Dynasties (960-1644 CE) [46]. The popularity of this pigment dropped after the invention of smalt blue in the 16th century [48], and it was basically out of use after the invention of Prussian blue during the 18th century [46].

New yellow pigments were used during classical antiquity. Orpiment (As_2S_3) is one of the earliest yellow pigments from the Egyptian civilization, detected on objects and paintings from the 31st to the 6th century BCE [49]. This pigment was also used in mural paintings from central Asia between the 6th and 13th century CE; the use of orpiment is recorded until the 19th century [49].

Naples yellow ($\text{Pb}_2\text{Sb}_2\text{O}_7$) is another synthetic pigment of Egyptian origins. It was employed as an opacifying agent and as an enamel colour around 1500 BCE [38]. According to Wainwright, et al. (1986) Naples yellow was largely used in Europe as a glass colorant during the 15th century; there is evidence it was used on paintings until the 16th century [50]. Felici, et al (2004), reported the presence of Naples Yellow in the mural paintings of the Trinità dei Monti, Italy, made by Andrea Pozzi in 1693 [51].

Lead-tin yellow (Pb_2SnO_4 or $\text{Pb}(\text{Sn}, \text{Si})\text{O}_3$), as well as Naples yellow, was used as a glass opacifier and ceramic glaze, and the earliest evidence of its use is in a Roman shard from the 4th century CE [52]. The use of lead-tin yellow as a pigment is documented in 15th century German paintings, including the wall paintings in the Cathedral St. Marien of Freiberg, Saxony. Lead-tin yellow was mainly used in Europe until the 18th century [52].

About the red pigments, realgar, cinnabar and red lead were common pigments since ancient times. The first record of Realgar (As_4S_4) was found in Egyptian tombs from the New Kingdom (16th to 11th century BCE) [49], and its use continued until the 16th century CE [41]. Red lead or minium (Pb_3O_4), commonly confused with cinnabar, was first synthesized during the Han Dynasty in China [41]. Its use has been recorded on the Roman Fayum portraits of the 2nd to 4th centuries CE, as well as in Chinese wall paintings from the 5th to the 9th centuries [41].

In what concerns the green hues, malachite ($\text{CuCO}_3 \cdot \text{Cu(OH)}_2$) was first found as a pigment in Tutankhamun's tomb dated from 1325 BCE [41]. A further use of malachite was found in the Nero's Golden house (1st century CE) from the Roman period, and the western Chinese mural paintings dated from the 9th to the 10th centuries CE [53]. Malachite became popular in Europe between the 15th and 16th centuries, and its use remained until the 19th century when synthetic green pigments of lower cost were produced [53]. Malachite was frequently applied in German wall paintings of churches dated from the 11th to the 18th centuries, and for Italian fresco painting, since malachite is considered quite suitable for fresco technique [47].

Green earth ($\text{K}[(\text{Al}, \text{Fe(III)}), (\text{Fe(II)}, \text{Mg})](\text{AlSi}_3, \text{Si}_4)\text{O}_{10}(\text{OH})_2$) is another ancient pigment mentioned by Vitruvius in the 1st century BCE [54]. Green earth is still widely used nowadays due to its stability and resistance to alkali and acid media. The pigment will be further described in subchapter 2.5.

Finally, lead white ($2\text{PbCO}_3 \cdot \text{Pb(OH)}_2$) was used since the Roman period, being Vitruvius one of the first authors that wrote about the synthesis of the pigment [55]. Lead white was widely employed in easel paintings until the 19th century CE; it was less common in wall paintings due to the subsequent darkening of the pigment after applying, phenomenon that is still under study [55].

2.4.3 Medieval period

In antiquity, Lapis lazuli, the natural form of ultramarine blue, was used in mineral form for jewelry and decorative objects [56]. There is no proof of its use as a pigment until the 6th – 7th century CE in the wall paintings of the cave temples in Bāmiyān, Afghanistan, [56]. Between the 14th and the 15th century, this blue pigment was applied in illuminated miniatures and Italian panel paintings, but the price was extremely high because of the excessive extraction and preparation costs, making people look for other alternatives like azurite [48, 56]. An affordable synthetic route to produce ultramarine blue was discovered until 1828 [56].

According to Kühn (1993), verdigris was widely used in Europe from the 13th to the 19th centuries, mainly for easel paintings [57]. Verdigris' use started to decrease with the synthesis of emerald green. However, it was still commercially available by 1928 [57].

Indian yellow ($\text{C}_{19}\text{H}_{16}\text{O}_{11}\text{Mg} \cdot 5\text{H}_2\text{O}$) dates from the 15th century. Its origins are still uncertain, but there is a theory that the pigment was brought to India by the Persians [58]. Indian yellow was extracted from the cow's urine whose diet consisted of mango leaves; it was mainly used for watercolor and tempera-like paintings in India and Europe [58]. In 1908, the production of this pigment was forbidden because of the animal abuse that was required for its obtention [41].

2.4.4 Post-industrial revolution and modern pigments

The 18th century is considered the period of the first chemical revolution when Antoine-Laurent Lavoisier published the basis of modern chemistry [59]. According to Cartechini et al (2021), this chemical revolution, together with the identification and isolation of new elements, were the base for the development of new pigments [38].

The following section mentions some of the most popular pigments used by artists in both painting and mural painting, intending to make visible the variety of pigments available during Almada Negreiros' career.

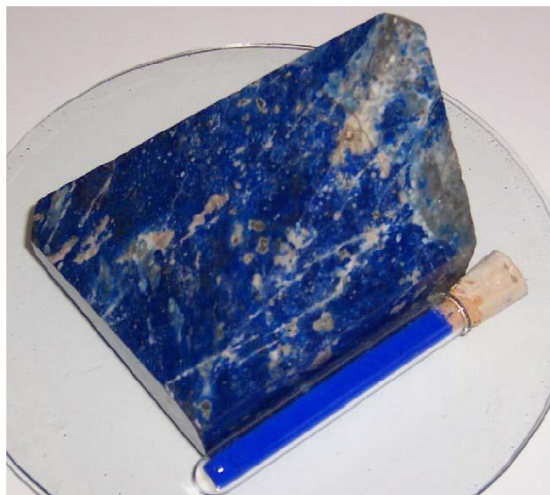


Figure 11. Lapiz azuli and synthetic ultramarine blue.
Image retrieved from: [38]

The first modern synthetic pigment, Prussian blue ($\text{Fe}_4[\text{Fe}(\text{CN})_6]_3 \cdot x\text{H}_2\text{O}$), was prepared by Heinrich Diesbach in 1704 [39]. Prussian blue was in vogue in both America and Europe, but its use decreased until the commercialization of the phthalocyanine pigments in the 1950's [60]. Prussian blue was the starter of a whole period of new synthetic pigments [47].

According to Fiedler and Bayard's work (1997), Scheele's green (CuAs_2O_4) was discovered by Carl Wilhelm Scheele in 1775. However, it was mainly used in paper hangings and wallpaper, and there is limited information about the use of this pigment in

artistic painting, except for a few cases like Edouard Manet's painting *Music in the Tuileries Gardens* [61]. Scheele's green was substituted by emerald green, a copper acetoarsenite, in 1814. Due to its bright green color, emerald green was used in a variety of paintings by Cezanne, Monet and Van Gogh [40]. Concerning mural painting, Zheng et al. (2022) found emerald green in the mural of the Lam Rim Hall in Beijing, China, dating from the 20th century [62]. The use of emerald green decreased because of its high toxicity, being phased out of the market by 1960 [61].

Titanium white (TiO_2), synthesized in 1795 [35], and barium sulfate (BaSO_4), commercially available in 1782, were substitutes of lead white [60]. Barium sulfate, also called baryte, became famous until the beginning of the 19th century, and nowadays it is used either as a pigment or as an extender [63]. An example of the use of baryte as an extender is the study made by the conservator Milene Gil and collaborators (2021) where they detected the presence barium sulfate in the paint layers of Almada Negreiros' artwork, during the first survey of the mural paintings in the Maritime Station of Alcântara [64].

Cobalt pigments emerged in 1780 when the Swedish chemist Sven Rinnman synthesized cobalt green ($\text{CoO} \cdot \text{ZnO}$). Cobalt blue ($\text{CoO} \cdot \text{Al}_2\text{O}_3$) was synthesized by the chemist Louis Jacques Thénard approximately twenty years later in 1802 [41]. Among the cobalt-based pigments, cobalt blue gained more popularity among artists, including George Field and Pierre-Auguste Renoir [41].

According to Abel (2012), chrome pigments started to be developed when the chemist Louis Nicolas Vaquelin synthesized chrome orange ($\text{Pb}_2 \cdot (\text{CrO}_4(\text{OH})_2)$) in 1797, followed by chrome oxide green in 1809 [65], and chrome yellow in 1816 [41]. Veridian, an hydrated chromium oxide, was prepared in 1838 by the color makers Pannetier

and Binet [65]. Chrome yellow was mainly used in watercolor painting, oil painting and coach painting during the second quarter of the 19th century, but its use decreased after its poor lightfastness was discovered [66]. More information regarding chrome oxide green and veridian will be given in the next subchapter.

The extraction and production of cadmium-based pigments started with the discovery of cadmium and natural sources of the element in 1817 [41]. Cadmium yellow (CdS) was the first one to be commercially available in 1900 [41]. Cadmium orange and cadmium red emerged by mixing cadmium sulfide and cadmium selenide Cd(S,Se). Monet was one of the painters who used cadmium yellow in his artwork [67]. Cadmium orange was identified in one of Henri Matisse's artworks (Le Château Chenonceaux, 1918), as well as in watercolor paintings [67]. Almada Negreiros also made use of cadmium-based pigments. In 2021, Gil et al., after carrying out both in-loco and laboratory analysis of two working palettes that belonged to Almada Negreiros, identified both cadmium yellow and red, alone and mixed with other pigments to give a different hue [68]. Fiedler and Bayard (1986) state that currently, cadmium pigments are still of big importance in the artist's pigments [67].

The evolution of pigments over time is connected as well with the evolution of dyes. According to Cartechini (2021) and Neugebauer, et al (2019), the revolution of color chemistry happened during the 19th and 20th centuries [38], due to the development of the coal-tar industry [69]. The need for a bigger color palette for textiles made chemists look for new types of colorants, with Perkin developing the first synthetic dye, *Mauveine*, in 1856 [47].

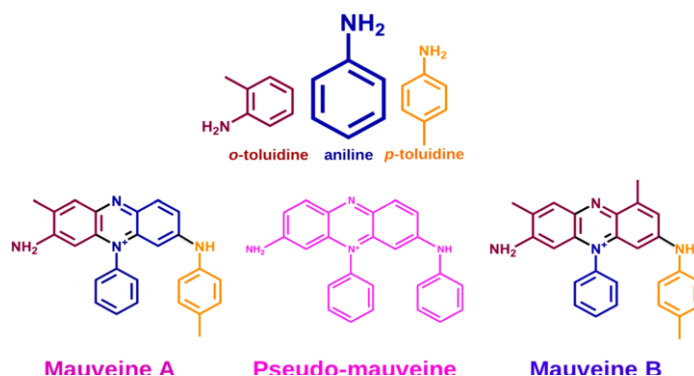


Figure 12. Reactants (up) and products (down) of the synthesis of mauveine. Image retrieved from: [70].

Mauveine was a mixture of around 13 derivatives of aniline, and the ones responsible for the color were mauveine A and B (Figure 11) [70]. The synthesis of this dye during the development of the coal-tar industry was crucial for the new generation of dyes and synthetic organic pigments (SOPs), which were used for painting, printing inks, and for the coloration of plastics and textiles [71].

SOPs are molecules made of insoluble organic groups, metal-organic complexes, and non-soluble salts of dyes [72]. The organic units are usually carbocyclic ring structures with a planar conjugated system, featuring C=O and NH functional groups [73] (Figure 12). These specific pigments became of extensive use in both painting and the textile and plastic industry due to the immense diversity of hues, in addition to the lower prices and their high tinctorial strength [72]. Unfortunately, due to the constant replacement

of pigments with poor fastness by new better ones, there is limited information about the stability of many synthetic organic pigments [69].

Synthetic organic pigments are classified according to the main organic structure. Table 1 shows a classification of synthetic organic pigments created from 1884 until the last quarter of the 20th century (1980's). It is based on Lomax and Learner's work on synthetic organic pigments published in 2006 [71], and it only includes the groups related to artists' pigments. This table was specifically selected since it covers the time Almada Negreiros made the mural paintings in the Maritime Station of Alcântara (1945).

According to Pause et al. (2021), before 1950, SOP groups like β -Naphthol pigment lakes; BON lake pigments (pigments produced with 2-hydroxy-3-naphthoic acid as coupling component); β -Naphthol; Pyrazolones; Hansa Yellows; Diarylides Naphthol AS; Iron complex Pigment Green B; Phthalocyanines, and Nickel Azo Yellow were already developed and in use [74]. Lithol Red is an example of an early synthetic pigment used for mural painting in Argentina, found in the lunette paintings of *Galerías Pacífico*, 1946 [75]. This sulfonated azo pigment was also found in the Harvard Murals, a set of monumental canvas paintings made by Mark Rothko in 1959 [76]. Nowadays, it is known that Lithol red has poor lightfastness and chemical instability [76].

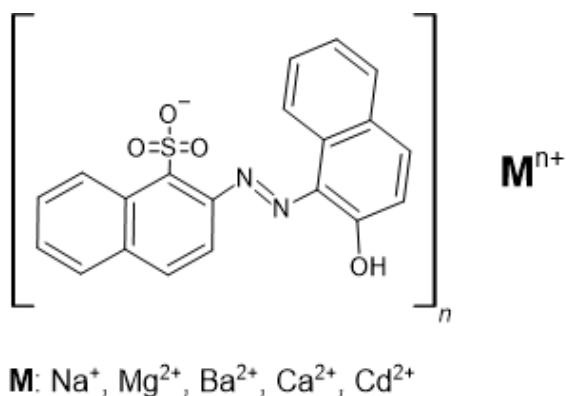


Figure 13. Chemical structure of Lithol red.

All that diversity of pigments was produced and commercialized by companies like *LeFranc*, *Schminke*, *Winsor & Newton*, *Roberson's* and *Royal Talens*. These were the main ones responsible for the manufacturing of modern artists' pigments [72]. Cruz (2005 and 2009) mentioned some of the companies that supplied pigments to Portugal in the 20th century were *Winsor & Newton*, *LeFranc* [77], *Morin & Janet* and *C. Bourguès* [78].

The variety of synthetic pigments, in conjunction with the new artistic movements, helped the artists to think more about creativity in art, doing experiments with new materials and methods. According to Paolo and Laura Mora (1984), the artworks by The Big Three (Subchapter 2.1) are a clear example of the use of new materials like synthetic resins, acrylics and vinyl on supports like canvas, masonite, aluminium, and celotex among others [79]. La Nasa's et al. work, published in 2021, presented a multi-analytical study done on the mural painting of the Polyforum Cultural Siqueiros (Mexico), painted by David Alfaro Siqueiros [80]. They identified the presence of hematite mixed with the synthetic organic pigments, PR 112, PR 122, PY 1 and PY 3, to increase the brightness and modify the hue, and polystyrene and alkyd resins as binders [80].

Many modern artists made (and still make) use of very unstable pigments by unknown techniques [81]. The identification of modern painting materials and their degradation processes are currently a challenge for conservators and scientists.

Table 1. Classification of SOPs produced until the 20th century. Adapted from: [71].

Pigment Class	Structure	Dates of use	Major uses
Arylide Yellows	Monoazo pigments with acetacetarylamine coupling components	First commercialization in 1910	Artists' paints
Beta naphthol	Monoazo pigments with beta-naphthol coupling component	Since 1895 until the early 1900s	Printing inks and artists' materials
Naphthol Reds	Monoazo pigments, derivatives of 2-hydroxy-3-naphthoic acid	First synthesized in 1911	Automotive, architectural and artists' paints
Benzimidazolones	Monoazo pigments with the 5-aminocarbonyl benzimidazolone grouping	First patented in the 1960s	Automotive, artists' paints, printing inks
Disazo Condensation	Disazo pigments with aromatic diamino carboamide linkage	First patented in the 1950s	Automotive, artists' paints, plastics
Pyrazolone	Mono or disazo pigments, contain the pyrazolone ring	First pigment (PY 100) introduced in 1884	Artist's paints, printing inks, plastics
Phtalocyanines	Metal porphyrins	Blue hues introduced in 1935. Green hues in 1938 and 1959.	Automotive and artists' paints, plastics, textiles
Nickel Azo-Yellow	Metallized azo pigments	Developed in 1945	Automotive and artists' paints
Quinacridones	Linear trans quinacridone derivatives	Introduced in 1955	Automotive and artists' paints, plastics, textiles
Perylene/Perinone	Perylenes: Diimides of perylene tetracarboxylic acid. Perinones: naphthalene-1,4,5,8-tetracarboxylic acid.	Introduced in 1950	Automotive, industrial and artists' paints, plastics
Diketopyrrolo-pyrrole	Based on 1,4-diketopyrrolo (3,4c) pyrrole ring system	Introduced in the 1980s	Automotive and artists' paints, plastics, textiles

2.5 List of the green pigments available for artists in the 20th century

To give a general context of the green pigments contemporary to Almada Negreiros' career, the following list shows the most representative green pigments available and in use for painting during the 19th and 20th centuries. It is not possible to give a complete list due to the variety of natural and synthetic pigments during this period. The idea is to explore the green painting palette and show the complexity of their study in modern mural paintings.

Green Earth (PG 23, CI 77009)

Called by names like terra verde, Grüne Erde, and terre verte; it is an allumino-silicate of iron and magnesium ($K[(Al, Fe(III)), (Fe(II),Mg)](AlSi_3, Si_4)O_{10}(OH)_2$) present in nature as celadonite, glauconite, cronstedtite and chlorite [54].

According to the senior conservator Carol A. Grissom (1986), the oldest use of the pigment was found in both ancient jars and mural paintings located in Pompeii [54]. It was mainly used for fresco mural paintings during the Roman period and for tempera paintings in the Medieval period [82]. Examples of the use of green earth in mural paintings are the Pompeiian paintings from the 1st century, the Bizantine wall paintings of Santa Sophia, in Trebizond, Turkey [54]; and the Andean church of *Our Lady of Copacabana de Andamarca* in Bolivia (18th century) [83]. Green earth is still commercially available.

Grissom (1986) indicates this pigment presents low tinting strength and hiding power. However, it is considered a very stable pigment against light and air. Green earth is compatible with all kinds of media and pigments, making it appropriate for fresco technique [54].

Malachite (PG 39, CI 77492)

The conservator scientists Rutherford John Gettens and Elizabeth West Fitzhugh reported in 1993 a diverse list of names for malachite like Bremen Green, Cooper Green, Hungarian Green, Olympian Green, among others [53], and the synthetic version of malachite is called Green Verditer. It consists of a basic copper (II) carbonate, ($CuCO_3 \cdot Cu(OH)_2$) found in both natural and synthetic forms [53]. Malachite is naturally associated with azurite, chrysocolla and cuprite [53].

As mentioned before, the first appearance of malachite is in Egyptian funerary paintings, and its use dropped until the 19th century [41].

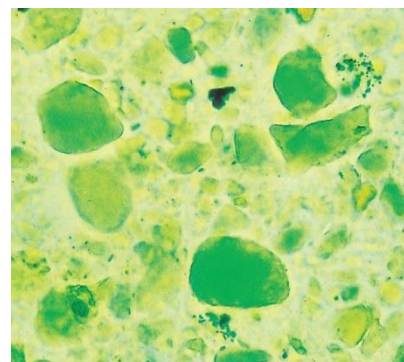


Figure 14. Particles of green earth pigment under normal transmission light. (500x). Image retrieved from: [54].

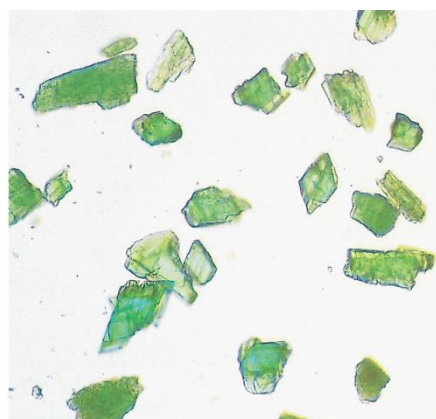


Figure 15. Coarse malachite under normal transmitted light. (121x). Image retrieved from: [53].

According to Gettens and Fitzhugh (1993), malachite presents good lightfastness and it is stable under normal atmospheric conditions, however, its stability depends on the particle size of the pigment [53]. They reported finely powdered malachite can suffer darkening, and it is relatively resistant to alkaline media as long as it is not heated, making it suitable for fresco techniques [53]. Nevertheless, malachite is not resistant to acidic media. The exposure of the pigment to high concentrations of CO₂ produces tenorite, CuO, which is a dark mineral [53].

Verdigris

This synthetic pigment called verdigris, ver-de-gris, verderame, Grünspan, verdete, or cadernillo; is a mix of different copper acetates. It can contain [57]:

1. $[\text{Cu}(\text{CH}_3\text{COO})_2]_2 \cdot \text{Cu}(\text{OH})_2 \cdot 5\text{H}_2\text{O}$ blue hue
2. $\text{Cu}(\text{CH}_3\text{COO})_2 \cdot \text{Cu}(\text{OH})_2 \cdot 5\text{H}_2\text{O}$ blue hue
3. $\text{Cu}(\text{CH}_3\text{COO})_2 \cdot [\text{Cu}(\text{OH})_2]_2$ blue hue
4. $\text{Cu}(\text{CH}_3\text{COO})_2 \cdot [\text{Cu}(\text{OH})_2]_3 \cdot 2\text{H}_2\text{O}$ green hue

In 1993, Hermann Kühn stated that verdigris was officially mentioned in literature since the Middle Ages, as well as the Renaissance and the Baroque period [57]. The pigment was detected from the 13th to 19th century in European paintings, being *The Last Supper*, by Giotto, dated to the 13th century one of the earliest paintings where verdigris was used [57]. From the 15th to the 17th centuries, verdigris was mainly used in easel paintings, being *The Girl with the Pearl Earring* (1665), by Jan Vermeer, one of the most iconic examples [57]. Its use declined after the synthesis of emerald green in the 19th century. However, it was present in the catalogue of *LeFranc* pigments in France until 1928 [57].

According to Kühn (1993) verdigris has good lightfastness, but it tends to have a chromatic alteration, from blue to green, that depends on the mixture of copper acetates present in the sample, as well as the binding medium [57]. Verdigris accelerates the drying process of oil-media, making it suitable for oil painting. However, resins should be avoided due to the formation of copper resins [57]. Regarding compatibility, this pigment should not be mixed with sulfur-containing pigments in aqueous media, due to the formation of copper sulfide [57].

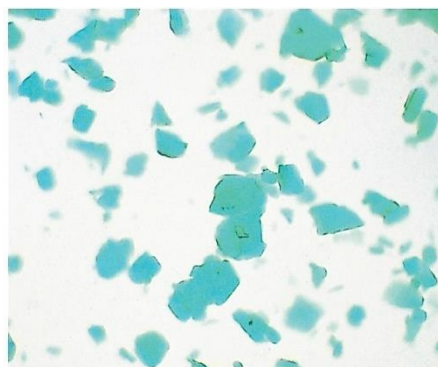


Figure 16. Particles of neutral verdigris under transmitted light (325x). Image retrieved from: [57].

Copper Resinate

Copper resinate or transparent copper resinate ($[\text{Cu}(\text{RCO}_2)_4\text{Cu}]$) is comprised of copper salts of resin acids like abietic acid, dehydroabietic acid, pimaric acid, isopimaric and sandaracopimaric acid [57].

Maurizio Aceto, who published in 2021 a review about the organic pigments used for mural paintings, mentioned copper resinate was produced since the 8th century [84]. The use of copper resinate was reported in 13th-14th century wall paintings located in the San Juan del Hospital Church in Valencia (Spain) [84]. Copper resinate was used as a glazing pigment for Northern easel painting, in the 15th and 16th centuries, and in Italian paintings during the 16th century (*St. John the Baptist preaching*, by Raphael, 1503). There is no common presence of this pigment after the 16th century. However, verdigris was found in an Arnold Böcklin's painting from 1873, *Triton and Nereide* [57].

Unfortunately, copper resinate has no discrete particles (particles that can be separated and distinguished from other particles) nor crystalline structure, making its identification a challenge. Aceto (2021) states this pigment fades easily, making it not adequate for mural painting [84]. It oxidizes under high exposure to short-wave UV light, giving a brown decolorated hue [57]. Alter, et al. studied in 2019 the darkening mechanism of copper resinate and verdigris, in linseed oil, under exposure to near ultraviolet light (~ 410 nm) [85]. They proposed a mechanism where, in presence of oxygen (O_2) a photoinduced radical reaction occurs where the oxygen substitutes two of the organic ligands of the complex and form a peroxo-Cu (II) dimer [85].

Emerald Green (PG 21, CI 77410)

According to Fiedler and Bayard's work (1997), emerald green was also known as Paris green, Schweinfurt Green, Veronese green, and Mitis' Green, but some manufacturers used to exchange Scheele's Green with emerald green names, which are different pigments [61]. Emerald green is a copper acetoarsenite, whose chemical formula is $3\text{Cu}(\text{AsO}_2)_2 \cdot \text{Cu}(\text{CH}_3\text{COO})_2$

Fiedler and Bayard (1997) stated this pigment was synthesized by Ignaz von Mitis and it was first introduced to the market in Germany in 1814 [61]. An uncountable amount of artists used the pigment because of its deep and bright green color, between them Edouart Manet, Claude Monet, Paul Cézanne, Edgar Degas, Vicent van Gogh and Paul Gauguin [61]. Emerald green was also used in mural painting, like the 19th century Napoleone Verga's mural painting located in Perugia, Italy [86], and in a rural Persian Wall painting [87]. Despite its toxicity, emerald green was still used as a pigment

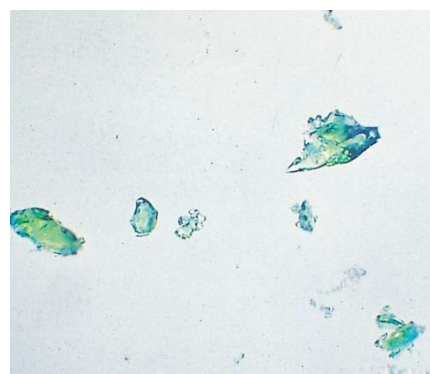


Figure 17. Fragments of copper resinate. Transmitted light (351x). Image retrieved from: [57].

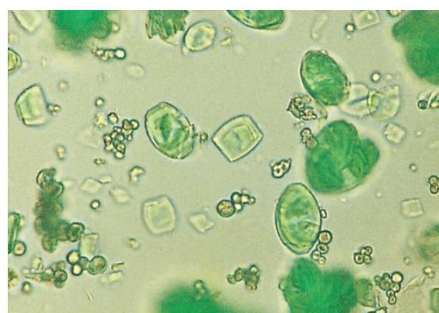


Figure 18. Emerald green. Transmitted light (820x). Image retrieved from: [61].

around 1960, but after that many companies, including Winsor and Newton, discontinued the pigment in their catalogs [61].

Emerald green has a good hiding capacity, and has a relatively good lightfastness and weatherfastness. It darkens with the presence of hydrogen sulfide, H_2S , which reacts to create CuS (the kinetics of the reaction decreases in oil media). As such, it is not compatible with lime or substances that contain sulfur [61].

Chromium Oxide (PG 17, CI 77288)

This pigment has other names like chrome sesquioxide, chrome oxide-opaque, vert-émeraude-dull, and chromoxidgrün [65].

With the chemical composition Cr_2O_3 , this pigment can be either synthetic or natural, where eskolaite is the natural source [65]. The use of chromium oxide as a pigment, according to the art historian Richard Newman, was described by Louis Nicolas Vaquelin in 1809 [65]. Chromium oxide was on the English pigment catalogues in the late 19th and early 20th centuries [65]. The high cost of production made the artists opt for other alternatives like emerald green; in fact, it was common to sell a mixture of Prussian blue with chrome yellow with the name of chromium oxide [65]. Moritz von Schwind and Arnold Böcklin were artists who used chromium oxide in their paintings. Regarding mural paintings, chrome oxide green was identified in the 20th century mural paintings of the Begoña's Galleries in Bilbao, Spain [88], and Piqué et al. reported in 1995 the use of chromium oxide in the green layer of one of the most important masterpieces of David Alfaro Siqueiros, *América Tropical*, made in 1932 [89].

According to Newman (1997), chromium oxide has high hiding power and tinting strength, lightfastness and weatherfastness; it is resistant to alkaline and acidic media, making it compatible with most pigments and painting techniques [65]. Chromium oxide is considered to be a permanent pigment [65].

Hydrated Chromium Oxide (PG 18, CI 77289)

Veridian ($\text{Cr}_2\text{O}_3 \cdot 2\text{H}_2\text{O}$) was commonly named vert-émeraude, Pannetier's green, Guignet's green, and Vert Émeraude [65]. However, it was frequently confused with emerald green during the 1890's [65].

Veridian was synthesized for the first time by the French color makers companies Pannetier and Binet in 1838 [65]. Its production was patented by Guignet in 1859 and the pigment was available for the artist soon afterwards [65]. Newman remarked that veridian and veronese green names were used

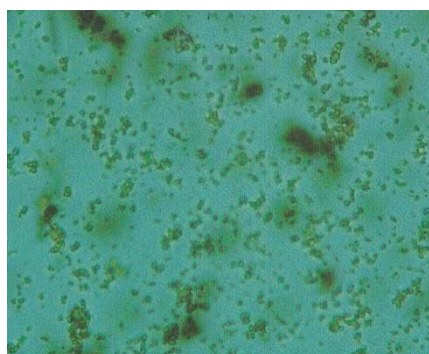


Figure 19. Chromium (III) oxide. Transmitted light (500x). Image retrieved from: [65].

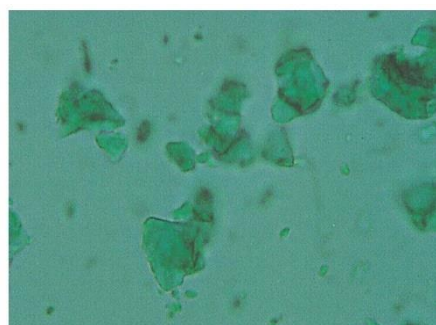


Figure 20. Hydrated chromium oxide. Transmitted light (440x). Retrieved from: [65].

interchangeably, however, veronese could be either emerald green or a mixture of chrome yellow and Prussian blue [65]. In fact, due to its high cost, veridian was usually sold as a mixture of Prussian blue with chromium yellow instead [65]. Its use declined in the 1950's after the discovery of phthalocyanine pigments [65]. Veridian was used by renowned artists like Paul Cézanne, Pierre-August Renoir, George Seurat, Edouard Manet, Claude Monet, and Vincent van Gogh [65]. Veridian, as well as chromium oxide, are still commercially available [65].

Newmann (1997) stated that, due to the medium hiding power and high tinting strength of veridian, baryte (BaSO_4) is usually added as an extender to facilitate the dispersion and grinding of the pigment. Veridian has good lightfastness and is basically compatible with all pigments and media [65]. As chromium oxide, veridian is considered to be a permanent pigment [65].

PG 12 (PG 12, CI 10020)

Pigment Green 12, also called Naphthol Green B, Naphthol Green, Acid Green 1, and Naphtolgrün B; is a barium lake of Acid Green (Figure 21) which is an iron complex of 1-nitroso-2-naphthol-6-sulfonic acid [69].

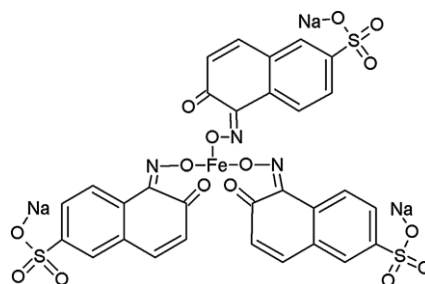


Figure 21. Chemical Structure of Naphthol Green (Acid Green 1). Retrieved from: [69].

According to Neugebauer, et al (2019), Naphthol Green B was synthesized by Otto Hoffmann in 1883 and patented the next year in Germany for dyeing wool and silk. It is still commercially available [69]. Five manufacturers of this pigment have been identified between 1883 and 1923. Unfortunately, there is no record of artists who made use of this pigment. However, companies of artists' pigments have commercialized pigments with PG 12 in their composition by the following names [69]:

- Winsor & Newton: *Alizarin Green*, modern watercolor pigment;
- Schoenfeld & Co: *Echtgrün*;
- Günther Wagner & Co: *Eilido-Grün*;
- Redeker & Hennis A.-G: *Saftgrün bläulich* and *Saftgrün gelblich*;
- Talens: *Vert de vessie*, *Vert olive*, *laque vert claire* and *Laque verte foncée*.

Neugebauer et al. mentioned this synthetic organic pigment has medium lightfastness [69]. There is no more information available about the properties of this pigment.

PG 8 (PG 8, 1006)

PG 8 is a synthetic organic pigment also known as Pigment Green B, Nitroso Green, and Pigmentgrün B. It is an iron complex of 1-nitroso-2-naphthol (Figure 22). In 2014, the senior researcher Matthijs de Keijzer stated that PG 8 was synthesized and reported by Otto Hoffmann in 1885 and commercialized by the company BASF in 1921 [90]. PG 8 was mainly used for wallpaper, rubber coloration, and the textile industry. However, use declined with the invention of phthalocyanine pigments in the early 1950s due to the outstanding stability of these new pigments [90]. There are few records of the use of PG 8 as artists' pigments. Saverwyns identified in 2010 the presence of PG 8 in *Relief Painting* (1915) by Liubov Popova, a renowned Russian painting from the avant-garde artistic trend [91]. PG 8 was also found in *As For apperance* (1963-1965) and *Colors in Four Corners* (1970) by the U.S.A painter Sam Francis [92]. The use of PG 8 in mural painting was reported in 2021 in Almada Negreiros' mural paintings of the Maritime Station of Alcântara, Lisbon [64]. Out of this case, no other examples have been found.

Keijzer (2014) mentioned PG 8 has medium light and weather fastness, but it is sensitive to alkalis and acids [90]. There is no more information about the properties of this pigment.

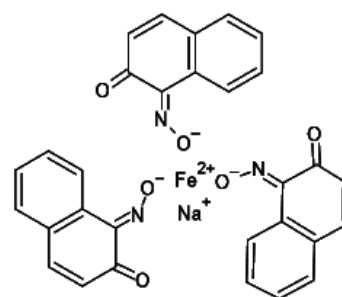


Figure 22. Chemical Structure of Nitroso Green (PG 8).

Phthalocyanine Green (PG 7; CI 74260)

PG 7 is also known as Phtalocyaningrün, vert de phtalocyanine, verde de ftalocianina, and Monastral Fast Green GS. The pigment consists of a copper complex of polychloro phthalocyanine (Figure 23). Keijer (2014) mentions phthalocyanine green was synthesized in 1935 by Georg Niemann, Willi Schmidt, Fritz Mühlbauer and Geord Wiest [90]. According to Lutzenberger and Stege (2009), the high stability and resistance of PG 7 make it nowadays used as an artist's pigment, lacquers, printing ink, and for the coloration of textiles, rubber and plastics [93]. PG 7 was identified in Max Beckmann's painting *Woman with mandolin in yellow and red* (1950) [93].

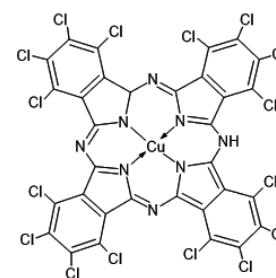


Figure 23. Copper (II) Phthalocyanine (C.I. Pigment Blue 15).

The chemist Suzanne Quillen Lomax mentioned in 2005 that PG 7 has very high lightfastness in watercolor, oil, acrylic, gouache and alkaline media, as well as tinting strength. In addition, it is resistant to acids and bases [94].

2.6 Properties and main causes of deterioration of pigments on mural paint layers

According to the conservators-restorers Paolo and Laura Mora (1984), the causes of deterioration of paint layers depend on mainly three factors: the materials used for the pictorial support and the paint layer (mortar, pigments, and binders); the painting technique and the execution of the mural painting; and the weather conditions to which it is subjected [79].

The type of pigments used is crucial for the successful durability of a paint layer. The performance of pigments can be described in terms of the hue, tinctorial strength, hiding power, dispersion, and fastness, among others. The following paragraphs describe a brief introduction about the pigment properties, as well as an introduction about the main causes of deterioration in mural paintings.

2.6.1. *Pigment properties*

Hue: it is directly related to a pigment's color (blue, green, red, yellow). In pigments, colors are associated with the interaction of electromagnetic radiation and matter by physical and/or chemical phenomena [38]. The physical phenomena related to color are dispersion, diffraction, polarization and scattering of light, which mainly depend on the structure of the compound, the shape and dimensions of the particle and the distribution along the pigment [95]. On the other hand, the chemical phenomena are related to the excitation of electrons by electromagnetic radiation (usually in the UV-Vis region) after absorbing radiation of specific energy, reflecting the complementary color [36]. The energy of absorption depends on the nature of the material [38].

For d-block metal complexes, the absorption in the visible light can be related to electronic transitions within the metal, electronic transitions between the ligand and the metal, charge transfer complexes; and for semi-conductors, the electronic transitions between the valence and conduction bands [38].

According to the ligand-field theory, the interaction between the metal and the ligands produces electronic repulsions that vary depending on the geometry and spatial orientation of the d orbitals [96]. The five d orbitals, which were before degenerated (same energy), split into two or three different energetic levels, in which electronic transition energy is in the range of visible light [96].

Charge transfer complexes consist of the exchange and redistribution of the electronic density between a donor and an acceptor [97]. For d-block metal complexes, ligands are commonly the donors and metals the acceptors; examples of this are hematite and yellow chromate-based pigments [38]. The charge transfer phenomenon can also happen with compounds without a metal center – e.g., the intense blue color of azurite is due to a charge transfer between the radical anion S_3^- presented in the mineral [38].

For semiconductors, like cadmium Yellow (CdS), the color is due to the electronic transition between the valence band (electron-full band) and the conduction band (empty-electron band) [38]. The transition energy from the highest occupied energy state and the lowest unoccupied energy state is equal to the band gap energy, where the band gap is a set of continuous “forbidden” energy levels for electrons [38].

For organic pigments, the hue is due to the presence of a conjugated double-bound system called chromophore, which is the main responsible for visible light absorption [36,38]. Hunge & Schmidt described in 2018 that there are functional groups called auxochromes which, attached to the chromophore, modify the wavelength of absorption and consequently the color [36]. Alkoxy, hydroxy, alkylamino, arylamino and alkyl groups are considered electron-donor auxochromes. Conjugated functional groups like NO₂, COOH, COOR, SO₂NH₂ or SO₂Ar, are considered electron-acceptor auxochromes [36].

Some pigments contain both metal and organic ligands whose color is due to both the organic part and the metal, giving a color which is the contribution of all the electronic transitions [38].

Tinctorial Strength: According to Nagose et al. (2018), the tinctorial strength of a pigment is the capability to give color to the medium, once applied, by absorbing visible light [98]. The capability to absorb light depends on the chemical structure of the pigment, the wavelength of the incident light, as well as the particle size. Oyarzún (2000) mentions tinctorial strength as a way to study the yield of the pigment: the less amount of pigment necessary to reach a specific color intensity, the higher the tinctorial strength [99].

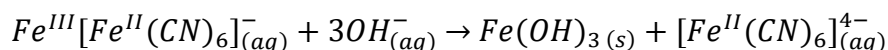
Hiding Power: it is defined by the capability of a pigment, once applied in a layer, to hide the surface background color. This property is related to the light scattering in the paint layer, which depends on its thickness, the absorption of light within the layer, and the chromatic differences between the pigment and the substrate [36].

Dispersion: it is associated with the even distribution of the pigment in the medium without agglomerates. Aspects like the chemical composition of the pigment and the medium, particle size distribution, particle shape, crystalline structure, and the interactions pigment-media are involved in the dispersive properties of the pigment [36].

Fastness: according to Hao and Iqbal (1977) fastness is the ability of the pigment to withstand specific chemical and physical phenomena, during and after application [73]. These phenomena are associated with the environmental conditions, the media in which the pigment is dispersed, and the characteristics of the substrate where the pigment is applied. Lightfastness and weather fastness are the most common properties studied in pigments and are measured by evaluating the fading or darkening of the pigment color as a function of exposure to specific light and/or weather conditions [73].

2.6.2. Main causes of deterioration of mural paintings (topics)

Incompatibility of pigments with the painting technique: when the fresco technique is used, caustic alkalis, like lime, can chemically modify the pigment and therefore modify the hue and its properties [100]. Prussian blue is one example of incompatibility for fresco technique, due to the fact this pigment is very sensitive to alkaline media [60]. The report of the chemist Mike Ware states the decomposition reaction of Prussian blue in alkaline media is the following [101]:



Lead white, minium, azurite, cinnabar, and synthetic organic pigments like BON lake pigments and Pigment Green 8; are examples of pigments that react in alkaline media, which is the media used for fresco technique [90,102].

The artist should be aware which pigments were compatible with the painting technique before any painting process [100]. According to Mora (1974) the most suitable pigments to use in fresco technique are calcium carbonate, all range of ochres, green earth, Egyptian blue, ivory or bone black, and wood charcoal [102]. Newman established in 1997 chromium oxide green and veridian are also compatible with all kinds of media, therefore making them compatible with the fresco technique [65].

Incompatibility of pigments with other pigments: chemical reactions can occur when pigments are in direct contact, either by mixing or by contact between pictorial layers; cadmium yellow is an example of it. According to Fiedler and Bayard (1986), cadmium yellow darkens with the presence of lead or copper-based pigments, by producing lead or copper sulfides [67]. Kühn and Curran (1986) emphasized chrome yellow should not be mixed with lead white in alkaline media due to the formation of chrome red ($PbO \cdot PbCrO_4$) [66].

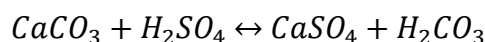
Light exposure: Ultraviolet light (UV) promotes the excitation of electrons and therefore the oxidation or ionization of atoms, or the formation of free radicals, which are very reactive species that can modify the chemical structure of pigments and organic binders [103]. Pigments with organic groups like SOPs, are usually more sensitive to light than inorganic pigments [100]. Cadmium yellow is an example for this type of deterioration. In exposure to light, moisture and air, cadmium yellow reacts by photo-oxidation, giving cadmium sulfate ($CdSO_4$) as degradation product [104].

Pollution: substances like carbon dioxide, sulfur dioxide, nitrogen dioxides, ozone, chlorides, and sulfates of alkali metals are considered pollutants [100]. The mechanism by which they promote the deterioration of mural paintings varies depending on the nature of the pollutant, the composition of the paint layer and mainly the presence of moisture or humidity, as shown in the next item.

Water and high level of humidity: water can be present in mural paintings by infiltration, rain exposure, rising damp, humidity condensation in cold walls or moisture produced by hygroscopic materials [100]. The excess of water and moisture in mural paintings is one of the most concerning problems for the conservation of mural paintings since water, in conjunction with other factors, can trigger chemical, physical, and biological deterioration mechanisms.

According to Mora (1974) and Thapa (1984) humidity and moisture can react with the pollutants present in the atmosphere and create reactive substances in the paint layer. Carbon dioxide (CO_2), sulfur dioxide (SO_2), and nitrogen dioxide (NO_2) react with water to form carbonic acid (H_2CO_3), sulfurous and sulfuric acid (H_2SO_3 and H_2SO_4), and nitric acid (HNO_3), respectively [102, 105]. These acids, even in small amounts, are reactive enough to dissolve and modify the paint layer composition, mainly

carbonates. In presence of sulfuric acid, calcium carbonate, commonly present in fresco technique, reacts in aqueous media to form calcium sulfate:



The acid formation can also be due to the pigment in contact with water. According to Subbaraman (1993), verdigris hydrolyses with water and forms acetic acid, which can damage the paint layer [106].

Besides promoting chemical reactions, water can dissolve or partially dissolve inorganic salts from the support, the intonaco, and the paint layer [79]. The dissolved salts are carried and transported until water evaporation, or the supersaturation of salts produces their crystallization. The crystallization can be over the paint layer surface (efflorescence), or inside the rendering or the support (sub-efflorescence) which can produce mechanical stress in all the components of the mural painting [106].

As mentioned before, water can contribute to physical and biological deterioration. Water that falls directly on the paint layer produces erosion. Indeed, at cold temperatures, water solidifies into ice and its expansion can produce damage to the support [106]. Finally, constant damp areas are a good environment to promote bio-colonization [106].

Biodeterioration: the environmental conditions, as well as the composition of the paint layer, can promote the development of microorganisms and therefore bio-colonization. Subbaraman mentioned in 1993 that the growth speed of microorganisms is fast when the relative humidity is over 65%, and lichen and even algae can grow in constantly damped areas [106]. In addition, Ciferri (1999) mentions that the presence of biodegradable substances (glues, emulsifiers, etc.), dirt, and soot, is a factor that can create a proper environment for microorganisms [107].

According to Allsopp, et al. (2004) microorganisms can produce mechanical, aesthetic, and chemical biodegradation [108]. The mechanical deterioration is related with the growth of microorganism within the paint layer, producing the cracking of the surface [108]. The presence of microorganisms, as well as their excretion and metabolic products, can make an aesthetic change in the mural painting by the appearance of stains on the wall [108]. The chemical biodegradation occurs when microorganisms consume materials from the paint layer and support as a source of energy [108]. The acidic secretions and metabolic products of microorganisms can also affect the chemical composition of the pictorial layer by the degradation of biodegradable substances and polymers, provoking the weakening of the paint layer from the rendering [106, 108].

Many deterioration factors can be damaging to the artwork at the same time, or even in conjunction, so it is extremely important to consider any factor that could promote the deterioration.

2.7 List of references

[1] Malott, M.E. (2019). How a Few Individuals Brought about a Cultural Cusp: From a Mexican Mural Program to a Movement. *Perspect Behav Sci*, 42, 773–814. <https://doi.org/10.1007/s40614-019-00211-4>

- [2] Goldman, S. M. (1982) Mexican Muralism: Its Social-Educative Roles in Latin America and the United States. *Aztlan--International Journal of Chicano Studies Research*, 13, 111-133.
- [3] Alberti, C. S. S. (2021). El muralismo como espacio de intercambio entre Italia y México, 1950-1980. *Anclajes*, 12 (2), 145-165. <https://doi.org/10.19137/anclajes-2021-25210>
- [4] Malott, M. E. (2020) Evolution of the Mexican Muralist Movement: A Culturo-Behavior Science Account. In Cihon, T. M. & Mattaini, M. A. (Eds.), *Behavior Analysis: Theory, Research, and Practice*, Springer, 357-384.
- [5] Moraga Valle, F. (2019). Educación, exilio y diplomacia: Vasconcelos, Mistral, Torres Bodet y la proyección internacional de sus ideas educativas, 1921-1964. *Revista De Historia De América*, 156, 61-94. <https://doi.org/10.35424/rha.156.2019.234>
- [6] Patterson, R. H. (1964) An Art in Revolution: Antecedents of Mexican Mural Painting, 1900-1920. *Journal of Inter-American Studies*, 6 (3), 377-387.
- [7] Fernández, T. & Tamaro, E. (2004). *Biografía de Diego Rivera*. Biografías y Vidas. La enciclopedia biográfica en línea. <https://www.biografiasyvidas.com/biografia/r/rivera.htm>
- [8] José Clemente Orozco Biography (2014). The Biography.com website. <https://www.biography.com/artist/jose-clemente-orozco>
- [9] *Historia*. (n. d.) Museo Cabañas. <https://museocabanas.jalisco.gob.mx/es/historia/>
- [10] Saldanha, A. (2013). Experiência Estética e Simbólica do Muralismo Português em Período Revolucionário. *e-escrita*, 4 (4), 297-317.
- [11] Hansen B. (2019). Medical History as Fine Art in American Mural Painting of the 1930s. *Canadian bulletin of medical history = Bulletin canadien d'histoire de la medecine*, 36 (1), 80–111. <https://doi.org/10.3138/cbmh.246-012018>
- [12] Esteban-Leal, P. (n.d.). *Guernica. Pablo Picasso (Pablo Ruiz Picasso)*. Museo Reina Sofia. <https://www.museoreinasofia.es/coleccion/obra/guernica>
- [13] Xennex (2011) *Death to the Invader*. David Alfaro Siqueiros. <https://www.wikiart.org/en/david-alfaro-siqueiros/death-to-the-invader-1942-1>
- [14] França, J. A. (2009). *A Arte em Portugal no Século XX (1911-1961)* (4th Ed.). Livros Horizonte. 10-100.
- [15] Fernández Pinto, P. (2013). El papel y la palabra: la construcción de una modernidad artística en Orpheu, Blast, The egoist y Poetry. In Galindo-Orrego, L. (Editor). *Lectores dentro y fuera de los textos literarios: Convergencias 2011*. Ediciones Uniades, 35-50.
- [16] Laureano Costa, S. & Pizarro, J. (2017) Almada's Notes for the Memory of Orpheu. *Pessoa Plural—A Journal of Fernando Pessoa Studies*. Brown Digital Repository. Brown University Library. <https://doi.org/10.7301/Z0V12305>

- [17] Baiôa, M., Fernandes, P. J. & Ribeiro de Meneses, F. (2003). The Political History of Twentieth-Century Portugal. *E-JPH*, 1 (2), 1-18.
- [18] Araquistain, L. (1928). Dictatorship in Portugal. *Council on Foreign Relations*, 7 (1), 41-53.
- [19] Candeias, A: (2004) Literacy, schooling and modernity in twentieth-century Portugal: what population censuses can tell us, *Paedagogica Historica*, 40:4, 509-530, <https://doi.org/10.1080/0030923042000250027>
- [20] Lobo, P. R. (2014). Almada and the Maritime Stations: The portrait of Portugal that the dictatorship wanted to erase. *Revista de História da Arte – série W*, 2, 342-352.
- [21] Dix, S. & Pizarro, J. (2011). *Portuguese Modernisms Multiple Perspectives on Literature and the Visual Arts*. Modern Humanities, Research Association and W. S. Maney & Son Ltd, 1-10.
- [22] Pinto dos Santos, M. (2016). On Being Modern: Possibilities of Resistance through Primitivism and Ingenuousness in Ernesto de Sousa and Almada Negreiros. *RIHA Journal* (0137) <https://doi.org/10.11588/riha.2016.1.70204>
- [23] Tavares, C. A. (2017). Duas narrativas para o meu país nos painéis de Almada Negreiros. *Convocarte: Revista de ciências da arte*, 1, 123-128.
- [24] Acciaiuoli, M., França, J. A., Espina, A., Gómez de la Serna, R. & de Sena, J. (1983). *Almada Negreiros*. Fundación Juan March, 9-16.
- [25] Ferreira, A. Q. (1994). *Análise e recepção da modernidade em Almada Negreiros: painéis das gares marítimas de Lisboa*. Lisboa: Fundação Engenheiro António de Almeida. 175-211.
- [26] Mendes-Madeira, M. (2018). Almada Negreiros, cinema e iconografia musical: os casos de Madrid e Lisboa. Cuadernos de Iconografía Musical. *FAM UNAM*. 109-138. <http://www.cuadernos-iconografiamusical.fam.unam.mx/index.php/CIM/article/view/90>
- [27] Goyri-O'Neill, J., Camisão-Soares, A. & Marques, C. (2013). The Relic in the Panels of Sao Vicente de Fora. *Acta medica portuguesa*, 26, 289-293.
- [28] Simão Palmeirim Costa & Pedro J. Freitas (2015) Almada Negreiros and the geometric canon, *Journal of Mathematics and the Arts*, 9 (1-2), 27-36, <https://doi.org/10.1080/17513472.2015.1012699>
- [29] Vieira, Y. F. (2012). Almada negreiros: Profecia e modernidade, ficção e iniciação. *Remate De Males*, 12 (1), 79–87. <https://doi.org/10.20396/remate.v12i1.8635909>
- [30] Sapega, E. W. & Beltrán, E. (2017). Almada en la ciudad: ¿encargo u obra? *Dearq*, 21, 32-43. <https://doi.org/10.18389/dearq21.2017.03>
- [31] Enriques da Silva, R. (2014). Almada, das artes e dos ofícios. *Revista de História da Arte – série W*, 2, 393-403.

- [32] *History* (n.d.) Faculdade de Direito Universidade de Lisboa. <https://www.fd.ulisboa.pt/school/history/>
- [33] Bandeira, F. (2000). *Gare Marítima de Alcântara / Salão e Auditório Almada Negreiros*. SIPA – Sistema de Informação para o Património Arquitetónico. http://www.monumentos.gov.pt/Site/APP_PagesUser/SIPA.aspx?id=5061
- [34] *A Escola Patrício Prazeres e os Murais do Almada Negreiros*. (2021). Agrupamento de escolas Patrício Prazeres. <https://aepp.pt/evento/a-escola-patricio-prazeres-e-os-murais-do-almada-negreiros/>
- [35] *Departamento de Matemática | Department of Mathematics* (n.d.) Universidade de Coimbra. <https://www.uc.pt/ruas/inventory/mainbuildings/matematicas>
- [36] Hunger, K. & Schmidt, M. U. (2018). *Industrial Organic Pigments* (4th Ed.). Wiley-VCH, 1-184.
- [37] Lewis, P. A. (1997). Colorants: Organic and Inorganic Pigments. In Nassau, K. (Ed.). *Color for Science, Art, and Technology*. North Holland, 283-312.
- [38] Cartechini, L.; Miliani, C.; Nodari, L.; Rosi, F. & Tomasin, P. (2021). The chemistry of making color in art. *Journal of Cultural Heritage*, 50, 188-210. <https://doi.org/10.1016/j.culher.2021.05.002>
- [39] Ardilla-Leal, L. D.; Potou-Piñales, R- A.; Pedroza-Rodríguez, A. M. & Quevedo-Hidalgo, B. E. (2021) A Brief History of Colour, the Environmental Impact of Synthetic Dyes and Removal by Using Laccases, *Molecules*, 26, 3813, 1:40. <https://doi.org/10.3390/molecules26133813>
- [40] Domingo, I., Chieli, A. (2021) Characterizing the pigments and paints of prehistoric artists. *Archaeol Anthropol Sci*, 13, 196. <https://doi.org/10.1007/s12520-021-01397-y>
- [41] Abel, A. (2012). The history of dyes and pigments: from natural dyes to high performance pigments. *Colour Design*, 557–587. <https://doi.org/10.1016/b978-0-08-101270-3.00024-2>
- [42]. Gettens, R. J., Feller, R. L. & Chase, W. T. (1993). Vermilion and Cinnabar. In Roy, A. (Editor). *Artists' Pigments. A Handbook of Their History and Characteristics*. Volume 2. National Gallery of Art, 159-182.
- [43] Argote, D. L., Torres, G., Hernández-Padrón, G., Ortega, V., López-García, P.A., and Castaño, V. M. (2020). Cinnabar, hematite and gypsum presence in mural paintings in Teotihuacan, Mexico, *Journal of Archaeological Science: Reports*, 32, 102375, <https://doi.org/10.1016/j.jasrep.2020.102375>
- [44] Rieder, J. (1997). Egyptian Blue. In West Fitzhugh, E. (Editor) *Artists' Pigments. A Handbook of their History and Characteristics*. Volume 3. Oxford university Press, 23-45.
- [45] Berke, H. (2007). The invention of blue and purple pigments in ancient times. *Chem. Soc. Rev.*, 2007,36, 15-30. <https://doi.org/10.1039/B606268G>

- [46] Gettens, R. J. & Fitzhugh, E. W. (1993). Azurite and Blue Vertider. In Roy, A. (Editor). *Artists' Pigments. A Handbook of Their History and Characteristics*. Volume 2. National Gallery of Art, 23-36.
- [47] Barnett, J. R.; Miller, S. & Pearce, E. (2006). Colour and art: A brief history of pigments. *Optics & Laser Technology*, 38, 445-453. <https://doi.org/10.1016/j.optlastec.2005.06.005>
- [48] Švarcová, S., Hradil, D., Hradilová, J. et al. (2021) Pigments—copper-based greens and blues. *Archaeol Anthropol Sci*, 13, 190. <https://doi.org/10.1007/s12520-021-01406-0>
- [49] West Fitzhugh, E. (1997). Orpiment and Realgar. In West Fitzhugh, E. (Editor) *Artists' Pigments. A Handbook of their History and Characteristics*. Volume 3. Oxford university Press, 47-79.
- [50] Wainwright, I. N. M., Taylor, J. M. & Harley, R. D. (1986) Lead Antimonate Yellow. In Feller, R. L. *Artists' Pigments. A Handbook of Their History and Characteristics*. Volume 1. Oxford University Press, 17-36.
- [51] Felici, A. C., Fronterotta, G., Piacentini, M., Nicolais, C., Sciuti, S., Vendittelli, M. & Vazio, C. (2004). The wall paintings in the former Refectory of the Trinità dei Monti convent in Rome: relating observations from restoration and archaeometric analyses to Andrea Pozzo's own treatise on the art of mural painting, *Journal of Cultural Heritage*, 5 (1), 17-25, <https://doi.org/10.1016/j.culher.2003.07.001>
- [52] Kühn, H. (1993). Lead-Tin Yellow. In Roy, A. (Editor). *Artists' Pigments. A Handbook of Their History and Characteristics*. Volume 2. National Gallery of Art, 83-112.
- [53] Gettens, R. J. & Fitzhugh, E. W. (1993). Malachite and Green Vertider. In Roy, A. (Editor). *Artists' Pigments. A Handbook of Their History and Characteristics* Volume 2. National Gallery of Art, 183-202.
- [54] Grissom, C. A. (1986) Green Earth. In Feller, R. L. *Artists' Pigments. A Handbook of Their History and Characteristics*. Volume 1. Oxford University Press, 141-186.
- [55] Gettens, R. J., Kühn, H. & Chase, W. T. (1993). Lead White. In Roy, A. (Editor). *Artists' Pigments. A Handbook of Their History and Characteristics*. Volume 2. National Gallery of Art, 67- 82.
- [56] Plesters, J. (1993). Ultramarine Blue, Natural and Artificial. In Roy, A. (Editor). *Artists' Pigments. A Handbook of Their History and Characteristics*. Volume 2. National Gallery of Art, 37-66.
- [57] Kühn, H. (1993). Verdigris and Copper Resinate. In Roy, A. (Editor). *Artists' Pigments. A Handbook of Their History and Characteristics*. Volume 2. National Gallery of Art, 131-158.
- [58] Baer, N. S., Joel, A., Feller, R. L. & Indictor, N. (1986) Indian Yellow. In Feller, R. L. *Artists' Pigments. A Handbook of Their History and Characteristics*. Volume 1. Oxford University Press, 17-36.

- [59] American Chemical Society. (1999) *Antoine-Laurent Lavoisier: The Chemical Revolution. International Historic Chemical Landmarks.* <http://www.acs.org/content/acs/en/education/whatischemistry/landmarks/lavoisier.html>
- [60] Berrie, B. H. (1997). Prussian Blue. In West Fitzhugh, E. (Editor) *Artists' Pigments. A Handbook of their History and Characteristics.* Volume 3. Oxford university Press, 191-217.
- [61] Fiedler, I., & Bayard, M. A. (1997). Emerald Green and Scheele's Green. In West Fitzhugh, E. (Editor) *Artists' Pigments. A Handbook of their History and Characteristics.* Volume 3. Oxford university Press, 219-272.
- [62] Zheng, Y.-X., He, X.; Li, X., Chen, K.-L., Guo, H., and Pan, X.-X. (2022) Raman Spectroscopy Analysis of the Mural Pigments in Lam Rim Hall of Wudang Lamasery, Baotou Area, Inner Mongolia, China. *Minerals*, 12, 456-464. <https://doi.org/10.3390/min12040456>
- [63] Feller, R. L. (1986) Barium Sulfate-Natural and Synthetic. In Feller, R. L. *Artists' Pigments. A Handbook of Their History and Characteristics.* Volume 1. Oxford University Press, 47-64.
- [64] Gil, M., Costa, M., Cvetkovic, M., Bottaini, C., Cardoso, A. M., Manhita, A., Dias, C. & Candeias, A. (2021). Unveiling the mural painting art of Almada Negreiros at the Maritime Stations of Alcântara (Lisbon): diagnosis research of paint layers as a guide for its future conservation. *Ge-conservacion*, 20, 105-117. <http://dx.doi.org/10.37558/gec.v20i1.1027>
- [65] Newman, R. (1997). Chromium Oxide Greens. Chromium Oxide and Hydrated Chromium Oxide. In West Fitzhugh, E. (Editor) *Artists' Pigments. A Handbook of their History and Characteristics.* Volume 3. Oxford university Press, 273-294.
- [66] Kühn, H. & Curran, M. (1986) Chrome Yellow and other chromate pigments. In Feller, R. L. *Artists' Pigments. A Handbook of Their History and Characteristics.* Volume 1. Oxford University Press, 187-218.
- [67] Fiedler, I. & Bayard, M. A. (1986) Cadmium Yellows, Oranges and Reds. In Feller, R. L. *Artists' Pigments. A Handbook of Their History and Characteristics.* Volume 1. Oxford University Press, 65-108.
- [68] Gil, M., Costa, M., Cardoso, A., Valadas, S., Helvaci, Y., Bhattacharya, S., Moita, P. & Candeias, A. (2021). On the Two Working Palettes of Almada Negreiros at DN Building in Lisbon (1939–1940): First Analytical Approach and Insight on the Use of Cd Based Pigments. *Heritage*, 4 (4), 4578-4595. <https://doi.org/10.3390/heritage4040252>
- [69] Neugebauer, W.; Sessa, C.; Steuer, C.; Allscher, T. & Stege, H. (2019). Naphthol Green- a forgotten artists' pigment of the early 20th century. History, chemistry and analytical identification. *Journal of Cultural Heritage*, 36, 153-165. <https://doi.org/10.1016/j.culher.2018.08.008>.

- [70] Cova, T.F.G.G., Pais, A.A.C.C. & Seixas de Melo, J.S. Reconstructing the historical synthesis of mauveine from Perkin and Caro: procedure and details. *Sci Rep* 7, 6806 (2017). <https://doi.org/10.1038/s41598-017-07239-z>
- [71] Lomax, S. Q. & Learner, T. (2006) A Review of the Classes, Structures, and Methods of Analysis of Synthetic Organic Pigments, *Journal of the American Institute for Conservation*, 45:2, 107-125.
- [72] Sundberg, B.N.; Pause, R.; van der Werf, I.D.; Astefanei, A.; van den Berg, K.J. & van Bommel, M.R. (2021). Analytical approaches for the characterization of early synthetic organic pigments for artists' paints, *Microchemical Journal*, 170, 106708. <https://doi.org/10.1016/j.microc.2021.106708>.
- [73] Hao, Z. and Iqbal, A. (1977). Some aspects of organic pigments. *Chemical Society Reviews*, 3, 203-213. <https://doi.org/10.1039/CS9972600203>
- [74] Pause, R., van der Werf, I. D. & Jan van den Berg, K. (2021). Identification of Pre-1950 Synthetic Organic Pigments in Artists' Paints. A Non-Invasive Approach Using Handheld Raman Spectroscopy, *Heritage*, 4 (3), 1348-1365. <https://doi.org/10.3390/heritage4030073>
- [75] Moretti, P., Gallegos, D., Marte, F., Brunetti, B., Sgamellotti, A. & Miliani, C. (2013). Materials and Techniques of Twentieth Century Argentinean Murals, *Procedia Chemistry*, 8, 221-230, <https://doi.org/10.1016/j.proche.2013.03.028>
- [76] Kennedy, A.R., Stewart, H., Eremin, K. and Stenger, J. (2012), Lithol Red: A Systematic Structural Study on Salts of a Sulfonated Azo Pigment. *Chem. Eur. J.*, 18, 3064-3069. <https://doi.org/10.1002/chem.201103027>
- [77] Cruz, A. J. (2009). Entre a tradição e a modernidade: os pigmentos ao dispor dos artistas e o conhecimento sobre esses materiais em Portugal no início do século XX. *Estudos De Conservação E Restauro*, 1, 93-112. <https://doi.org/10.34618/ecr.1.3168>
- [78] Cruz, A. J. (2005). A pintura de Columbano segundo as suas caixas de tintas e pincéis. *Conservar Património*, 1, 5-19.
- [79] Mora, P., Mora, L. & Philippot, P. (1984). *Conservation of Wall Paintings*, Butterworths, 56-68.
- [80] La Nasa, J., Campanella, B., Sabatini, F., Rava, A., Shank, W., Lucero-Gomez, P., De Luca, D., Legnaioli, S., Palleschi, V., Colombini, M. P., Degano, I., Modugno, F. (2021). 60 years of street art: A comparative study of the artists' materials through spectroscopic and mass spectrometric approaches, *Journal of Cultural Heritage*, 48, 129-140. <https://doi.org/10.1016/j.culher.2020.11.016>
- [81] Berrie B. H. (2012). Rethinking the history of artists' pigments through chemical analysis. *Annual review of analytical chemistry* (Palo Alto, Calif.), 5, 441-459. <https://doi.org/10.1146/annurev-anchem-062011-143039>
- [82] Fanost, A., Gimat, A., de Viguerie, L., Martinetto, P., Giot, A., Clémancey, M., Blondin, G., Gaslain, F., Glanville, H., Walter, P., Mériguet, G., Rollet, A. & Jaber, M. (2020). Revisiting the identification of commercial and historical green earth pigments.

Colloids and Surfaces A: Physicochemical and Engineering Aspects, 584, 124035.
<https://doi.org/10.1016/j.colsurfa.2019.124035>

[83] Tomasini, E., Castellanos-Rodríguez, D., Gómez, B.A., de Faria, D.L.A., Rúa-Landa, C., Siracusano, G., & Maier, M.S. (2016). A multi-analytical investigation of the materials and painting technique of a wall painting from the church of Copacabana de Andamarca (Bolivia), *Microchemical Journal*, 128, 172-180, <https://doi.org/10.1016/j.microc.2016.04.020>

[84] Aceto, M. (2021). Pigments—the palette of organic colourants in wall paintings. *Archaeol Anthropol Sci* 13, 159 <https://doi.org/10.1007/s12520-021-01392-3>

[85] Alter, M., Binet, L., Touati, N., Lubin-Germain, N., Le Hô, A. S., Mirambet, F., & Gourier, D. (2019). Photochemical origin of the darkening of copper acetate and resinate pigments in historical paintings. *Inorganic chemistry*, 58 (19), 13115-13128. <https://doi.org/10.1021/acs.inorgchem.9b02007>

[86] Rosi, F., Miliani, C., Borgia, I., Brunetti, B. and Sgamellotti, A. (2004), Identification of nineteenth century blue and green pigments by in situ x-ray fluorescence and micro-Raman spectroscopy. *J. Raman Spectrosc.*, 35, 610-615. <https://doi.org/10.1002/jrs.1180>

[87] Holakooei, P., Karimy, A-H. & Nafisi, G. (2018) Lammerite as a Degradation Product of Emerald Green: Scientific Studies on a Rural Persian Wall Painting, *Studies in Conservation*, 63 (7), 391-402, <https://doi.org/10.1080/00393630.2017.1419658>

[88] Lama, E., Prieto-Taboada, N., Etxebarria, I., Bermejo, J., Castro, K., Arana, G., Rodríguez-Laso, M. D. & Madariaga, J. M. (2021). Spectroscopic characterization of xx century mural paintings of punta begoña's galleries under conservation works, *Microchemical Journal*, 168, 106423. <https://doi.org/10.1016/j.microc.2021.106423>

[89] Piqué, F., Derrick, M., Parker, A., Schilling, M., & Scott, D. (1995). Original Technique of the Mural America Tropical by David Alfaro Siqueiros. *MRS Proceedings*, 352, 365-371. <https://doi.org/10.1557/PROC-352-365>

[90] Keijzer, M. D. (2014). The delight of modern organic pigment creations. In: van den Berg, K. J.; Burnstock, A.; de Keijzer, M.; Krueger, J.; Learner, T.; Tagle, A.; & Heydenreich, G. (Eds.) *Issues in contemporary oil paint*, Springer, Cham., 45-73. http://dx.doi.org/10.1007/978-3-319-10100-2_4

[91] Saverwyns, S. (2010). Russian avant-garde... or not? A micro-Raman spectroscopy study of six paintings attributed to Liubov Popova. *Journal of Raman Spectroscopy*, 41 (11), 1525-1532. <https://doi.org/10.1002/jrs.2654>

[92] Defeyt, C., Mazurek, J., Zebala, A., & Burchett-Lere, D. (2016). Insight into Sam Francis' painting techniques through the analytical study of twenty-eight artworks made between 1946 and 1992. *Applied Physics A*, 122 (11), 1-6. <https://doi.org/10.1007/s00339-016-0485-x>

[93] Lutzenberger, K., & Stege, H. (2009). From Beckmann to Baselitz-towards an improved micro-identification of organic pigments in paintings of 20th century art. *Preservation Science*, 6, 89-100.

- [94] Lomax, S. Q. (2005). Phthalocyanine and quinacridone pigments: their history, properties and use. *Studies in Conservation*, 50 (sup1), 19-29. <https://doi.org/10.1179/sic.2005.50.Supplement-1.19>
- [95] Eastaugh, N., Walsh, V., Chaplin, T., & Siddall, R. (2013). *Pigment compendium: optical microscopy of historical pigments*. Elsevier, -XIV <https://doi.org/10.4324/9780080454573>
- [96] Petrucci, R. H., Harwood, W. S. & Herring, F. G. (2003) *Química General* (8th Ed.) Pearson Educación, 985-1023.
- [97] Housecroft, C. E. & Sharpe, A. G. (2005) *Inorganic Chemistry* (2nd ed.). Pearson Education. 570-571.
- [98] Nagose, S., Rose, E., & Joshi, A. (2019). Study on wetting and dispersion of the Pigment Yellow 110. *Progress in Organic Coatings*, 133, 55-60. <https://doi.org/10.1016/j.porgcoat.2019.04.045>
- [99] Oyarzún, J. M. (2000) *Pigment Processing. Physico-chemical Principles*. Vincentz, 75.
- [100] Mora, P., Mora, L. & Philippot, P. (1984). *Conservation of Wall Paintings*, Butterworths, 165-215.
- [101] Ware, M. (2008). Prussian blue: artists' pigment and chemists' sponge. *Journal of Chemical Education*, 85 (5), 612. <https://doi.org/10.1021/ed085p612>
- [102]. Mora, P. (1974). *Causes of deterioration of mural paintings*. International Centre for the Study of the Preservation and the Restoration of Cultural Property, 11-30. https://www.iccrom.org/sites/default/files/2018-02/1974_mora_causes_deterioration_111773_light.pdf
- [103] Alonso-Villar, E. M., Rivas, T., & Pozo-Antonio, J. S. (2021). Resistance to artificial daylight of paints used in urban artworks. Influence of paint composition and substrate. *Progress in Organic Coatings*, 154, 106180. <https://doi.org/10.1016/j.porgcoat.2021.106180>
- [104] Comelli, D., MacLennan, D., Ghirardello, M., Phenix, A., Schmidt Patterson, C., Khanjian, H., ... & Nevin, A. (2019). Degradation of cadmium yellow paint: New evidence from photoluminescence studies of trap states in Picasso's *Femme (Époque des "Demoiselles d'Avignon")*. *Analytical chemistry*, 91(5), 3421-3428. <https://doi.org/10.1021/acs.analchem.8b04914>
- [105] Thapa, B. S. (1984). Deterioration and restoration of painting. *Ancient Nepal*, 37-40. https://himalaya.socanth.cam.ac.uk/collections/journals/ancientnepal/pdf/ancient_nepal_79_04.pdf
- [106] Subbaraman, S. (1993). Conservation of mural paintings. *Current Science*, 64 (10), 736-753. <http://www.jstor.org/stable/24122234>

- [107] Ciferri, O. (1999). Microbial Degradation of Paintings. *Applied and Environmental Microbiology*, 65 (3), 879-885. <https://doi.org/10.1128/AEM.65.3.879-885.1999>
- [108] Allsopp, D., Seal, K., & Gaylarde, C. (2004). Introduction. In Allsopp, D., Seal, K., & Gaylarde, C. (Eds.) *Introduction to Biodeterioration*. Cambridge University Press, 1-10. <https://doi.org/10.1017/CBO9780511617065.003>

Chapter 3: Case Study and Methodology

3.1. Introduction to the Maritime station of Alcântara: geographic location and some notes about the history of the construction and of the surrounding environmental conditions

The Maritime Station of Alcântara is in Lisbon, in the parish of Alcântara, near the bank of the Tagus River (coordinates: 38,699285°, -9,174199°; WGS84) (Figure 1) [1].

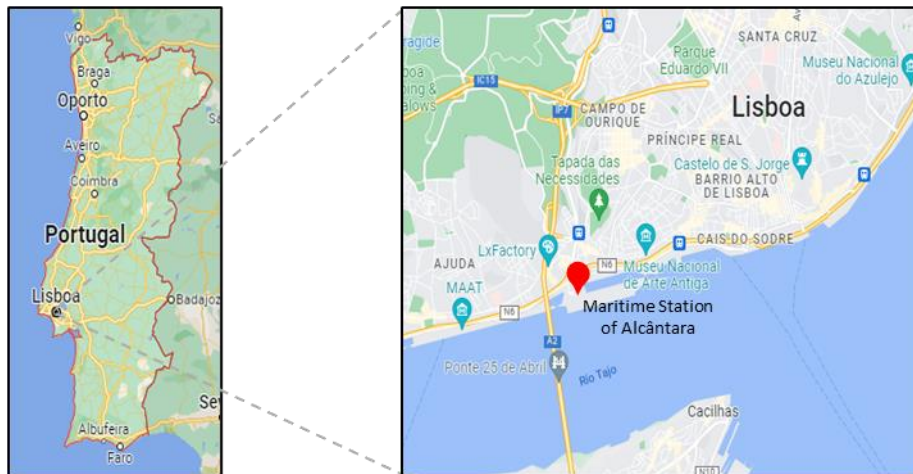


Figure 1. Geographic location of the Maritime Station of Alcântara. Images adapted from Google Maps 2022 © all rights reserved.

The Maritime station was part of the riverside area urbanization project that started in 1926 [2]. The commission for the construction of the building was required due to the new law, imposed in 1928, where all the ocean liners that passed through Lisbon had to be docked [2,3], in addition to the fact Lisbon gained popularity as a port of call and destination [3].

In 1934, the construction of the Maritime Stations was assigned to the architect Porfírio Pardal Monteiro [2]. He designed the Maritime Station of Alcântara between 1934 and 1939, with the misfortune that some of the architectural elements needed to be removed due to budget constraints [2]. The preparatory works for the construction started in 1939, and the Maritime Station of Alcântara was built between 1940 and 1943 (Figure 2) [1,2].



Figure 2. Maritime Station of Alcântara (1943). On the left: facade over the ground. On the right: facade over the sea. Images retrieved from: [3].

According to Bandeira (2000), the materials used for the construction were reinforced concrete, mixed masonry, and brickwork, painted plaster, limestone stonework, marble, wood and cast iron [1].

The Maritime Station of Alcântara was inaugurated on July 17, 1943. However, the mural paintings were not executed by that time. Almada Negreiros started the process to make the mural paintings in 1943 and finished the eight panels in 1945 [3].

The construction of the Maritime Station occurred when Alcântara was not an industrial area anymore. According to the historian Frédéric Vidal (2014) and Magda Pinheiro (2008), from 1840 to the 1890s Alcântara was considered one of the most important industrial areas of Lisbon, being the textile, metallurgic, mechanic, and chemical industries the main ones [4,5]. The industrial expansion in the eastern part of Lisbon, as well as the migration of the textile industries to the northern part of Portugal, converted Alcântara from an industrial area to an industrial heritage place [5].

Frédéric Vidal (2014) mentioned the promotion of industrial heritage in Alcântara starting in the 1980s [4]. From the 1920s onwards, Alcântara was considered one of the “popular neighborhoods”, as mentioned by Frédéric Vidal in 2015 [6]. Nowadays, this parish is one of the new touristic attractions of the capital, being the LX Factory, a former industrial area from the 19th century, one area for art galleries, design companies and leisure activities [6].

In terms of the location and climate of the city, Lisbon is located on the Atlantic coast of the European southern part, next to the northern edge of the Tagus estuary (38°44' latitude North and 9°8' longitude West) [7]. The Mediterranean and Atlantic influences generate high temperatures and low rainfall in summer times; and high rainfall, with dry and cold winds from the Peninsula's interior, during winter times [8].

The meteorologist Pedro M. A. Miranda, and collaborators, stated that from 1946 to 1975 the main temperature cooled down, followed by fast warming between 1976 and 2000 [9]. This last period was characterized by an important rainfall reduction [9]. The Instituto Português do Mar e da Atmosfera reported that, between 1971 and 2000, the maximum temperatures were between 28.5 °C in August, and 13.1°C in January; and the minimum temperatures between 16.1 °C in August and 6.7 °C in January [10]. Regarding relative humidity, the same institute reported, from 1971 to 2000, an interval range of relative humidity between 62% to 84% [10]. In 2022, Silva, et al. stated that Lisbon is subjected to heatwaves where the maximum temperatures are over 35°C [11]. The year of 2018, considered one of the hottest years of current times, is an example of the previous mentioned, where five heatwaves were reported between summer and autumn [12].

An important topic to mention is the presence of air pollutants in Lisbon. According to Mojardino et al. (2018) particulate matter of diameter below 10 µm (PM₁₀) and nitrogen dioxide (NO₂) are the pollutants of biggest concern in Lisbon [13], because their concentrations have exceeded the limits stated by Directive 2008/50/EC [13,14]. In cities, PM can be produced by the combustion of solid fuels and the erosion of the road due to traffic [14]. Emissions of NO₂ and NO_x are related to fossil-fuel combustion, either by stationary sources or motor-based vehicles [14]. Soares et al.

(2021) mentioned between 2010 and 2018, there was an increment in the concentration of ozone (O_3) in the metropolitan area of Lisbon. The presence of ozone can be the product of the reaction between nitrogen oxides and volatile organic compounds (VOC) when exposed to sunlight [15, 16].

3.2. Identification of the mural paintings and criterium of selection for in loco and laboratory analysis

The eight mural paintings are located in the waiting room of the Maritime Station, on the western and eastern walls of the first floor (Figure 3a/b). Both the eastern and western walls have 4 panels of 7.2 m high per 3.8 m wide each. The western wall has the triptych depicting the legend of Nau Catrineta (Panels 1, 2 and 3), and the

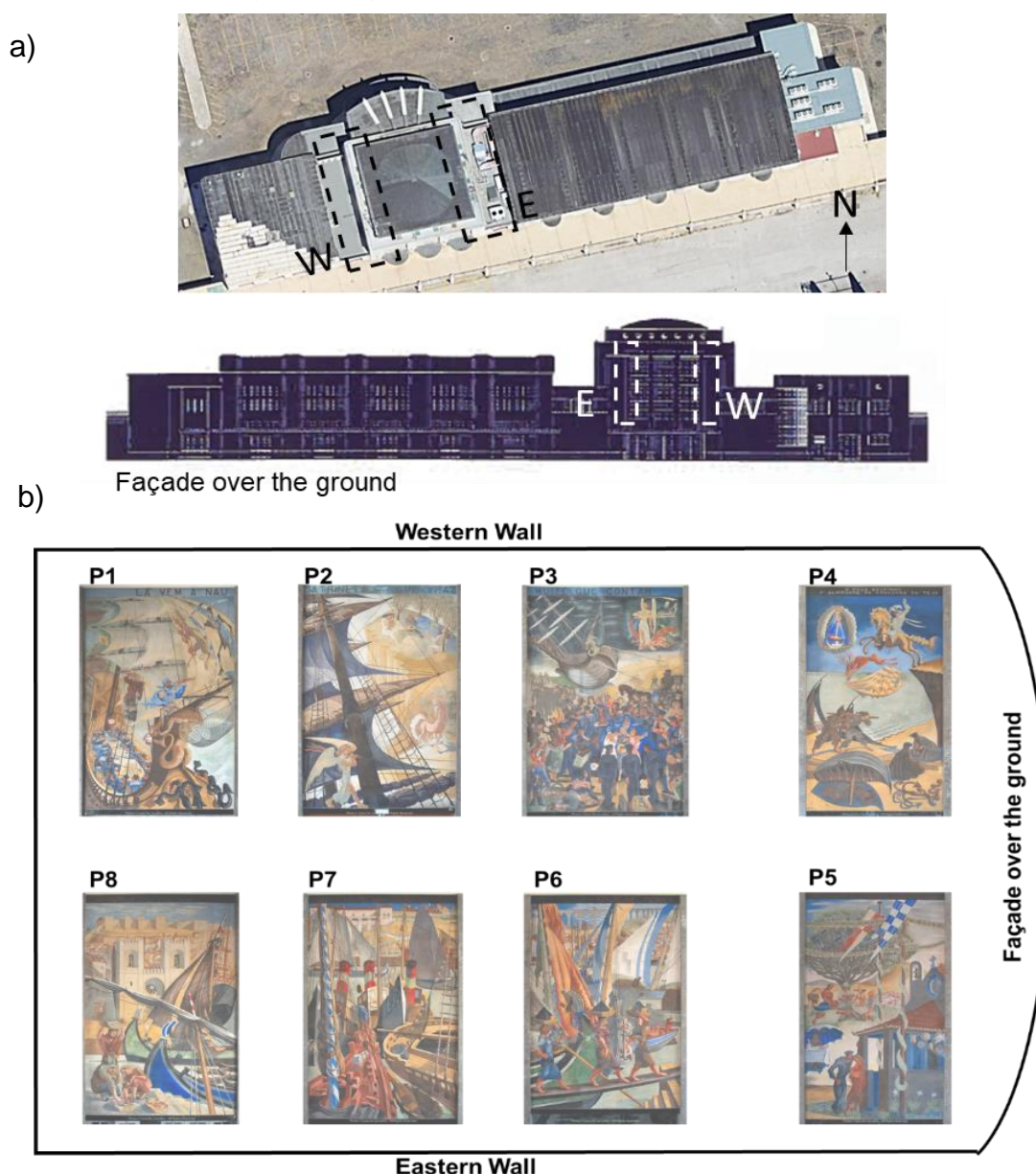


Figure 3. a) Location of the Western and eastern walls of the waiting room from satellite view and from the façade over the ground. The white and black squares indicate the location of the eight mural paintings inside the waiting room. Images retrieved from: [1, 17], b) Disposition of the eight mural paintings in the waiting room. Images adapted from Guta Carvalho-June 2020 © all rights reserved

individual painting of the miracle of Dom Fuas Roupinho (Panel 4). The eastern wall has the individual painting and represents a picnic in a procession day (Panel 5) and finally, the second triptych represents everyday life in Lisbon riverside (Panels 6, 7 and 8).

As mentioned in the first chapter (1.1) the focus of the research was on the green paint layers. Figure 4 shows the contour line drawing of the eight panels from the Maritime Station of Alcântara; the areas in green signalize the paint layers where green hues were detected. Light green hues are predominant in the painting color palette, and it covers an extensive area in the panels.

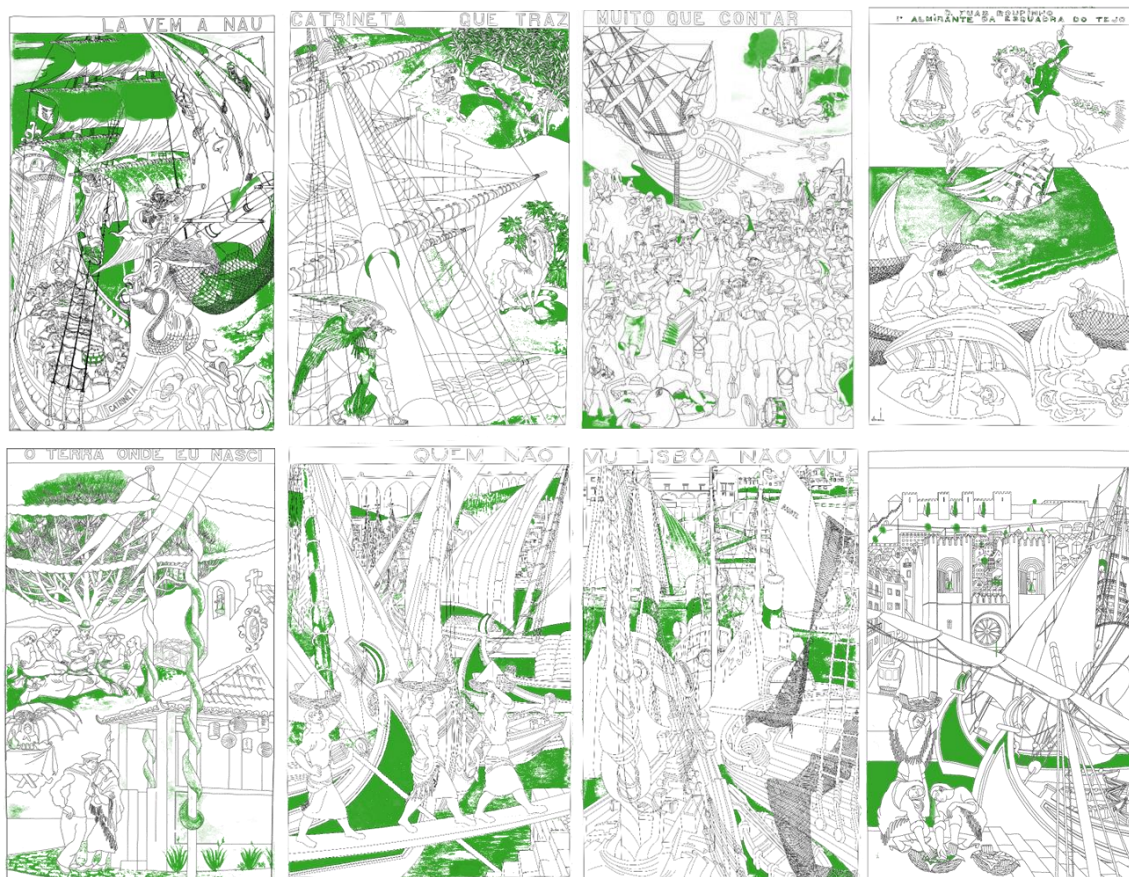


Figure 4. Contour line drawing of the mural paintings of the Maritime Station of Alcântara. The green areas represent the paint layers where green hues were detected.

In fact, the light green paint layers present a high degree of flaking and loss of cohesion. The state of conservation of the light green hues was mentioned in the diagnostic survey of the eight mural paintings performed in 2021 [18]. However, there was no deeper research about the deterioration factors that could affect the green paint layers. Figure 5 shows examples of light green deteriorated areas found by visual inspection, which are mainly concentrated in panels 2, 3, 5, 6, and 8. The purpose of this project was to study the green painting palette, the painting technique used in the green areas, and identify the mean deterioration factors that are damaging the green paint layers. The state of conservation of the green paint layers, analyzed during the study, can be found in Appendix I.



Figure 5. Photographic documentation in visible and visible ranking light of deteriorated paint layers.

3.3. Identification of powdered green pigments

As stated in the introduction, a set of eleven powdered green pigments was analyzed as a complement to the study of the green paint layers (Table 1): Three pigments were purchased in 2005 in old drugstores in the Alentejo region; four were found at Almada Studio from Le-Franc and Osaka; two are from the former Tijomel ceramic manufacture (1941-1992) and finally, two were purchased in 1998 and 2022 in art known suppliers (Windsor & Newton and Kremer Pigmente).

The analysis of these pigments provided a better understanding of the kind of green pigments that were available for artistic purposes in Portugal during the 20th century. Besides, it helped to match up and see if there is any kind of interrelation with the pigments found at Almada studio and on the green paint layers at the maritime station of Alcântara.

Table 1. Description of the green powdered pigments analyzed.

Pigments Ref.	Pigments label	Manufacturer	Date of purchase
a) Pigments retrieve from Almada studio			
LF22	Vert à la chaux	LeFranc-Paris	1938/39 (hypothesis)
LF23	Vert emeraude	LeFranc-Paris	1938/39 (hypothesis)
LF30	Vert à la chaux	LeFranc-Paris	1938/39 (hypothesis)
O1	Viridian	Osaka -Japan	before 1979
B) Pigments from other sources			
WN 0210720	Windsor green	Windsor and Newton	1998
FA 5	Royal green	Unknown -Old Drugstore-Ferreira do Alentejo	2004
FA 4	Vert à la chaux [altered]	Unknown -Old Drugstore-Ferreira do Alentejo	2004
FA 3	Vert à la chaux	Unknown -Old Drugstore-Ferreira do Alentejo	2004
5W	Chrome Green 665 GS	Wengers LTD	1941-1992*
13 BCW	Chrome Green "O" W34	Blyte color works	1941-1992*
K41700	Veronese Green Earth	Kremer	2015

* These pigments were used as colours at the tijomel ceramic manufacture that was active between 1941 and 1992

3.4. Experimental conditions

The methodology to carry out the in loco non-invasive and laboratory analyses is shown in the flow chart of Figure 6. The principles of each technique and the analytical conditions will be presented in the following subsections.

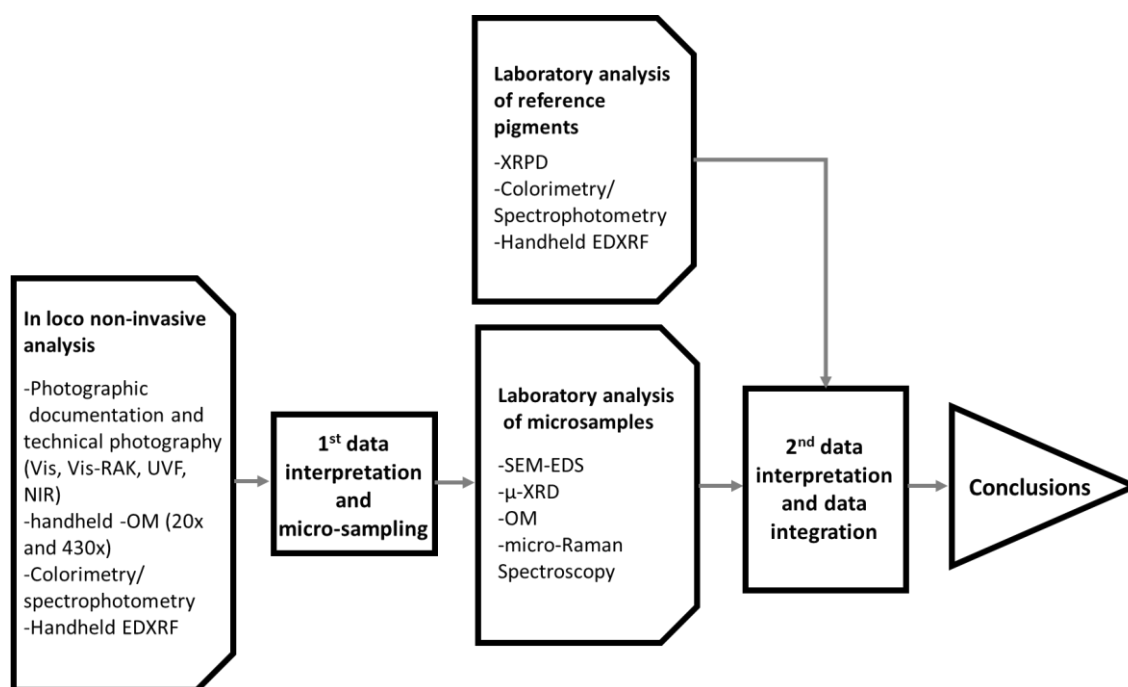


Figure 6. Methodology flow chart

3.4.1 In loco non-invasive analyses

3.4.1.1. Photo documentation and technical photography (TP)

Technical and material research in loco began with a thorough examination of the painting features and the current painting condition. The first photographic documentation was carried out in the visible light range (Vis) and in visible raking light (Vis-RAK) with a high-resolution digital camera for a global overview of the paintings and details of the green paint layers. This first record allowed a comprehensive insight into the current situation and allowed the selection of the eleven areas highlighted in Figure 7 for technical photography, non-invasive analysis in loco and microanalysis in the laboratory.

Technical photography (TP) generically comprises a collection of broadband spectral images acquired with a modified camera for full spectrum using various light sources and filters [19]. TP in art and conservation is very useful as a first approach to discriminate and map different types of pigments, organic materials that have been used originally or in past interventions (e.g., adhesives, retouching materials), but also underdrawings made with absorbent materials [19].



Figure 7. Areas selected for the in loco and laboratory analyses. Images adapted from Guta Carvalho (June 2020 © all rights reserved).

The images of the selected paint areas were acquired at 360-400 nm (UV), 400-780 nm (Vis) and 1000 nm (NIR). The photographic records in visible (Vis), visible raking (Vis-RAK) and Ultraviolet fluorescence induced in the visible range (UVF) were made with a Nikon D3200 digital camera with 24 Mpx and an objective 18-55 mm f:3.5-5.6 GIL. Photographic records in the near-infrared (NIR) were made with a transformed Nikon D3200 digital camera with 24Mpx and an objective 18-55 mm f:3.5-5.6 GIL.

In what concerns the light sources, halogen lamps (1000W-230V) were used for Vis, Vis-Rak and NIR. Raking light at 10-15° from the painting surface was used to observe and record flaking, and other features related to the artist's procedure, such as brushstrokes, type of incisions, tool marks and mortar joints.

UVF photography was used to ascertain the presence of organic matter associated with original painting materials and past intervention products used to fix the flaking paint layers.

UVF photography was performed using a Labino® MPXL UV PS135 light (35W PS135 UV Midlight 230V) with a UV filter included (310-400nm and a peak at 365nm), a midlight distribution angle of 20° and a start-up time full power after 5-15 seconds.

3.4.1.2. Handheld Optical Microscopy (h-OM)

Optical microscopy consists in the magnification of small objects or areas to study specific features that are not possible to see by the naked eye [17]. For mural painting studies, it is possible to analyze in loco technical and material details such as the type of brushstrokes and pigment mixtures, but also deterioration features such as fissures, stains, and salt formation. h-OM enabled the preliminary assessment of the mural panels and was essential to select the areas for non-invasive analysis and for micro-sampling.

In light optical microscopy, a set of lenses is fixed in a hollow tube to magnify an object, using visible light as a source of illumination [17]. For digital microscopes, a camera receives the magnified picture and displays it on a computer screen. In this research handheld OM was carried out by using two digital microscopes DinoLite ProX AM 4000. Both digital microscopes were used for each punctual area of analysis. The first one was used in magnification 20x for the mapping of the paint layer, and the second one in magnification 434x to analyze the pigment particles. Punctual areas in poor state of preservation were not analyzed to avoid the risk of damaging the paint layer.

3.4.1.3. Colorimetry and Spectrophotometry

By this non-invasive technique, we can quantify the perception of color by measuring the light transmission or reflectance of a material in the visible light range [18, 19]. The technique was carried out to analyze and document the current green painting palette of the case study.

Color is a visual response that differentiates materials by the properties of the light reflected or transmitted [18]. Given the concept of color, colorimetry is the science that studies color to represent it by numerical parameters [20]. In 1976, the International Commission on Illumination (CIE) designed a new system called *CIELAB*, based on additive color mixture, to manage the color parameters in a three-dimensional space [21]. The parameters for the CIELAB space are L^* , a^* and b^* [20]:

- L^* (z-axis) represents the lightness of the material: it goes from 100 (perfect reflecting diffuser) to zero (no reflectance).
- a^* and b^* are coordinates that describe the redness ($+a^*$) and the greenness ($-a^*$) attributes, represented along the x-axis, while the yellowness ($+b^*$) and blueness ($-b^*$) attributes are represented along the y-axis (Figure 8).

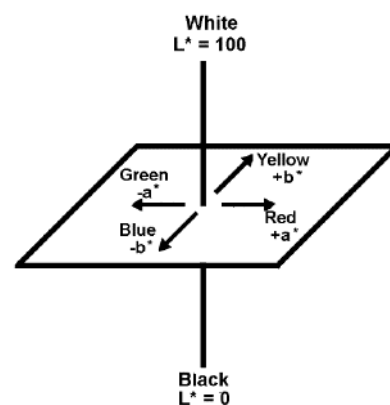


Figure 8. CIE Lab Color space chart.
Image retrieved from: [22]

Spectrophotometry, on the other hand, measures the interaction of electromagnetic radiation with matter [23]. The measuring consists of irradiating the sample with a continuous wavelength light source and detecting the relative intensity of electromagnetic radiation reflected or transmitted by the material at individual wavelengths of the spectrum [20]. The results can be represented in a chart of reflection (or transmission) as a function of wavelength, giving what is called the spectral curve [20]. When spectrophotometry is made in the visible light range, the bands presented in the spectral curve describe the color composition of the sample. Table 2 presents the spectral colors with their respective wavelength range, according to Artioli (2010) [24].

Table 2. Wavelength range of colors in the visible light spectrum.

Color	Wavelength (nm)
Red	700–635
Orange	635–590
Yellow	590–560
Green	560–490
Blue	490–450
Violet	450–400

A total of 47 points in the green pictorial layers were measured using a Data Color Check Plus II (Lawrenceville, NJ), equipped with an integrating sphere and applying the following parameters: diffuse illumination 8 viewing (following the CIE standard No. 15.2. Colorimetry), SCE and Standard Illuminant/Observer D65/10. The aperture size was USAV (Ø5 mm). The spectral curves in the visible range were acquired from 360 to 750 nm with a bandwidth of 10 nm. The results were obtained in the CIE L*a*b color space.

3.4.1.4 Handheld energy dispersive X-ray fluorescence (h-EDXRF)

Handheld EDXRF is a non-invasive technique used to analyze the main elemental composition of materials.

In XRF, X-rays, a part of the spectrum of electromagnetic radiation with a wavelength from 10 nm to 0.01 nm, are generated in an X-ray tube and interact with the sample. The incident X-rays can be absorbed by the sample. When the energy of the incident X-rays is the same as the binding energy of the inner-shell electrons, one of these electrons can be expelled from the atom, creating a vacancy, and causing the atom to become very unstable [25]. To recover its stability, one of the electrons from the outer shells will occupy the vacancy, leaving a new vacancy in its shell, and a photon will be released with an energy equal to the difference between the binding energies of their respective atomic shells and with the wavelength of an X-ray [25]. This energy is unique for each element, and, as such, the X-ray produced will be characteristic of the element present in the sample [25]. Therefore, the elemental composition of a sample can be determined by analyzing the energy of the characteristic X-rays from the

sample. The electronic occupation of vacancies continues until the atom recovers its stability [25].

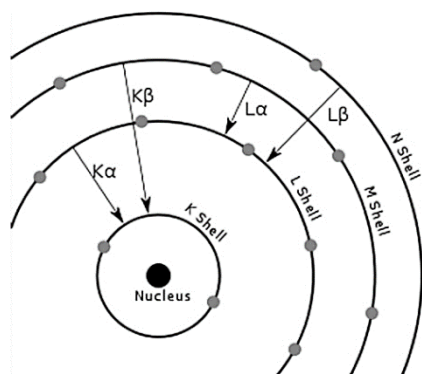


Figure 9. Electron transitions in X-ray fluorescence. Image retrieved from: [25].

It is important to point out that the incident X-rays have a higher energy than the characteristic X-rays emitted by the sample [26], and that the electronic shells and the electron transitions are labelled according to Figure 9 [25]. As such, if a vacancy is created in the K shell, and if an electron from the L shell occupies the vacancy, the transition is called $K\alpha$; however, if an electron from the M shell occupies the vacancy, the transition is called $K\beta$ and so on [25].

Handheld EDXRF was carried out to analyze the bulk elemental composition of the green paint layers. For mural painting, the penetration depth for XRF studies is usually uncertain due to the complexity of composition in artworks. It depends on both the energy of the X-ray fluorescence, and the critical penetration depth, which is related to the density and elemental composition of the sample [27]. The lighter the element, the lower the energy of X-ray fluorescence, and the more difficult it is to detect. Therefore, the critical penetration depth in light elements is in the order of micrometers, while the one for heavier elements, like lead, is around 1-10 mm [27].

The last statement is important to mention since, in the present work and the previous one regarding the mural paintings of the Maritime Station of Alcântara, both light and heavy elements were found to be distributed in a non-homogeneous way [18]. For this case study, it is not possible to estimate the penetration depth of h-EDXRF.

A Bruker™ Tracer III SD® handheld X-ray fluorescence spectrometer (Bruker, Germany), equipped with a rhodium target delivering a polychromatic X-ray beam of 3×3 mm and a silicon drift detector (XFlash®) was used to measure 50 paint areas covering the green painting palette. All spectra were recorded using S1PXRF software (Bruker™) and processed using Artax (Bruker™) software to obtain semi-quantitative data.

For the paint layers, the spectra were obtained using a voltage and a current intensity of 40 kV and 30 μ A, respectively, with an acquisition real time of 30 s. The acquisition real time was settled regarding the number of analyses and the time restrictions during the in loco study.

For the reference pigments, the spectra were obtained with the same equipment, using a voltage of 40 kV, and a current of 30 μ A at normal atmosphere, with an acquisition real time of 60 s.

3.4.2. Laboratorial analysis of microsamples

Microanalyses were carried out at Hercules laboratory on 21 microsamples collected from deteriorated paint layers (flaking and powdering areas) and paint layers in a better condition (sampling location in attachment). The goals were to study the

stratigraphy of the paint layer and the chemical and mineralogical composition of the pictorial layers; enabling to ascertain the painting technique and diagnose the state of conservation of the paint layers together with the deterioration features.

3.4.2.1 Optical Microscopy (OM)

Optical microscopy in Vis e UV mode was carried out in two steps on the microsamples:

- 1) overview of the micro fragments without any previous treatment, to study morphology, topography, the presence of salts and pigment particles, and deterioration features like powdering, fissures, and disaggregation,
- 2) analysis of cross-sections to study the stratigraphy of the paint layer (number of layers, thickness, appearance), to evaluate the possible presence of organic material, and to study the elemental composition and elemental distribution, which can provide information about the painting technique.

For the first step, 3D magnified images of the micro fragments were acquired with an HRX-01 HIROX Digital Microscope equipped with a 5 MP sensor to suit 4 K resolution and motorized HR lenses. The HR-5000E lens at 0° of inclination related to the normal were used to observe the object at 140x, 200x, 400x, 800x and 1000x magnifications under the top lighting system (96% intensity).

For the second step, the analyses of the cross-sections were carried out with a Leica DM2500M reflected light optical microscope in dark field illumination mode at 100x, 200x and 500x magnification; the photographs were acquired with the Leica MC 170HD digital camera equipped with the corresponding Leica software. UV radiation, produced by a high-pressure burner 103W/2 UV lamp with an excitation filter BP 340-380, a 400 dichromatic mirror and a suppression filter Lp425, size K was used to spot the presence of organic materials.

3.3.2.3 X-ray Diffraction (XRD)

X-ray diffraction is a technique that uses the interaction of X-rays and a sample to identify its mineralogical composition [25].

According to Snyder (1999), diffraction is a phenomenon where electromagnetic waves, after being scattered from an object, interfere constructively and destructively with each other [28]. In 1913, William Henry Bragg and William Lawrence Bragg pointed out that the diffraction patterns are related to the atomic disposition within the crystals, and they made a mathematic model to describe that arrangement of atoms by the X-ray diffraction patterns [29]. Figure 10 describes the phenomenon

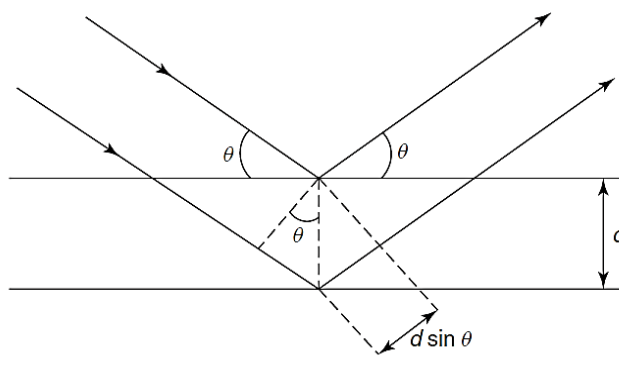


Figure 10. X-ray diffraction phenomenon. Image retrieved from: [25].

when two X-ray waves of equal wavelengths, get to adjacent layers. The wave path to reach the upper layer is shorter than the wave path to reach the lower layer, by a distance of $2d\sin\theta$. The two incident waves will be in phase if and only if the difference between the paths is equal to a multiple of the X-ray wavelength according to the following equation:

$$n\lambda = 2d\sin\theta$$

The former equation is denoted as Bragg's Law [29]. Therefore, by knowing the wavelength, and the angle of incidence of the X-rays, it is possible to determine the distance between layers of atoms. This phenomenon is specific for X-ray radiation since its wavelength is around the magnitude of the distance between planes of atoms [25].

For the analysis, the diffractogram patterns of a sample are compared with an XRD database to identify the crystalline structures present. In this case, XRD was used to analyze powdered samples (XRPD – X-ray powder diffraction) and fragments or micro fragments (micro-XRD or μ -XRD) in order to ascertain the mineralogical composition of the different paint layers.

Micro-XRD was performed with a Bruker D8 Discover[®] diffractometer with a Cu K α radiation and a 0.3 mm collimator. The micro fragments were mounted on a zero-background sample holder. The diffractograms were collected by using an angular range of 3–75°. The step time was adjusted for each sample, taking into account their size and complexity, in order to guarantee the identification of the crystalline phases present. The DIFFRAC.SUITE EVA[®] software and the International Centre for Diffraction Data PDF-2 database were used for the identification of the crystalline phases.

A Bruker D8 Discover[®] diffractometer with a Cu K α radiation was also used to identify the mineralogical composition of the pigments in powdered form (Chapter 3.3). The samples were placed in powder specimen holders and analyzed in an angular range of 3°–75° 2 θ , step size of 0.05°, and step time of 1 s. The same databases were used for the identification of the crystalline phases present.

3.3.2.4 Scanning Electron Microscopy with Energy Dispersive Spectroscopy (SEM-EDS)

Scanning electron microscopy takes advantage of the wave-particle duality of electrons, and the fact that accelerated electrons have a shorter wavelength than visible light, enabling the interaction with smaller surfaces (from micrometers to nanometers) and giving an image after the transduction of signals [30]. Instead of a light beam, SEM microscopes use a high-energy electron beam to scan the area of study. The particles generated from the interaction of the sample with the electron beam are then collected and detected.

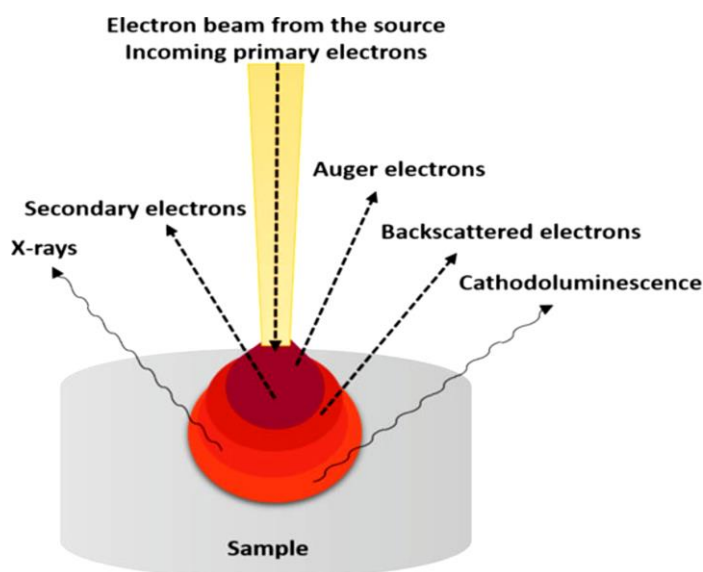


Figure 11. Outcome species during the interaction of the electron beam with the sample. Image retrieved from [31]

Figure 11 shows the particles that can be produced when the electron beam interacts with the sample. They provide information about specific properties of the sample, and require specific detectors to be analyzed. Given the nature of this study and the instrument used, only X-rays, backscattered electrons and secondary electrons will be described in the following paragraphs.

Backscattered electrons and secondary electrons are the basis for SEM imaging [30]. According to Akhtar et al. (2018)

backscattered electrons are incident electrons that are elastically scattered due to electromagnetic repulsions [31]. They remain with the same energy, and they provide information about the variations in surface composition, depending on the atomic density of the materials: the higher the atomic density of the material, the brighter the area on the image [32, 31].

Secondary electrons are formed during inelastic interactions with the primary or backscattered electrons, producing atomic ionization. They provide information about the topology and morphology of the sample [30].

Because of the ionization of atoms, the electrons reorganize to regain atom stability and characteristic X-rays are released [30]. The process that occurs during the generation of characteristic X-rays is identical to the one mentioned in the XRF section. Therefore, it is possible to perform elemental analysis of the areas of study by the detection of the characteristic X-rays emitted by the sample using energy dispersive spectroscopy (EDS).

It is important to note that one of the conditions to perform SEM analysis is that the sample must be conductive, otherwise, an accumulation of secondary electrons will create a positive charge in the sample and hence an unclear signal [30]. To analyze nonconductive samples, a thin conductive coating is generally applied. However, there is a way to avoid coating by using environmental or variable pressure scanning electron microscopy (E-SEM or VP-SEM). For this technique, a low-pressure vacuum is applied, and the charge generated by the secondary electrons is compensated by ionizing the gas molecules in the air [30].

SEM-EDS was applied to study the micro morphology and perform point analysis and elemental mapping of the samples, as well as to ascertain the presence of salt efflorescence. The samples were set in a carbon tape and analyzed with a variable pressure scanning electron microscope Hitachi S-3700N coupled to a Bruker™ XFlash 630M SDD EDS Detector®. The samples were analyzed in backscattering mode

(BSE) at low vacuum (40 Pa) using an accelerating voltage of 20 kV. The use of variable pressure equipment allowed the analysis of samples without coating.

3.3.2.6 Micro-Raman Spectroscopy

In micro-Raman spectroscopy, the molecular structure of a specimen is determined by analyzing its rotational-vibrational transitions during the Raman Effect, which is the inelastic scattering of electromagnetic radiation [33].

Usually, when a molecule does not absorb an incident photon, the photon is scattered without any loss of energy, denoted as Rayleigh scattering [33]. However, inelastic scattering can occur when part of the energy of the photon is absorbed because of the transition to a new rotational-vibrational state in the molecule, modifying the energy for the scattered photon [33, 34]. If the energy of the scattered photon is lower than the incident photon, the phenomenon is called Stokes Raman scattering. If the energy of the scattered photon is higher than the incident one, the phenomenon is called anti-Stokes Raman scattering (Figure 12) [35].

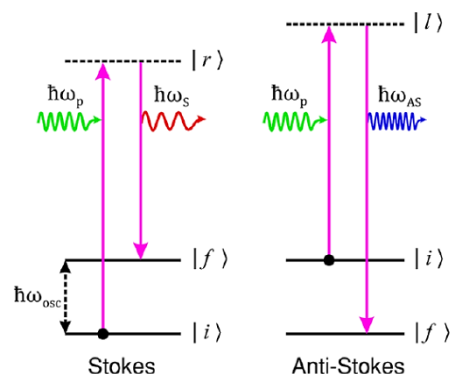


Figure 12. Stokes and anti-stokes scattering. Image retrieved from: [35].

The vibrational spectra are characteristic of every molecule, so we can distinguish between different inorganic, organic and biological species [36]. The condition to analyze a molecule by Raman spectroscopy is that it must be Raman active. A molecule is Raman active when its vibrations or rotations produce a change in the polarizability of the molecule [33].

As aforementioned, micro-Raman spectroscopy was performed at the Raman Research Group of Ghent University. In order to identify the pigments and minerals, ten microsamples were studied by using a confocal Raman Spectrometer Senterra R200-L, equipped with a red diode laser (785 nm) and a green Nd-YAG laser (532 nm), coupled with an Olympus microscope and a thermo-electrically cooled CCD spectrometer. The measuring time, laser power, and number of accumulations were set to obtain a good signal-to-noise ratio while avoiding thermal damage.

3.5 List of references

- [1]. Bandeira, F. (2000). *Gare Marítima de Alcântara / Salão e Auditório Almada Negreiros*. SIPA – Sistema de Informação para o Património Arquitetónico. http://www.monumentos.gov.pt/Site/APP_PagesUser/SIPA.aspx?id=5061
- [2] Monteiro, J. P. (2012) *Nove Décadas de Obra. Arte, Design e Técnica na Arquitectura do atelier Pardal Monteiro*, Volume 1. Universidade Técnica de Lisboa, Portugal. http://pardalmonteiro.com/Para_o_projeto_global-Volume_I.pdf

- [3] Lobo, P. R. (2014). Almada and the Maritime Stations: The portrait of Portugal that the dictatorship wanted to erase. *Revista de História da Arte – série W*, 2, 342-352.
- [4] Vidal, F. (2014) Urban transformation and diffusion of tourist practices: visiting Alcântara at the turn of the twentieth century, *Journal of Tourism and Cultural Change*, 12:2, 118-132. <https://doi.org/10.1080/14766825.2014.915086>
- [5] Pinheiro, M. (2008) Cidade e Caminhos-de-ferro. *Centro de Estudos de História Contemporânea Portuguesa*, 43.
- [6] Vidal, F. (2015) Sociability and collective action in a Lisbon workingclass neighbourhood: The social representations of Alcântara in the early twentieth century. *Portuguese Journal of Social Science*, 14(2), 143-156. https://doi.org/10.1386/pjss.14.2.143_1
- [7] Alpuim, T. and El-Shaarawi, A. (2009), Modeling monthly temperature data in Lisbon and Prague. *Environmetrics*, 20, 835-852. <https://doi.org/10.1002/env.964>
- [8] *Portugal. National circumstances relevant to adaptation actions* (2021). European Climate Adaptation Platform Climate-ADAPT. <https://climate-adapt.eea.europa.eu/en/countries-regions/countries/portugal>
- [9] Miranda, P., Coelho, M. F., Tomé, A., Valente, M., Carvalho, A., Pires, C., Pires, H.O., Pires, V. & Ramalho, C. (2002). 20th Century Portuguese Climate and Climate Scenarios. In Forbes, F. D. K. & Moita R. (Eds.) *Climate Change in Portugal: Scenarios, Impacts and Adaptation*. *Gradiva*, 27-38. https://www.researchgate.net/publication/257427857_20th_Century_Portuguese_Climate_and_Climate_Scenarios_in_Climate_Change_in_Portugal_Scenarios_Impacts_and_Adaptation
- [10] *Clima. Alterações Climáticas em Portugal* (2015). Instituto Português do Mar e da Atmosfera. <http://portaldoclima.pt/pt/>
- [11] Silva, R., Carvalho, A. C., Pereira, S. C., Carvalho, D., Rocha, A. (2022). Lisbon urban heat island in future urban and climate scenarios, *Urban Climate*, 44, 101218. <https://doi.org/10.1016/j.uclim.2022.101218>
- [12] Reis, C., Lopes, A., Correia, E., & Fragoso, M. (2020). Local Weather Types by Thermal Periods: Deepening the Knowledge about Lisbon's Urban Climate. *Atmosphere*, 11(8), 840. *MDPI AG*. Retrieved from <http://dx.doi.org/10.3390/atmos11080840>
- [13] Monjardino, J., Barros, N., Ferreira, F., Tente, H., Fontes, T., Pereira, P. & Manso, C. (2018) Improving Air Quality in Lisbon: modelling emission abatement scenarios, *IFAC-PapersOnLine*, 51 (5), 61-66. <https://doi.org/10.1016/j.ifacol.2018.06.211>
- [14] Santos, F. M., Gómez-Losada, A., & Pires, J. C. M. (2019) Impact of the implementation of Lisbon low emission zone on air quality, *Journal of Hazardous Materials*, 365, 632-641, <https://doi.org/10.1016/j.jhazmat.2018.11.061>

- [15] Soares, A. R., Deus, R., Barroso, C., & Silva, C. (2021). Urban Ground-Level O₃ Trends: Lessons from Portuguese Cities, 2010–2018. *Atmosphere*, 12(2), 183. <https://doi.org/10.3390/atmos12020183>
- [16] Atkinson, R. (2000) Atmospheric chemistry of VOCs and NO_x. *Atmospheric Environment*, 34, 2063-2101, [https://doi.org/10.1016/S1352-2310\(99\)00460-4](https://doi.org/10.1016/S1352-2310(99)00460-4)
- [17] Google (n.d.) [Gare Marítima de Alcântara] Retrieved November 11, 2022, from <https://goo.gl/maps/HaajQp9NtszDs3BL9>
- [18] Gil, M., Costa, M., Cvetkovic, M., Bottaini, C., Cardoso, A. M., Manhita, A., Días, C. & Candeias, A. (2021). Unveiling the mural painting art of Almada Negreiros at the Maritime Stations of Alcântara (Lisbon): diagnosis research of paint layers as a guide for its future conservation. *Ge-conservacion*, 20, 105-117. <http://dx.doi.org/10.37558/gec.v20i1.1027>
- [19] Cosentino, A. (2015). Practical notes on ultraviolet technical photography for art examination. *Conservar Património*, 21, 53-62. <http://dx.doi.org/10.14568/cp2015006>
- [17] Price, T. D. & Burton, J. H. (2011) *An Introduction to Archaeological Chemistry*. Springer Science+Business Media, 73-125.
- [18] Ohta, N. & Robertson, A. R. (2005) *Colorimetry*. Fundamentals and Applications. John Wiley & Sons, XV.
- [19] Cavaleri, T., Giovagnoli, A. & Nervo, M. (2013). Pigments and Mixtures Identification by Visible Reflectance Spectroscopy, *Procedia Chemistry*, 8, 45-54. <https://doi.org/10.1016/j.proche.2013.03.007>
- [20] Johnston-Feller, R. (2001). *Color Science in the Examination of Museum Objects: Nondestructive Procedures*. Getty Conservation Institute. 190-221. http://hdl.handle.net/10020/gci_pubs/color_science
- [21] Westland S, (2012). The CIE System. In: Chen, J., Cranton, W. & Fihn, M. (Eds.), *Handbook of Visual Display Technology*, Springer-Verlag. 139-146. https://doi.org/10.1007/978-3-319-14346-0_11
- [22] HUNTERLAB (1996) *CIE L*a*b* Color Scale*. Application Note, 8, 1-4. http://lib3.dss.go.th/fulltext/glass/GlassTheories/CIE_Lab_info.pdf
- [23] Germer, T. A., Zwinkels, J. C., Tsai, B. K. (2014) Chapter 2 - Theoretical Concepts in Spectrophotometric Measurements, In Germer, T. A., Zwinkels, J. C. & Tsai, B. K. (Eds.) *Experimental Methods in the Physical Sciences*, Academic Press, 46, 11-66, <https://doi.org/10.1016/B978-0-12-386022-4.00002-9>
- [24] Artioli, G. (2010). *Scientific Methods and Cultural Heritage: An introduction to the application of materials science to archaeometry and conservation science*, Oxford, 275. <https://doi.org/10.1093/acprof:oso/9780199548262.001.0001>
- [25] Stuart, B. H. (2007) *Analytical Techniques in Materials Conservation*. John Wiley & Sons, 229-242.

- [26] Shackley, M.S. (2011). An Introduction to X-Ray Fluorescence (XRF) Analysis in Archaeology. In: Shackley, M. (Eds.) *X-Ray Fluorescence Spectrometry (XRF) in Geoarchaeology*. Springer, 7-43. https://doi.org/10.1007/978-1-4419-6886-9_2
- [27] Potts, P. J. and West, M. (2008). Portable X-ray Fluorescence Spectrometry. Capabilities for In Situ Analysis. *The Royal Society of Chemistry*, 1-12.
- [28] Snyder, R. L. (1999). X-Ray Diffraction. In: Lifshin, E. (Eds.). *X-ray Characterization of Materials*. Wiley-VCH, 171-210.
- [29] Price, T.D., Burton, J.H. (2011). *Methods of Analysis. In: An Introduction to Archaeological Chemistry*. Springer, 73-126. https://doi.org/10.1007/978-1-4419-6376-5_4
- [30] Stuart, B. H. (2007) *Analytical Techniques in Materials Conservation*. John Wiley & Sons, 72-103.
- [31] Akhtar, K., Khan, S.A., Khan, S.B., Asiri, A.M. (2018). Scanning Electron Microscopy: Principle and Applications in Nanomaterials Characterization. In: Sharma, S. (Eds.) *Handbook of Materials Characterization*. Springer, 113-145. https://doi.org/10.1007/978-3-319-92955-2_4
- [32] Artioli, G. (2010). *Scientific Methods and Cultural Heritage: An introduction to the application of materials science to archaeometry and conservation science*, Oxford, 66-68. <https://doi.org/10.1093/acprof:oso/9780199548262.001.0001>
- [33] Stuart, B. H. (2007) *Analytical Techniques in Materials Conservation*. John Wiley & Sons, 136-156.
- [34] Vandenabeele, P. (2013) *Practical Raman Spectroscopy- An Introduction*. John Wiley & Sons, 1-7.
- [35] Jones, R.R., Hooper, D.C., Zhang, L., Wolverson, D. & Valev, V. K. (2019) Raman Techniques: Fundamentals and Frontiers. *Nanoscale Res Lett*, 14, 231. <https://doi.org/10.1186/s11671-019-3039-2>
- [36] Cialla-May, D., Schmitt, M. & Popp, J. (2019). Theoretical principles of Raman spectroscopy, *Physical Sciences Reviews*, 4 (6), 2019, 20170040. <https://doi.org/10.1515/psr-2017-0040>

Figure 2 shows the optical microscopy images in the visible range of six paint layers that are representative of the variations found. By OM is possible to recognize the paint layers are opaque, non-homogeneous, and present different green hues. All of them, except for the paint layer P2A 3, present evidence of salt neo formations distributed in uneven areas.

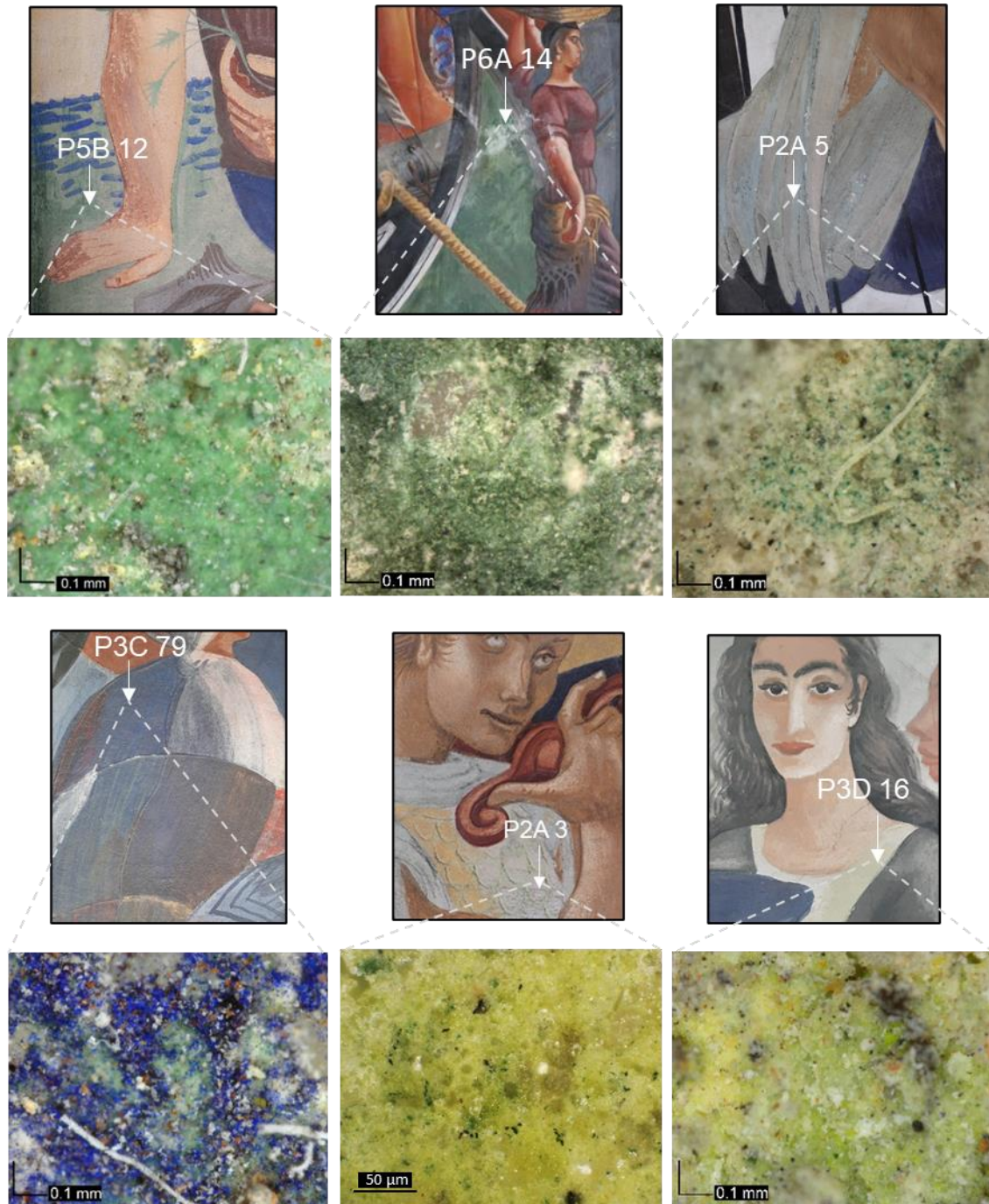


Figure 2. Handheld optical microscopy of five green paint layers from the Maritime Station of Alcântara at 430x magnification. The P2A 3 paint layer was analyzed by optical microscopy at 1000x magnification.

About the use of green pigments in the mural paintings, the green paint layer P5B 12 is part of the background that constitutes the grass, with light white irregular brushstrokes in the surroundings. The paint layer P6A 14 was used as the main

background color for the ship's bow. The paint layer P2A 5 comes from a light green brushstroke applied to highlight the undulations of the angel's robe. P3C 79 is a green area that was exposed below the blue brushstroke of the bag. The paint layer P2A 3 is a predominant yellow layer, mixed with a green pigment, over which a white highlight was applied. Finally, P3D 16 is a very thin and light green brushstroke applied to make a shadow in the yellow background.

The before mentioned shows Almada Negreiros made use of green pigments for the background, for the modification of the hue in pigments, and for shading and highlighting areas. In addition, the optical microscopy of the cross sections revealed the presence of mixtures of green and yellow-orange pigments. Figure 3 shows the three cross sections of the paint layers P2A 3 (sample mentioned in Figure 2), P3A 15, and P3A 8; where the mixtures of pigments were identified.

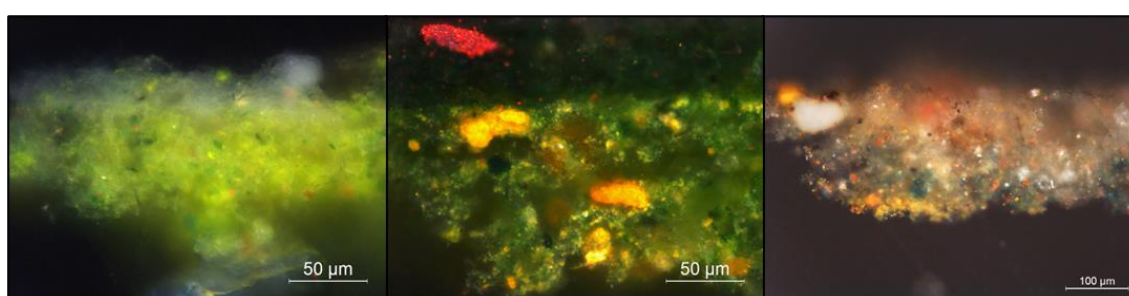


Figure 3. From left to right: optical microscopy of samples P2A 3, P3A 15 and P3A 8 cross sections at 500x, 500x and 200x magnification, respectively. The samples show mixtures of green and yellow particles in different amounts.

The presence of yellow and orange pigment particles mixed within the green paint layers, and the presence of warmer-colour layers in the underlayer, can explain the yellow span of the green paint layers in the CIE a^*b^* color space, including a small section of the red shades.

Besides the hue, the lightness of the paint layers was studied by the CIE color space a^*L^* chart (Figure 1) where many of the paint layers have a light green color. The current lightness of the green paint layers can be related to different factors. It can be related to the execution of the mural paintings; the possible use of white pigments to lighten the green color, or the application of the pigment with milk lime for the painting technique that was employed. However, it can also be related to some of the decay mechanisms that the pigments could have been undergone in the lightest shades.

To sum up the previously mentioned and show the different reflectance regions of the green pigment palette, Figure 4 displays the spectral curves of the six representative paint layers that were discussed above (Figure 2). According to Figure 4, the paint layer P3C 79 has an absorption band

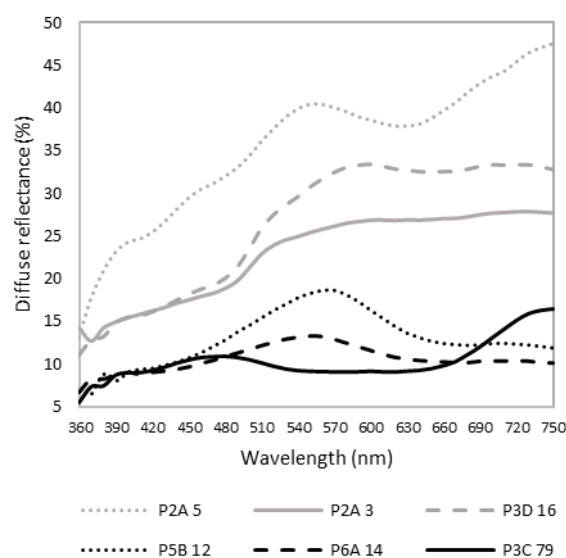


Figure 4. Reflectance spectra of the six selected green paint layers.

between 420 and 530 nm, covering both the blue and green regions, which is attributed to the blue brushstroke over the green pigment.

The paint layers P6A 14, P5B12, P3D 16 and P2A 5 have absorption bands between the 490-630 nm region (green to near orange region). Special attention must be paid to the spectrum of sample P2A 5, which presents a shoulder at 450 nm, and the absorption band at 560. According to Feller (2001) the two absorption bands at 465 and 600 nm, are indicative of chromium oxide green [1]. The before mentioned, as well as the detection of chromium, by h-EDXRF, in the sample, are indicative of the presence of a chromium-based pigment.

After the analysis of the green painting palette by colorimetry/ spectrophotometry, the bulk composition of the paint layers was determined by h-EDXRF to recognize possible chromophores that could be responsible for the green colour. The location of the h-EDXRF measurements is described in Appendix III. The label correlation with the colorimetry/ spectrophotometry can be found in Appendix IV.

Regarding the elements identified by this technique, calcium was present in all samples and can be associated with calcium-based salts on the surface of the paint layer, or the presence of calcite in the intonaco or even the arriccio.

Iron was also detected in all samples, suggesting that their green hue is related to the use of an iron-based pigment. It is important to note that iron was not detected as a component of the mortar, as the elemental analysis of the areas that correspond to the intonaco analyzed by SEM-EDS, did not reveal the presence of this transition metal (Figure 5).

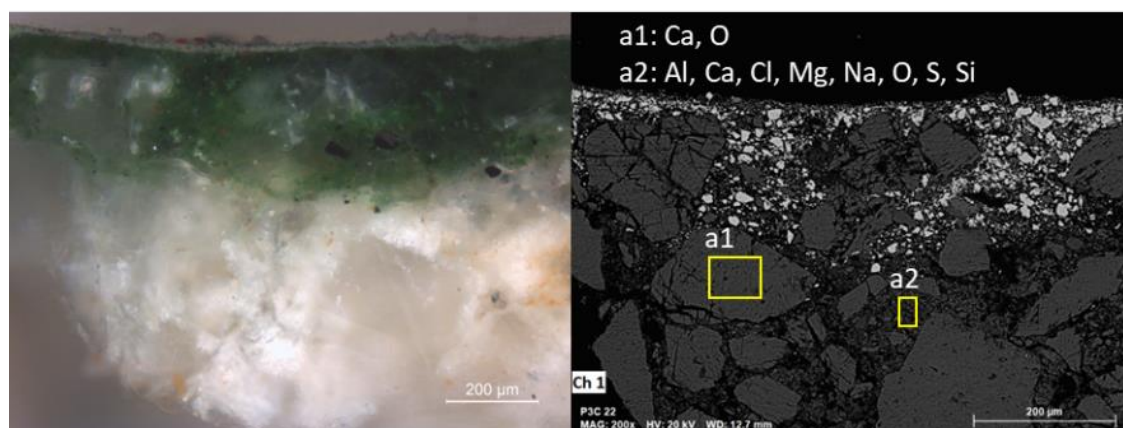


Figure 5. On the left: optical microscopy P3C 22 cross section at 100x magnification. On the right: SEM-EDS elemental analysis of the areas a1 and a2 from sample P3C 22. The main elements detected from the areas are described on the top.

Along with iron, chromium was also detected by h-EDXRF. In fact, these two transition metals were the only elements identified by h-EDXRF that could be present in green pigments. As seen in Figure 6 a), the areas measured by h-EDXRF can be divided into two main groups according to the Fe-Cr relationship. The first group (empty circles) is characterized by the absence of chromium, while the samples included in the second group (black circles) have variable amounts of chromium. The possible combined use of chromium-based and iron-based pigments was further corroborated by the detection of these elements in sample P3C 22 (Figure 6 b).

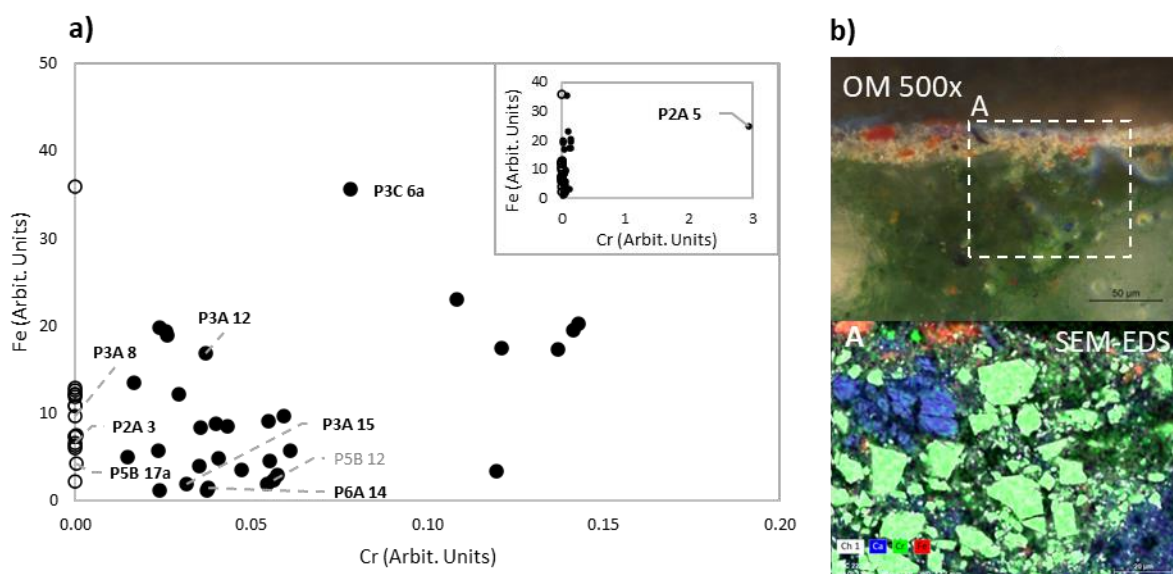


Figure 6. a) Handheld-EDXRF Fe-Cr bi-plot revealing the presence of two groups: one in which iron was exclusively detected (empty circles) and one in which iron and variable amounts of chromium were detected (black circles). In bold are the paint layers that were sampled for further analysis in the laboratory. **b)** OM and SEM-EDS of P3C 22, showing the presence of chromium in the green pictorial layer.

Chromium oxide and hydrated chromium oxide, known to be expensive green pigments, were already available by the time Almada Negreiros painted the panels in the Maritime Station of Alcântara [2]. Nevertheless, the presence of chromium can also be related to the use of chromium yellow, which mixed with Prussian blue imparts a green hue to the paint layer [2].

This practice was common since the last quarter of the 19th century, and the mix was called *green cinnabar* and *chrome green* [3]. In fact, given the known budget limitations for the commission of the Maritime Station of Alcântara [4], Almada Negreiros could have used chrome green pigments in a few selected areas, or, alternatively, employed the cheaper mixture of Prussian blue and chrome yellow.

In order to do a thorough research into the pigment identification, the painting technique, the state of conservation of the paint layers and deterioration features; 21 samples were analyzed in the laboratory. The microsample location is described in Appendix V. The table below summarizes the results obtained from the analysis of microsamples of green paint layers that are discussed and illustrated in this section. The results displayed in this table (Table 1) include both in loco analysis, carried out in the sampling area, and the laboratory analyses that were most relevant for the identification of the pigments used by Almada Negreiros. The results compendium of analyses performed for the 21 samples can be found in Appendix VI.

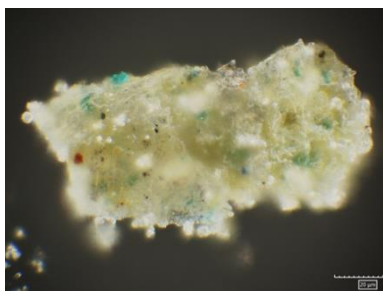


Figure 7. OM of sample P2A 5 at 2000x magnification

Even though both chromium and iron were detected by both h-XRF and SEM-EDS in several samples, chromium-based pigments were not identified by μ -XRD. In fact, in most cases, as seen in Table 1, μ -XRD did not reveal the presence of any mineral phases responsible for imparting green hues to the paint layer. P2A 5, the previously discussed sample about the presence of chromium, was one of the samples that were not able to analyze by this technique. Figure 7 shows the OM at 2000x magnification of the sample P2A 5. Both green and blue pigment particles are visible in the micro fragment.

Table 1. Analysis of results for the identification of green pigments. (PY 1- Pigment yellow 1, PG 8- Pigment green 8, PG 1-Pigment green 1)

Sample ID	CIELAB chromatic coordinates			h-EDXRF (in bold major elements for pigment identification)	μ -XRD	micro-Raman Spectroscopy
	L	*a	*b			
P2A 3	56.71	0.1	13.02	Ba, Ca , Cu, Fe, K, Mn, Ni, S , Si, Sr , Zn	-	PY 1, PG 8, baryte
P2A 5	67.99	-2.96	11.97	Ba, Ca , Cl , Cr , Cu, Fe , K, Mn, Ni, Pb , S , Si, Sr , Ti , Zn	-	-
P3A 8	55.86	0.32	7.8	Ba, Ca , Cl , Cr , Cu, Fe , K, Mn, Ni, Pb , S , Si, Sr , Ti , Zn	Gypsum, quartz	PG 1, carbon black, hematite, gypsum
P3A 12	30.95	0.19	1.45	Ba, Ca , Cl , Cr , Cu, Fe , K , Mn , Ni, S , Si, Sr , Ti , Zn	Quartz, gypsum, calcite, clinochlore, plagioclase, sepiolite	-
P3A 15	35.37	-3.45	6.53	Ba, Ca , Cl , Cr , Cu, Fe, K, Ni, Pb , S , Si, Sr , Zn	Baryte, gypsum, calcite	PG 8, hematite, baryte
P3C 6a	61.85	-0.4	10.58	Ba, Ca , Cr , Fe , K, Mn, S, Si, Sr , Ti , Zn	Gypsum, quartz, rutile, clinochlore, calcite, baryte	-
P3C 22	-	-	-	-	Calcite, baryte, gypsum	-
P5B 10	-	-	-	-	-	PG 8, baryte
P5 B 17	48.15	-5.4	9.39	Ba, Ca , Cl , Cr , Cu, Fe , Mn, Ni, S , Si, Sr , Zn	Gypsum, calcite, baryte	PG 8, carbon black, gypsum
P6A 14	41.45	-4.95	6.76	Ba, Ca , Cl , Cr , Cu, Fe, K , Ni, S , Si, Sr , Zn	Gypsum, calcite, baryte	PG 8
P8A 31a	-	-	-	-	Baryte	PG 8, ultramarine blue, calcite, gypsum

The only two samples that presented mineral phases responsible of the green hue were P3C 6a and P3A 12: the identification of clinochlore, an aluminosilicate of iron and magnesium, suggests that green earth is responsible for their green color. Figure 8 shows the diffractogram of sample P3C 6a, as well as an elemental map performed on the sample with the SEM-EDS which evidences the presence of the elements that can be associated with green earth minerals.

While the artists' pigments book does not mention clinochlore in the minerals that green earth can contain, chlorite is considered a green earth mineral [5], and clinochlore belongs to the chlorite group [6]. The variety of defects and impurities in

clinochlore modifies its optoelectrical properties [7], giving rise to a spectrum of colours from olive green to pale pink and yellow hues. The abundance of this natural mineral makes it possible to be used to produce green earth pigments [7].

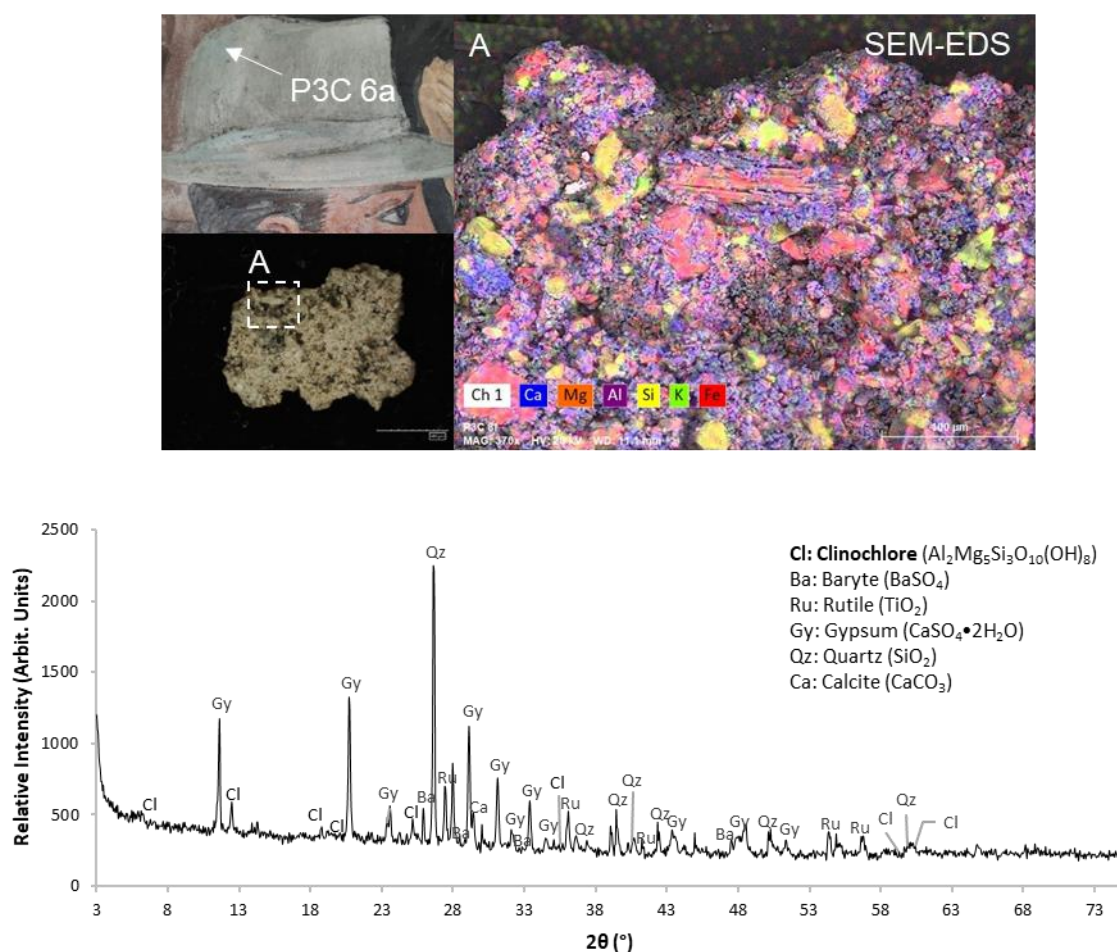


Figure 8. On top: sampling location of P3C 6a, OM of the sample at 140x magnification, and SEM-EDS elemental mapping of the area A. On the bottom: μ -XRD diffractogram of sample P3C 6a, showing the presence clinochlore.

This is not the first case this controversial mineral is present in paintings or mural paintings. In 2021, Fulcher et al. found, in the pharaonic town of Amara West, palettes with a very light green pigment, which composition included clinochlore, an unexpected pigment from the period and the site as the palettes date to around 1300-1050 BCE [8]. Clinochlore was also found in the preparatory layers of the 17th century wall paintings from the Petros and Paulos Church, located in Ethiopia, and in the green paint layers with glauconite [9].

Clinochlore was not the only green pigment used by Almada Negreiros. Micro-Raman spectroscopy, on the other hand, enabled the identification of synthetic organic pigments in seven microsamples: P2A 3, P3A 8, P3A 15, P5B 10, P5B 17, P6A 14 and P8A 31a. With the exception of sample P3A 8, all the samples contained an iron-based synthetic organic pigment, PG 8 identified based on the very strong Raman band at 752 cm^{-1} , the strong bands at 668 cm^{-1} and 633 cm^{-1} and the medium bands at 1355 cm^{-1} and 878 cm^{-1} (Figure 9) [10].

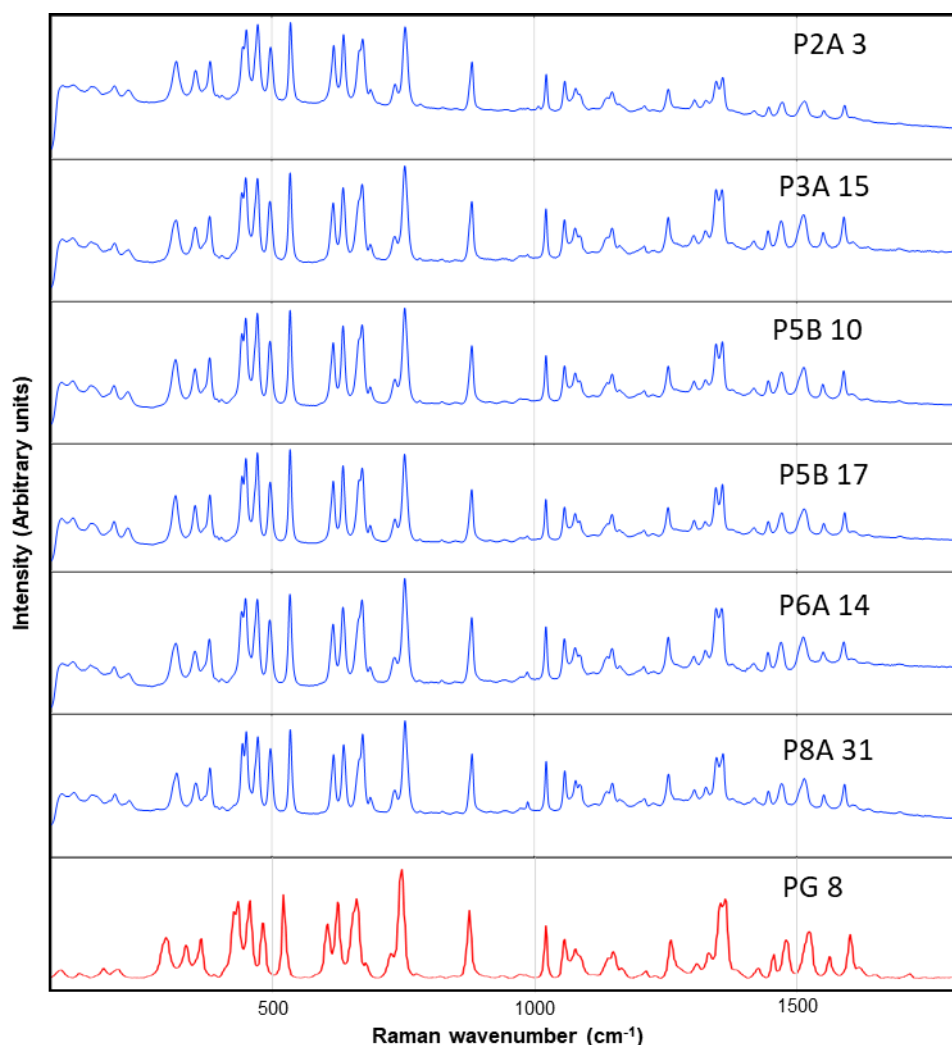


Figure 9. Raman spectrum of samples P2A 3, P3A 15, P5B 10, P5B 17, P6A 14 and P8A 31 (785 nm), and PG 8 (Spectrum retrieved from the database of the SOPRANO project: <https://soprano.kikirpa.be/>).

The importance of the use of micro-Raman spectroscopy in this study is clearly displayed, for instance, in sample P3A 15, a micro fragment composed of a mixture of green and yellow pigments (Figure 10).

Analyses by SEM-EDS and μ -XRD did not enable the identification of the green pigment present in this micro-sample. The SEM-EDS elemental mapping revealed the presence of a high concentration of iron in a few dispersed particles (Figure 10). These iron-rich particles could be hematite (Fe_2O_3) or goethite ($\text{FeO}[\text{OH}] \cdot n\text{H}_2\text{O}$), but the micro-Raman spectroscopy study over the yellow particles showed the presence of characteristic Raman bands at 224, 408 and 498 cm^{-1} , and the strong band at 290 cm^{-1} (figure 10) can be attributed to hematite [11]. The presence of PG 8 and hematite in the sample can explain the detection of iron by h-EDXRF. Hematite in yellow particles, could imply the presence of yellow ochre in the sample, since Elias, et al. (2006) stated yellow ochres contains hematite (Fe_2O_3 , red hue) and goethite ($\text{FeO}[\text{OH}] \cdot n\text{H}_2\text{O}$, yellow hue), which proportions modify the hue of the pigment [12].

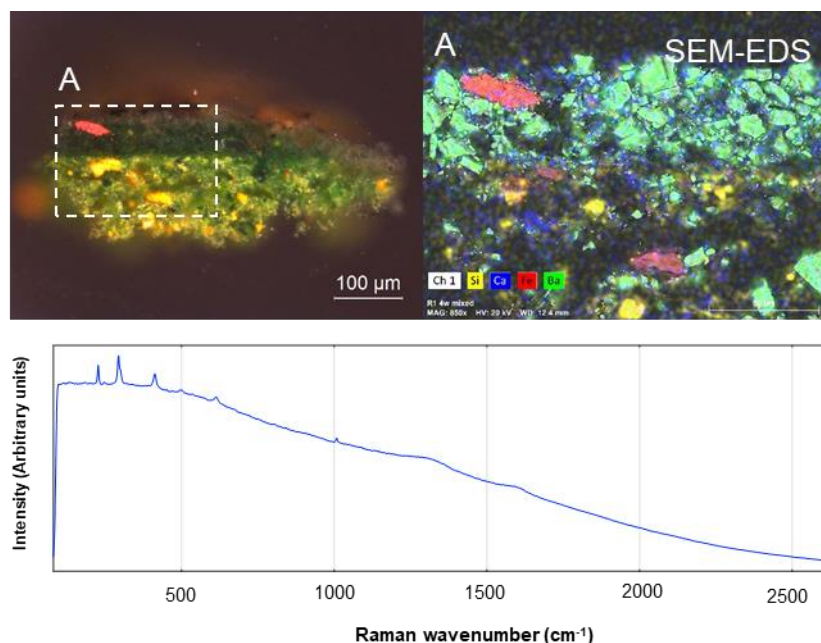


Figure 10. Upper left picture: optical microscopy of P3A 15 cross section at 200x magnification. Upper right picture: SEM-EDS image of area A. Lower picture: Raman spectrum of sample P3A 15 (785 cm^{-1}). The bands were attributed to hematite [11].

On the other hand, point analysis performed on the coarse grains from the upper green layer (Figure 10) revealed high concentrations of barium and sulfur, suggesting the presence of baryte (BaSO_4), which is consistent with the results obtained by μ -XRD (Figure 11). According to Feller (1987) baryte is a white pigment which was first used in 1782 as an alternative to the toxic pigment lead white [13]. Due to its chemical stability and its refractive index (1.64), baryte is mostly used as an extender [13]. The identification of baryte in nine samples could indicate it was mainly used as a filler.

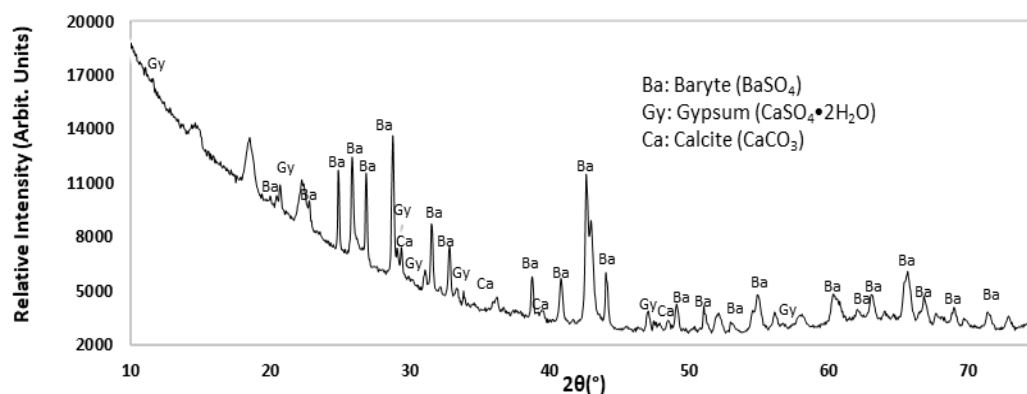


Figure 11. μ -XRD diffractogram of the micro fragment P3A 15. The diffractogram shows the presence of baryte, gypsum and calcium in the sample.

Besides the synthetic pigment PG 8, the green synthetic pigment PG 1 was identified by micro-Raman spectroscopy in sample P3A 8 (Figure 12). The triplet located at 1217, 1182 and 1159 cm^{-1} , as well as the bands at 1615 and 1581 cm^{-1} ; are the main bands for the identification of PG 1 [14]. Information about the historical context and first use of this pigment is scarce. PG 1, also called *Fanal green*, *Brilliant green*, and *Fanatone Bronze Green*, belongs to the triaryl carbonium pigment class [15]. There is

no information about the first synthesis or its properties. However, we know that triaryl carbonium dyes were used in the textile industry since 1859. Lakes were made later, but the poor lightfastness caused their discontinuation [14].

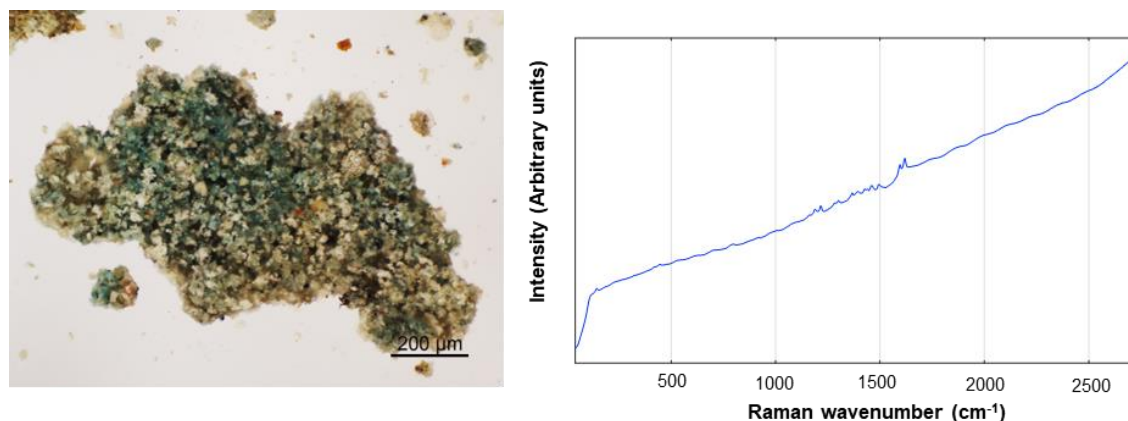


Figure 12. On the left: OM of microsample P3A 8 at 200x magnification. On the right: Raman spectrum of sample P3A 8 (785 nm). The bands were attributed to the synthetic pigment PG 1 [14].

The last synthetic pigment identified was PY 1, a yellow pigment mixed with PG 8 in the sample P2A 3. However, in this case, PG 8 was mixed with Hansa Yellow (PY 1) causing the sample to display a yellow-green colour (Figure 13). Hansa Yellow is a synthetic organic pigment from the family of the monohydrazone pigments, which has Raman characteristic bands at 1134, 1310, 1487 and 1621 cm^{-1} [16].

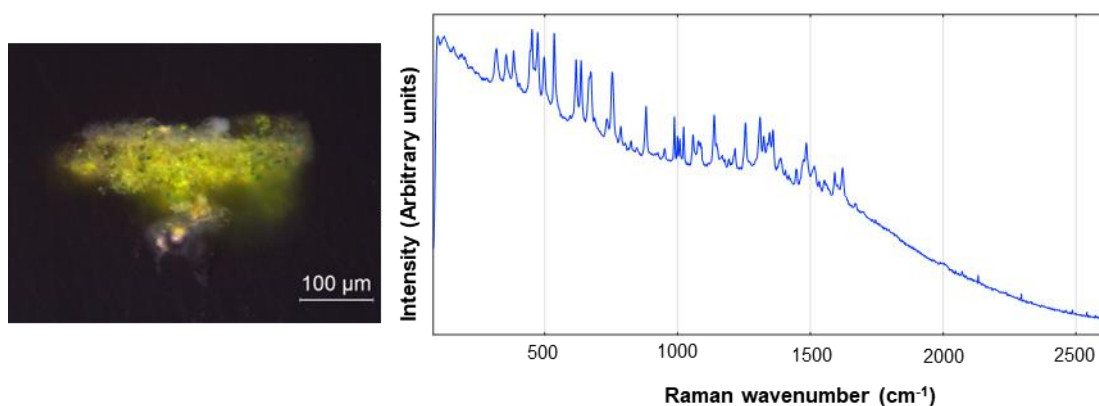


Figure 13. On the left: OM of microsample P2A 2 cross section at 200x magnification. On the right: Raman spectrum of sample P2A 3 (785 nm). The bands were attributed to the synthetic pigments PG 8 [10] and PY 1 [16].

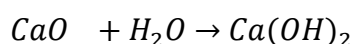
As a final note, it is important to highlight that three different green pigments (green earth, PG 8, and PG 1) were identified in panel number 3 in the basket with fruits that the lady is holding (Figure 14). This clearly indicates that Almada made use of a wide variety of green pigments to achieve the different hues of the fruits, and shows how careful and precise he was with his colour selection.



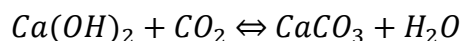
Figure 14. Location of samples P3A 15, P3A 12 and P3A 8, with their respective pigment identification, in the basket of fruits. On the right, the OM of the microsamples at 140x and 200x magnification are showed.

4.1.2. Painting technique

The mural paintings in the Maritime station of Alcântara are classified as fresco [17]. In fresco technique, the artist paints over a layer of fresh lime mortar, making the pigments get fixed by the carbonation of the calcium hydroxide present in the mortar [18]. The fresh lime mortar consists of a mixture of quicklime (CaO), inert aggregates, and water. During the mixing process, the quicklime reacts with water and forms calcium hydroxide, also called slaked lime (Ca(OH)_2), under the following reaction:



Once the fresh lime mortar is applied, the carbonation process occurs when the calcium hydroxide (Ca(OH)_2), exposed to air, interacts with the carbon dioxide from the atmosphere and reacts to form calcium carbonate (CaCO_3) according to the following chemical reaction [20-18]:



As the drying process of the mortar continues, the calcium hydroxide from the mortar migrates to the surface and undergoes the same reaction. When the paint layer is applied before the mortar gets dry, the formed calcium carbonate acts as a pigment binder and the pigment particles get attached to the surface [18].

Between the fresco technique, there are two variations. The term *buon* fresco is used when the pigment is mixed with water and applied to the fresh lime mortar. For the lime fresco technique, the pigment is mixed with a solution of calcium hydroxide before its application to the fresh lime mortar [18, 19].

As stated above, a fresco execution implies the presence of a fresh mortar surface. Depending on the dimensions of the mural painting, the speed of work, and the number of executants, the artist can apply a whole horizontal layer of intonaco along the width of the mural painting [18]. The joints are called *pontatas* and they appear as horizontal joints of mortar.

If the artist cannot paint the whole pontata in one day, the area is divided into smaller sections so the artist can apply intonaco on the section and paint it in one day. The joints that result from these areas are called *giornatas*, and they are usually vertical [18].

In what concerns the case study, Figure 15 shows the identification of a mortar joint by raking light (RAK) found in one of the areas analyzed in panel 3. From the prior diagnostic study of these mural paintings, Gil, et al. (2021) identified the execution of fresco technique in brownish, blue, and red paint layers [20]. Nevertheless, there are still doubts concerning the use fresco technique for all the paint layers, considering the monumental dimensions of the panels, and the fact Almada Negreiros worked alone during the execution of the mural paintings.

The determination of the painting technique for the green paint layers is of main interest to determine possible causes of the flaking and powdering.



Figure 15. Mortar joints located in panel 3. The arrows show the direction of the mortar overlapping.

Based on the fact the mural paintings of this case study are classified as fresco, it should be expected the presence of calcium matrix due to the presence of calcium carbonate. Figure 16 shows the SEM and SEM-EDS analysis of sample P5B 10. The SEM image shows the pigment particles are very loose, which means they have lost part of the binding medium. The calcium elemental map on the right shows there is calcium along the matrix of the paint layer, which can imply the paint layer could have been applied by fresco technique.

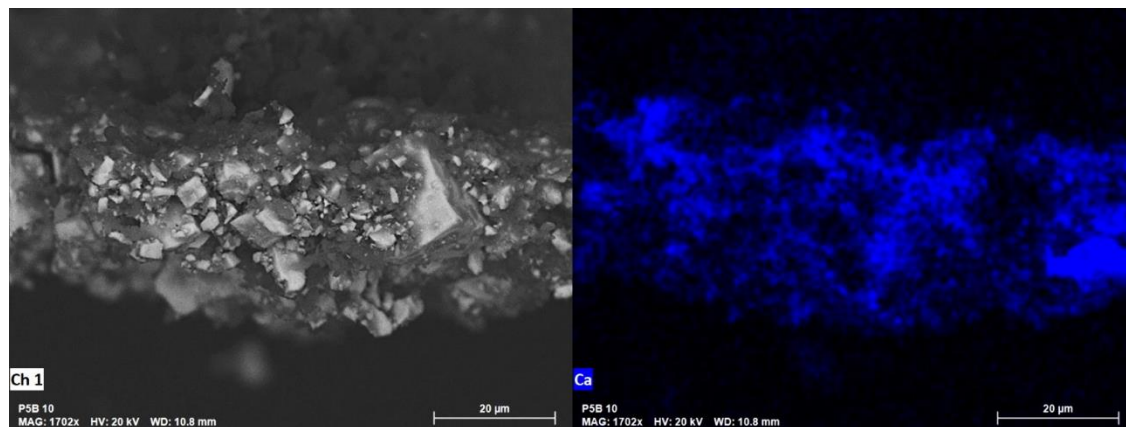


Figure 16. On the left: SEM image of sample P5B 10. On the right: calcium elemental map of sample P5B 10 by SEM-EDS.

According to Piovesian et al. (2012), a paint layer executed by fresco technique can be identified by two main features [19]. The first one is the thickness of the paint layer, which is usually up to 50 µm. The second one is the absence of a calcium-rich crust at the interface between the intonaco and the paint layer [19].

In order to look for these main features, the cross section of the same sample (P5B 10) was analyzed by SEM-EDS (Figure 17). As shown on the OM of the P5B10 cross section, the thickness of the dark green paint layer is 97 µm, almost the double of the thickness described by Piovesian et al. [19]. The thickness of the sample, as well as the uneven distribution of calcium in the paint layer indicates the paint layer was most likely applied by a different painting technique.

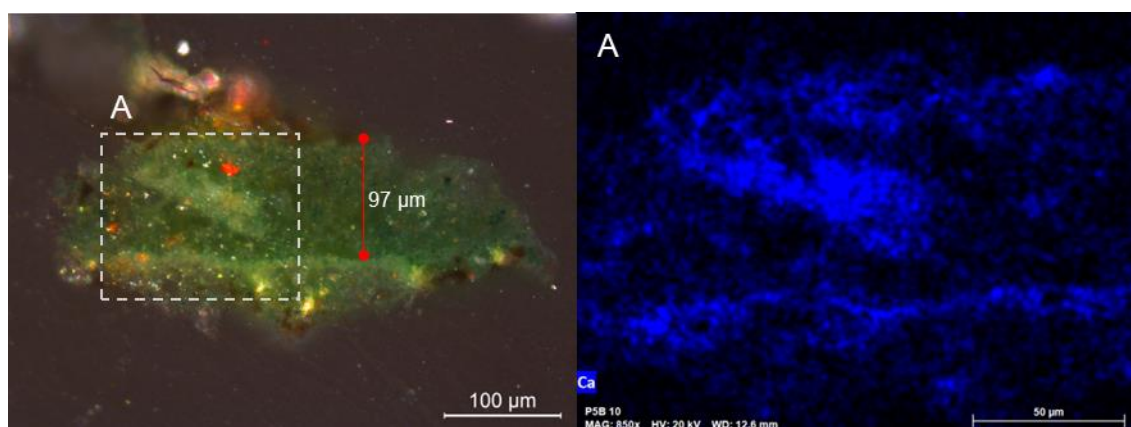


Figure 17. On the left: OM of P5B 10 cross section at 200x magnification. On the right: calcium elemental map of the area A by SEM-EDS.

In addition, there is a non-well defined calcium line that separates the dark green layer from the underlayer. The lack of intonaco on the sample does not allow to define the stratigraphy of the sample, and therefore it is not possible to define the execution in which the underlayer was applied.

As mentioned in the previous paragraphs, the paint layer P2A 3 comes from a deteriorated yellow-green area that presents powdering. The brushstroke over the yellow paint layer is of main importance since it shows an example of a calcium-rich layer (Figure 18). By the SEM image is possible to see and differentiate the white brushstroke that is over the layer. The calcium elemental map by SEM-EDS shows calcium all over the brushstroke, that can be related to the use of limewash to highlight the area.

Comparing to the white brushstroke, the yellow underlayer has not a considerable amount of calcium, that can be related with the deterioration of the layer. The painting technique for the paint layer was not possible to identify by the analytical techniques performed.

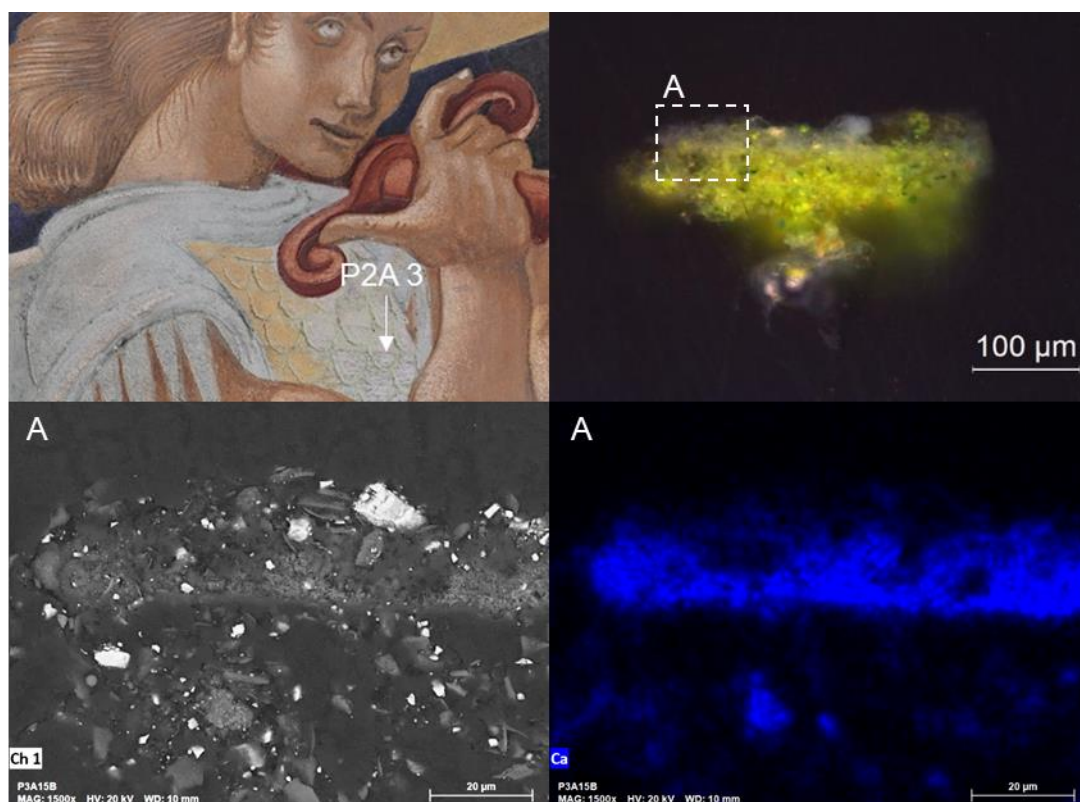


Figure 18. Upper left picture: location of the microsample P2A 3. Upper right picture: optical microscopy of P2A 3 cross section at 200x magnification. Lower left picture: SEM image of area A. Lower right picture: calcium elemental map of area A by SEM-EDS.

The bad state of preservation of the paint layers was one of the main problems for the analysis of painting technique, reasons why there is not a definite conclusion about the way the green paint layers were executed. However, we cannot exclude the possibility that Almada made use of secco technique. The scope of this study could not include the detection and identification of organic binders by infrared spectroscopy (IR) and pyrolysis-gas chromatography coupled with mass spectrometry (Py-GC-MS).

It is highly recommended to perform these analyses in future studies to confirm Almada Negreiros did not make use of other painting techniques.

It is important to point out that even when calcite was a mineral identified in seven out of eight samples analyzed by μ -XRD, the identification of a calcium carbonate matrix was not straightforward, in addition to the fact gypsum (CaSO_4) was detected in the same number of samples. The presence of gypsum will be discussed in the following section.

4.1.3. Decay mechanisms

After the identification of green pigments and painting technique were discussed, three hypotheses were raised about the main causes of deterioration of the green paint layers, which are the following:

- a) Technical drawbacks related to the pigments and the painting technique
- b) Salts
- c) Bio contamination

According to the previously mentioned in chapter 2, green earth is a very stable pigment which is appropriate for use in fresco technique [5]. On the other hand, PG 8 is not the most suitable pigment for fresco technique. PG 8 is an iron (III) complex of 1-nitroso-2-naphthol, and it was mainly used in the textile industry [21]. Between its properties, de Keijzer mentioned that this pigment has poor lightfastness, and it is reactive to alkaline and acidic media [21].

Slaked lime ($\text{Ca}(\text{OH})_2$), a very alkaline material, is an essential component of lime based technique as it is the case of fresco. If Almada Negreiros made use of PG 8 in any of the layers made by fresco, it is highly probable that the pigment was hydrolyzed in presence of the hydroxyl anions (OH^-) from the fresh lime mortar, modifying the electronic distribution of the pigment and therefore its fading. Based on that, it is stated as a hypothesis that the light green paint layers could be the result of a chromatic alteration.

The other synthetic pigment of concern is PG 1. Due to the lack of information about the origins and properties of PG 1, it is not possible to give a proper conclusion about its compatibility with the painting technique and with the pigments. Considering that PG 1 is mainly used for the textile industry, and the fact triaryl carbonium pigments usually have poor lightfastness [22], we can infer PG 1 is not resistant enough for mural painting.

However, it is possible that, more than a pigment, PG 1 was used as an adulterant. Grissom (1986) mentioned green earth was commonly adulterated with PG 1; the mixture was called lime green, and it was used mainly in lime media [5]. Green earth and PG 1 were not found simultaneously in the same sample. However, this does not discard the idea that Almada Negreiros could have made use of adulterated green earth.

In what concerns salts, sulphates were the most common salts present in the efflorescence. Gypsum (CaSO_4), baryte (BaSO_4) and calcite (CaCO_3) were the salts

identified in the ten micro fragments analyzed by μ -XRD (Table 2), whose analyses can be found in Appendix VII. Gypsum can be the product of the reaction of calcium carbonates with sulfur dioxide (from air pollution) and water [23]. However, there are other sources of sulfates that can trigger the formation of salts, like magnesium sulphate (MgSO_4) from sea spray, sulphates from construction materials like Portland cement, and sulphates as by-products of the oxidation of sulfur-containing compounds by microorganisms [23].

Table 2: Salts identified in micro fragments by μ -XRD

Sample ID	Salts		
	Gypsum	Calcite	Baryte
P3C 6a	•	•	•
P3A 12	•	•	
P3A 15	•	•	•
P3A 8	•		
P3C 22	•	•	•
P5B 17/17a	•	•	•
P5B 17b	•		
P6A 14	•	•	•
P8A 31a			•
P8A 35	•		

This is not the first-time salts are identified in the mural paintings of the Maritime Station of Alcântara – gypsum, thenardite (Na_2SO_4), syngenite ($\text{K}_2\text{Ca}(\text{SO}_4)_2 \cdot \text{H}_2\text{O}$), aphthitalite ($\text{K}_3\text{Na}(\text{SO}_4)_2$), and anhydrite (CaSO_4) have all previously been identified by μ -XRD [20]. Gil et al. (2021) pointed out that the eight mural paintings cover the areas between the first and second floors of the maritime station, crossing the edge that delimits the division between floors [20]. The thermal bridge produced by this edge can promote the condensation of water, and therefore the promotion of salt redissolution, the reaction with external agents, and the formation of

efflorescence and sub-efflorescence [20].

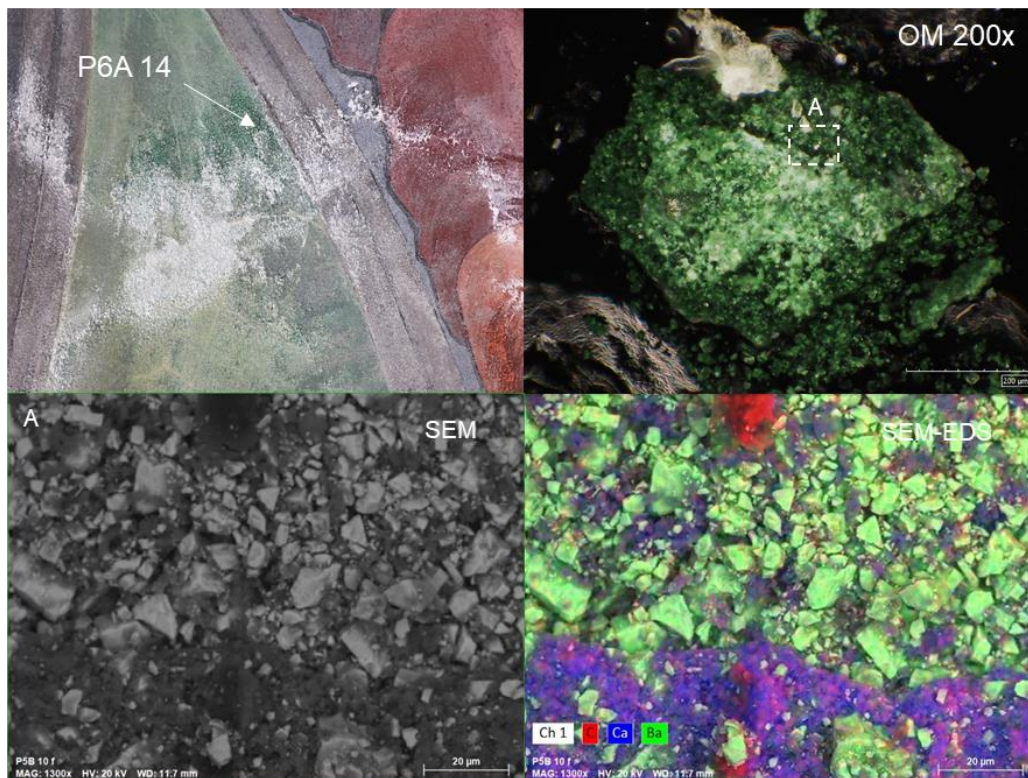


Figure 19. Upper left picture: location of the microsample P6A 14. Upper right picture: optical microscopy of P6A 14 micro fragment. Lower left picture: SEM image of area A. Lower right picture: elemental map of area A by SEM-EDS.

Figure 19 shows sample P6A 14, located in the area of the edge between floors, from one of the paint layers most affected by salt efflorescence. The SEM image of the paint surface shows most of pigment particles loose and exposed, which explain the loss of cohesion (or powdering) observed. According to Subbaraman (1993), water infiltrating into the pictorial layer can dissolve or loose the binder, producing the loss of the pigment particles in the paint layer [24].

Besides the loss of cohesion, flaking is a consequence of the crystallization of salts within or between paint layers. According to Borrelli (1999) the physical stress produced during crystallization, or the expansion of crystals due to hydration, can gradually over time cause loss of adhesion, giving place to the presence of flaking [23].

Finally, signs of bio colonization were found in two samples analyzed by SEM (Figure 20). Although a more in-depth study could not be carried out, it is known one of the main causes of bio colonization is the high relative humidity circumstances that are present in the Maritime Station of Alcântara.

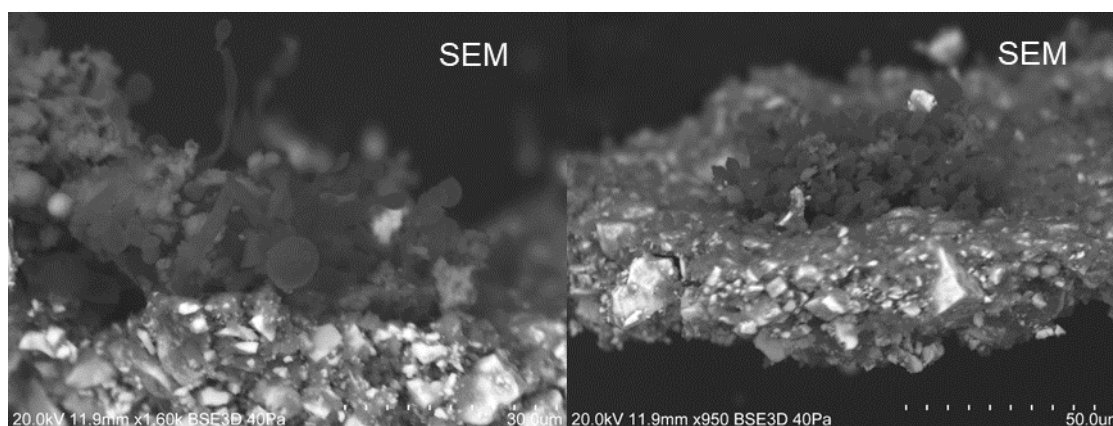


Figure 20. SEM images where signs of bio colonization were detected.

4.2. Characterization of green pigments in powder: a complementary study

In order to have a deeper understanding of the green pigments available in Portugal during the 20th century, the study of eleven pigments in powder was carried out by a series of analyses which involved colorimetry/spectrophotometry, h-EDXRF, XRPD, and micro-Raman Spectroscopy. A summary of the results obtained can be found in Table 3, while photographic evidence of the six pigments not retrieved from Almada Negreiro's studio is given in Figure 21.

Table 3. Summary of the results of colorimetry in the Vis, h-EDXRF, XRPD, and micro-Raman spectroscopy analysis carried out in the eleven green pigments in powder.

Pigments Ref.	Pigments label	CIE chromatic coordinates			h-EDXRF (in bold major elements for pigment identification)	XRPD	micro-Raman spectroscopy
		L*	a*	b*			
a) Pigments retrieve from Almada studio							
LF22	Vert à la chaux	49.14	3.70	-5.52	Al, Ba, Ca , Cr, Cu, Fe , K , Mn , Ni, Pb, S , Si , Sr, Ti , Zn	Quartz, plagioclase, alkali feldspar, calcite, clays/ micas	-
LF23	Vert emeraude	33.39	-3.64	-11.97	Al, Ba, Ca , Cr, Cu, Fe , K , Mn , Ni, Pb, Rb , S , Si , Sn, Sr, Ti , Zn	Quartz, gypsum, hematite, clays/ micas	-
LF30	Vert à la chaux	65.61	-33.79	2.29	Ba , Ca, Cr , Cu, Fe,K, S, Si , Sr , Zn	Baryte	Baryte
O1	Viridian	45.69	-34.23	12.35	Ba , Ca, Cr , Cu, Fe , K, Pb , S, Si , Sr , Zn	Baryte, quartz	Prussian Blue, Chrome Yellow, Baryte
B) Pigments from other sources							
WN 0210720	Windsor green	20.39	-37.24	-0.51	Br , Ca, Cl , Cu , Fe, Ni, Sn, Ti , Zn	PG 7	-
FA 5	Royal green	35.86	-17.92	0.26	Ba , Ca , Cr, Cu, Fe , Mn, Ni, Pb , S , Si , Sr , Zn	Baryte, calcite, quartz, litharge	-
FA 4	Vert à la chaux [altered]	41.15	1.40	-12.31	Ba , Ca , Cr, Cu, Fe , K , Mn , Ni, Pb, Rb , S , Si , Sr, Ti , Zn	Quartz, calcite, muscovite, smectite, Gypsum, plagioclase, alkali feldspar, kaolinite	-
FA 3	Vert à la chaux	58.24	-25.95	5.44	Ba , Ca , Cr, Cu, Fe , K , Mn , Ni, Pb , Rb , S , Si , Sr, Ti , Zn	Quartz, calcite, caolinite, muscovite, gypsum, baryte	-
5W	Chrome Green 665 GS	52.61	-12.55	11.47	Ba , Ca , Co , Cr , Cu, Fe, Ni, P , Pb , Si , Zn	Eskolaite, quartz, cochromite, kaolinite	-
13 BCW	Chrome Green "O" W34	45.57	-14.84	15.91	Cr , Fe, Ni, Sn	Eskolaite	-
K41700	Veronese Green Earth	66.11	-9.27	14.46	-	Gypsum, calcite, clinocllore, quartz	-

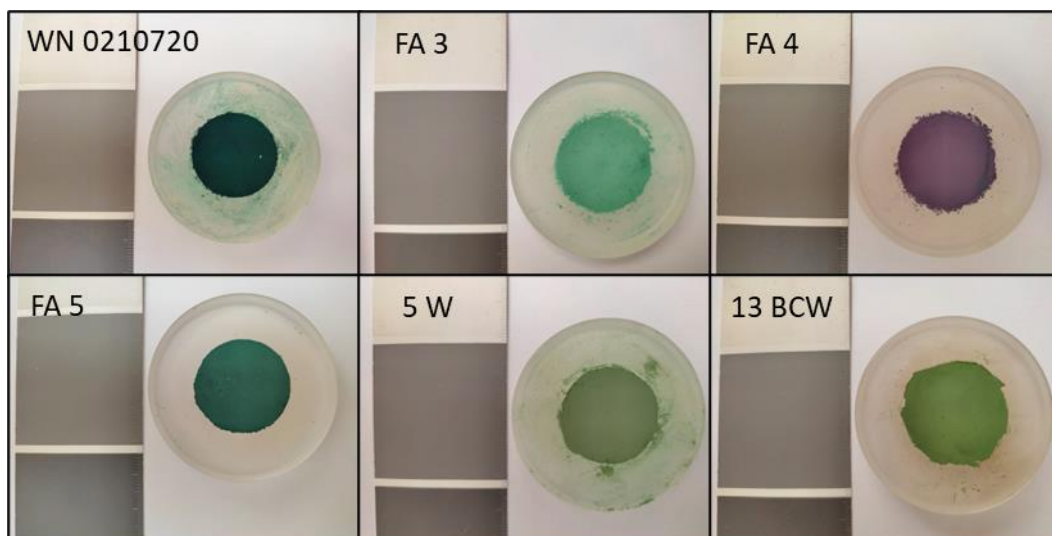


Figure 21. Pigments in powder under study. The six pigments came from external sources

It is important to note that the pigment FA 4 (Vert à la chaux) is labelled as a green pigment, but it does not display a green hue but a violet one. It can be due to a chromatic alteration or a simple mislabeling. It is the same for the pigment LF 22, found in Almada Negreiro's studio, which is also labelled as Vert à la chaux and does not display a green hue.

Figure 22 shows the CIE a^*b^* and a^*L^* colour space plots to analyze the hue and lightness distribution of the pigments in powder. The green hues span from -3.64 to -37.24 in the a^* axis; and from -11.97 to 15.91 in the b^* axis. The pigments FA 4 and

LF 22 were excluded from the range due to the color hue that does not correspond to the green area.

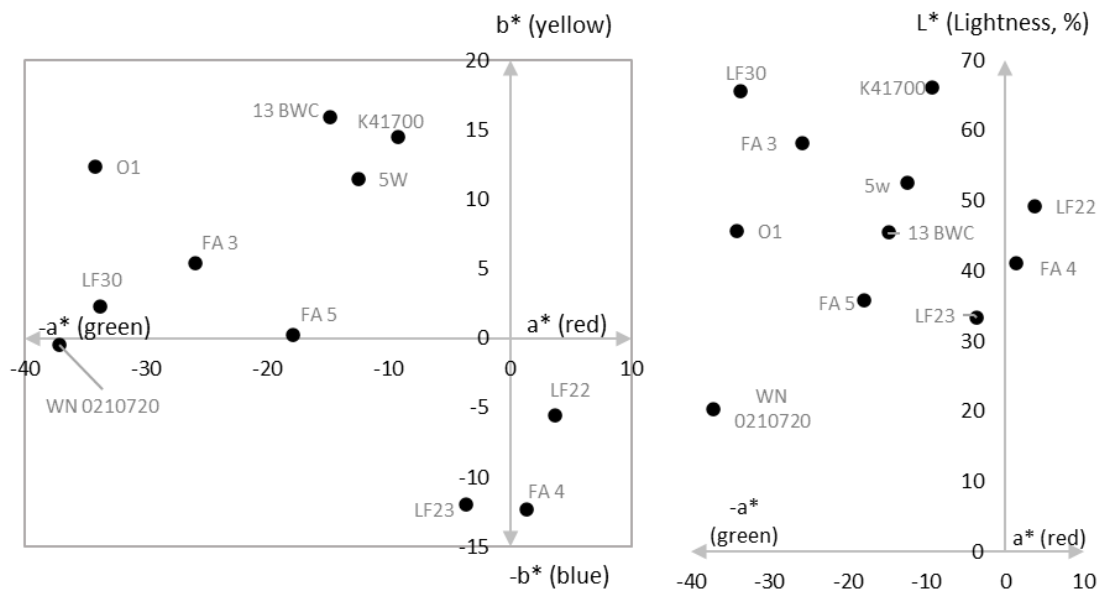


Figure 22. Colorimetric analysis of the pigments in powder. On the left: CIE Color Space a^*b^* . On the right: CIE Color Space a^*L^* .

About the lightness of the pigments in powder, they have a lightness between 30% and 70%, with the exception of WN 0210720, the darkest pigment, which presents a lightness of 20.39%. The green contribution to the color is much higher for the pigments in powder ($-37.24 \leq a^* \leq -3.64$) compared to the green paint layers ($-8.9 \leq a^* \leq -0.07$).

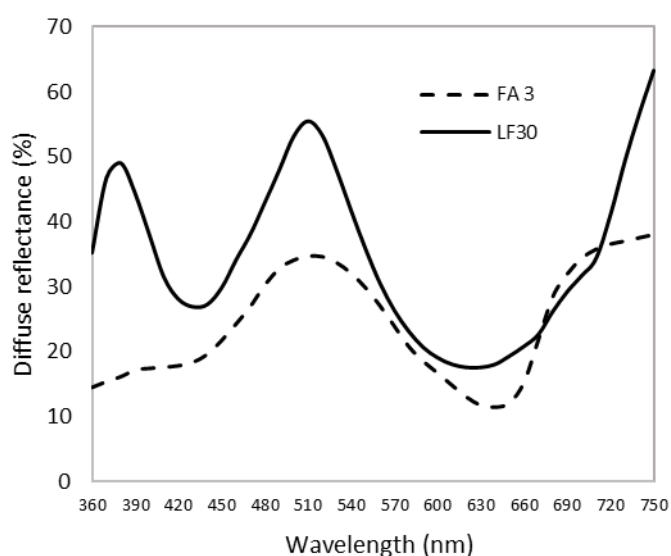


Figure 23. Reflectance spectra of FA 3 (from external sources) and LF30 (from Almada's studio).

By the CIE colour space a^*b^* chart it is possible to recognize that LF30 and FA 3 are pigments whose hue is different but they were labelled by the same name (Vert à la chaux). That could imply that the pigments have different compositions.

Figure 23 shows the reflectance spectra of two pigments in powder FA 3, and LF 30.

LF30 has two main absorption bands at 380 and 510 nm. According to Feller (1987) these double absorptions are characteristic of chromium oxide

green, but the author pointed out that the absorption bands for pure chromium oxide green are at 465 and 600 nm [25]. The presence of chromium in the elemental composition of LF30, as well as the double absorption bands in the reflectance spectrum might imply the presence of chromium oxide green. Compared to LF 30, FA 3 has an absorption band at 520 nm (green region) and a rise in reflectance in the far-red region at 660 nm, which means that the pigments LF 30 and FA 3, even when they have the same label, they have different chromophores.

In what refers pigment LF 30, baryte was the only mineral detected by both XRPD and micro-Raman spectroscopy, implying it was added as a filler. The same filler was also detected in many of the micro fragments of the paint layers. The presence of a chromium-based chromophore, as well as the contain of baryte as a filler, makes possible to hypothesize the pigment LF 30 could have been used by Almada Negreiros for the mural paintings under study.

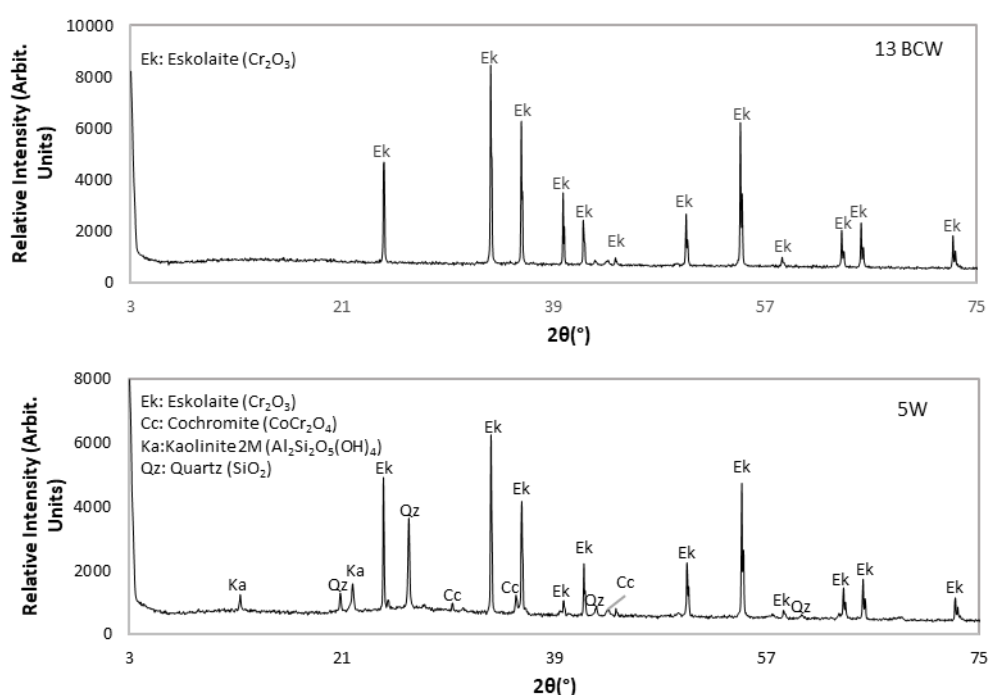


Figure 24. XRPD diffractograms of pigments 13 BCW and 5W.

Nevertheless, h-EDXRF and XRPD were essential to characterize 5W and 13 BCW from a chemical and mineralogical perspective. By h-EDXRF chromium was identified in both pigments, but cobalt was also present in pigment 5W. Figure 24 shows the diffractograms for samples 5W and 13 BCW where eskolaite and cochromite were detected. As mentioned in chapter 2.4, eskolaite is the mineral associated with the chrome oxide green pigment, but cochromite is not mentioned as an artist pigment. According to the handbook of mineralogy, cochromite is a black mineral whose streak has a greenish-grey color [26].

PG 7, hematite (Fe_2O_3), litharge (PbO) and clinocllore were identified by XRPD in the pigments WN 0210720, LF 23, FA 5 and K41700, respectively (Appendix VIII). Clinocllore, the mineral that belongs to the chlorite group, was found in both the pigment powder labelled as green earth, and in two samples from the Maritime Station of Alcântara. That proves that clinocllore is used as a pigment and that it is

commercially available under the name of green earth, even though it is not described in Artist's pigments as a phase belonging to the green earth minerals.

A surprising result was the one given by micro-Raman spectroscopy of pigment O1, labelled as viridian. Based on the characteristic bands at 460 and 1000 cm^{-1} , those at 2150 and 2090, and 276 cm^{-1} and finally those at 360 cm^{-1} and 842 cm^{-1} baryte [27], Prussian blue [28] and chrome yellow [29], respectively, were identified in pigment O1 (Figure 25).

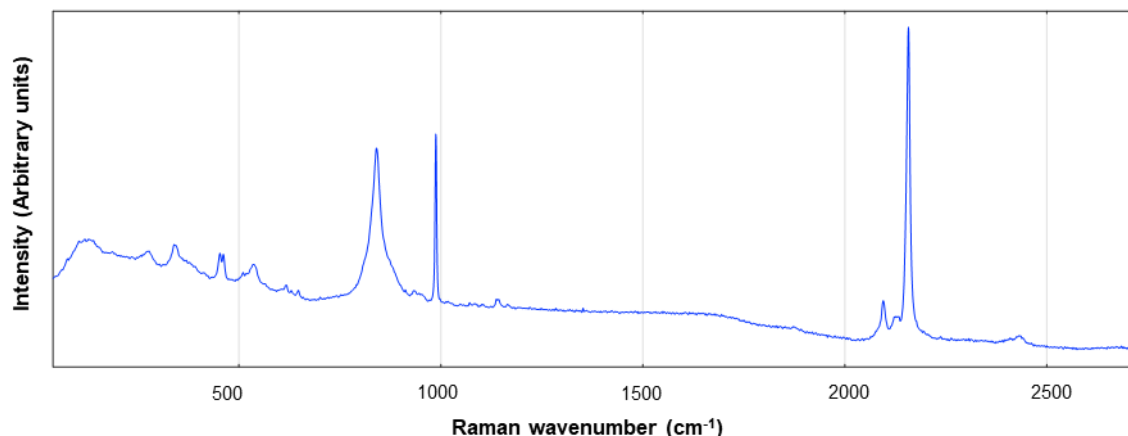


Figure 25. Raman spectrum of pigment O1 (785 nm). The bands were attributed to baryte [27] and the pigments Prussian blue [28] and chrome yellow [29].

Viridian is a hydrated chromium oxide ($\text{Cr}_2\text{O}_3 \cdot 2\text{H}_2\text{O}$) whose synthesis was very expensive. As such, it was common to sell mixtures of Prussian blue and chrome yellow by the name of viridian, as well as by the name of chromium green.

4.3. List of references

- [1] Johnston-Feller, R. (2001). *Color Science in the Examination of Museum Objects: Nondestructive Procedures*. Getty Conservation Institute. 190-221. http://hdl.handle.net/10020/gci_pubs/color_science
- [2] Newman, R. (1997). Chromium Oxide Greens. Chromium Oxide and Hydrated Chromium Oxide. In West Fitzhugh, E. (Editor) *Artists' Pigments. A Handbook of their History and Characteristics*. Volume 3. Oxford university Press, 273-294.
- [3] Kühn, H., & Curran, M. (1986). Chrome Yellow and Other Chromate Pigments. In Feller, R. L. *Artists' Pigments. A Handbook of Their History and Characteristics*. Volume 1. Oxford University Press, 187-217.
- [4] Lobo, P. R. (2014). Almada and the Maritime Stations: The portrait of Portugal that the dictatorship wanted to erase. *Revista de História da Arte – série W*, 2, 342-352.
- [5] Grissom, C. A. (1986) Green Earth. In Feller, R. L. *Artists' Pigments. A Handbook of Their History and Characteristics*. Volume 1. Oxford University Press, 141-186.
- [6] Brigatti, M.F., Galán, E. & Theng, B.K.G. (2006). Structure and Mineralogy of Clay Minerals. In Bergaya, F., Theng, B.K.G. & Lagaly, G. (Eds.). *Handbook of clay science*, Elsevier, 19-86. <https://doi.org/10.1016/B978-0-08-098258-8.00002-X>

- [7] de Oliveira, R., Guallichico, L. A. G., Policarpo, E., Cadore, A. R., Freitas, R. O., da Silva, F. M. C., Teixeira, V. C., Paniago, R. M., Chacham, H., Matos, M. J. S., Malachias, A., Krambrock, K. & Barcelos, I. D. (2022). High throughput investigation of an emergent and naturally abundant 2D material: Clinocllore, *Applied Surface Science*, 599, 153959, <https://doi.org/10.1016/j.apsusc.2022.153959>
- [8] Fulcher, K.; Siddall, R.; Emmett, T.F.; & Spencer, N. (2021) Multi-Scale Characterization of Unusual Green and Blue Pigments from the Pharaonic Town of Amara West, Nubia. *Heritage*, 4, 2563-2579. <https://doi.org/10.3390/heritage4030145>
- [9] Gebremariam, K. F., Kvittingen, L., & Banica, F.-G. (2016) Physico-Chemical Characterization of Pigments and Binders of Murals in a Church in Ethiopia. *Archaeometry*, 58, 271- 283. <https://doi.org/10.1111/arcm.12163>
- [10] Coccato, A., Bersani, D., Coudray, A., Sanyova, J., Moens, L., and Vandenabeele, P. (2016) Raman spectroscopy of green minerals and reaction products with an application in Cultural Heritage research. *J. Raman Spectrosc.*, 47: 1429-1443. <https://doi.org/10.1002/jrs.4956>
- [11] Marucci, G., Beeby, A., Parker, A. W., & Nicholson, C. E. (2018). Raman spectroscopic library of medieval pigments collected with five different wavelengths for investigation of illuminated manuscripts. *Analytical methods*, 10(10), 1219-1236. <https://doi.org/10.1039/C8AY00016F>
- [12] Elias, M., Chartier, C., Prévot, G., Garay, H., & Vignaud, C. (2006). The Colour of Ochres Explained by Their Composition. *Materials Science and Engineering B-advanced Functional Solid-state Materials*, 127 (1) 70-80. <http://dx.doi.org/10.1016/j.mseb.2005.09.061>
- [13] Feller, R. L. (1986) Barium Sulphate. In Feller, R. L. *Artists' Pigments. A Handbook of Their History and Characteristics*. Volume 1. Oxford University Press, 47-64.
- [14] Sundberg, B.N., Pause, R., van der Werf, I.D., Astefanei, A., van den Berg, K.J. & van Bommel, M.R. (2021) Analytical approaches for the characterization of early synthetic organic pigments for artists' paints, *Microchemical Journal*, 170, <https://doi.org/10.1016/j.microc.2021.106708>
- [15] Hunger, L. & Schmidh, M. U. (2018). *Industrial Organic Pigments* (4th ed.). Wiley-VCH, 634.
- [16] Royal Institute for Cultural Heritage (2010). *PY1 Raman 785 nm*. SOP Spectral Library SOPRANO. https://soprano.kikirpa.be/index.php?lib=sop&id=PY1_A_785_kikirpa
- [17] Tavares, C. A. (2017). Duas narrativas para o meu país nos painéis de Almada Negreiros. *Convocarte: Revista de ciências da arte*, 1, 123-128. <http://hdl.handle.net/10451/27734>
- [18] Mora, P., Mora, L. & Philippot, P. (1984). *Conservation of Wall Paintings*, Butterworths, 1-17.

- [19] Piovesan, R., Mazzoli, C., Maritan, L. & Cornale, P. (2012), Fresco and Lime-Paint: an Experimental Study and Objective Criteria for Distinguishing Between These Painting Techniques. *Archaeometry*, 54: 723-736. <https://doi.org/10.1111/j.1475-4754.2011.00647.x>
- [20] Gil, M., Costa, M., Cvetković, M., Bottaini, C., Cardoso, A., Manhita, A., Dias, C., Candeias, A. (2021). Unveiling the mural painting art of Almada Negreiros at the Maritime Stations of Alcântara (Lisbon): diagnosis research of paint layers as a guide for its future conservation. *Ge-conservacion*. 20. 105-117. <https://doi.org/10.37558/gec.v20i1.1027>
- [21] de Keijzer, M. (2014). The Delight of Modern Organic Pigment Creations. In: van den Berg, K. J.; Burnstock, A.; de Keijzer, M.; Krueger, J.; Learner, T.; Tagle, A.; & Heydenreich, G. (Eds.) *Issues in Contemporary Oil Paint*. Springer, Cham., 45-73. https://doi.org/10.1007/978-3-319-10100-2_4
- [22] Hunger, L. & Schmidth, M. U. (2018). *Industrial Organic Pigments* (4th ed.). Wiley-VCH, 613-614.
- [23] Borrelli, E. (1999). Salts. In Borrelli, E. (Editor). *Conservation of Architectural Heritage, Historic Structures and Materials*. ICCROM, 3-23.
- [24] Subbaraman, S. (1993). Conservation of mural paintings. *Current Science*, 64 (10), 736-753. <http://www.jstor.org/stable/24122234>
- [25] Johnston-Feller, R. (2001). *Color Science in the Examination of Museum Objects: Nondestructive Procedures*. Getty Conservation Institute. 225-237. http://hdl.handle.net/10020/gci_pubs/color_science
- [26] Anthony, J. W., Bideaux, R. A., Bladh, K. W. & Nichols, M. C. (2005) Handbook of Mineralogy, *Mineralogical Society of America*. <http://www.handbookofmineralogy.org/pdfs/cochromite.pdf>
- [27] *Baryte X050028* (n.d.) The RRUFF™ Project Database. <https://rruff.info/baryte/display=default/X050028>
- [28] Moretti, G, Gervais, C. (2018) Raman spectroscopy of the photosensitive pigment Prussian blue. *J Raman Spectrosc.*, 49, 1198-1204. <https://doi.org/10.1002/jrs.5366>
- [29] Edwards, H. G. M. (2011) Analytical Raman spectroscopic discrimination between yellow pigments of the Renaissance, *Spectrochimica Acta Part A: Molecular and Biomolecular Spectroscopy*, 80(1) 14-20. <https://doi.org/10.1016/j.saa.2010.12.023>

Chapter 5: Conclusions and future perspectives

The present study is focused on the green paint layers of the eight monumental mural paintings located in the Maritime Station of Alcântara, Lisbon (Portugal). This impressive artwork was made by the Portuguese artist Almada Negreiros in 1945. He used a bright chromatic palette that today shows different states of conservation, being the green paint layers the most concerning ones due to the severe flaking and powdering in the lightest shades. The main goal of this research was to understand this decay phenomenon by the identification of the pigments, the painting technique, and the external deterioration factors.

Parallel to this research, seven green pigments in powder, from external sources, were also analyzed for a deeper understanding of the type of green artists' pigments available in Portugal during the 20th century. In addition, it helped to compare and identify if there is any kind of relationship with the pigments from the paint layers under study.

The colorimetric study of the paint layers has shown that the green color palette is most characterized by green-yellow hues. The yellow shades are attributed to both mixtures of green and yellow-orange pigments, and to the interference of yellow paint underlayers.

Almada made use of green pigments in an extensive area of the mural paintings. They were used to paint the background and to make shades and highlights in the mural painting.

Regarding the green pigments used by Almada in the mural paintings, the analytical setup used enabled the identification of two main types:

- a) green earths, identified by the presence of clinocllore in two samples
- b) the synthetic pigments PG 8 and PG 1 found in six and one sample, respectively

Other chromophores were also identified in five green paint layers such, as hematite (a red iron oxide), a yellow synthetic pigment PY1, ultramarine blue and carbon black. From the prior pigments, only PY1 was used intentionally by the artist. Hematite can be related to the presence of ochre pigments, and the remain seems to be unintentionally mixed within the pigments.

The presence of chromium-based pigments was confirmed by h-EDXRF, it was not possible to identify which chromium-based pigments were used with the analyses performed.

The degree of disruption of the green paint layers, as well as the presence of neoformed salts, increased the complexity of the process of identifying the painting technique, and it was not possible to reach reliable conclusions. Further analysis must be carried out on the green paint layers that exhibit a better state of conservation to clarify the painting technique used by Almada Negreiros. In addition, analyses by Fourier-transform infrared spectroscopy (FTIR) and pyrolysis-gas chromatography coupled with mass spectroscopy (Py-GC/MS) will be used in the future to identify the

presence of organic binders, and to confirm (or discard) the use of the secco technique for the green paint layers.

Based on the results obtained, one of the main causes of deterioration of the green paint layers is the presence of neoformed salts. For the Maritime Station of Alcântara, the presence of salts is linked to water infiltration that dissolves the soluble salts from the support and the painting materials, and transports them until they crystallize due to water evaporation or supersaturation.

Cycles of dissolution and crystallization of the salts in, and between paint layer weakens its main structure, causing loss of cohesion; promotes mechanical stress and therefore the flaking of the paint layers.

Besides the presence of salts, signs of bio-colonization were found in two samples analyzed by SEM-EDS. The growth of microorganisms, as well as their excreta and metabolic activity can promote both physical and chemical deterioration of the paint layers. This is a topic that needs further studies in order to verify and identify the species present.

Likewise, the role of the presence of the synthetic organic pigment PG 8 in the decay mechanisms of the green paint layers must be further explored. In fact, if Almada made use of the fresco technique for applying the green paint layers, it might be possible that the paint layers, where PG 8 was used, underwent a chromatic alteration due to the sensibility of the pigment against alkaline media.

Future research must, therefore, still be undertaken in order to provide information that can aid future conservation works carried out in Almada Negreiros' mural paintings in the Maritime Station of Alcântara.

In what refers to the parallel study carried out on green powder pigments, eskolaite, a mineral related to chromium oxide green, was identified in two of the pigments 5W and 13 BCW from external sources. Clinocllore was identified in the pigment labelled as *Veronese green earth* which confirms the use of this mineral as a green pigment.

From the pigments in powder found in Almada Negreiros' studio, a mixture of Prussian blue with chrome yellow was identified in the pigment labelled as *Viridian*, whose name is not in accordance with the composition. This shows that the misname of this specific pigment was also common in Portugal during the 20th century.

The pigment in powder LF30, labelled as *Vert à la chaux*, showed a reflectance spectrum in which absorption bands are related to chromium oxide green pigments. The previously mentioned, and the fact baryte was found as a filler in both LF 30 and the paint layers, raises the hypothesis that Almada may have made use of this pigment for the mural paintings of the Maritime Station of Alcântara. However, more extensive research is needed to identify the chromium chromophore responsible for the green color.

From the study of the green pigments in powder, it was possible to conclude that green chromium oxide, green earth and mixtures of Prussian blue and chrome yellow, were the green pigments available in the market in Portugal during the 20th century. There

is still a thorough research missing on modern pigments of this century in Portugal. However, the present work provides a first step towards this line of future research.

Appendix

Appendix I: State of conservation of the green paint layers

Appendix I

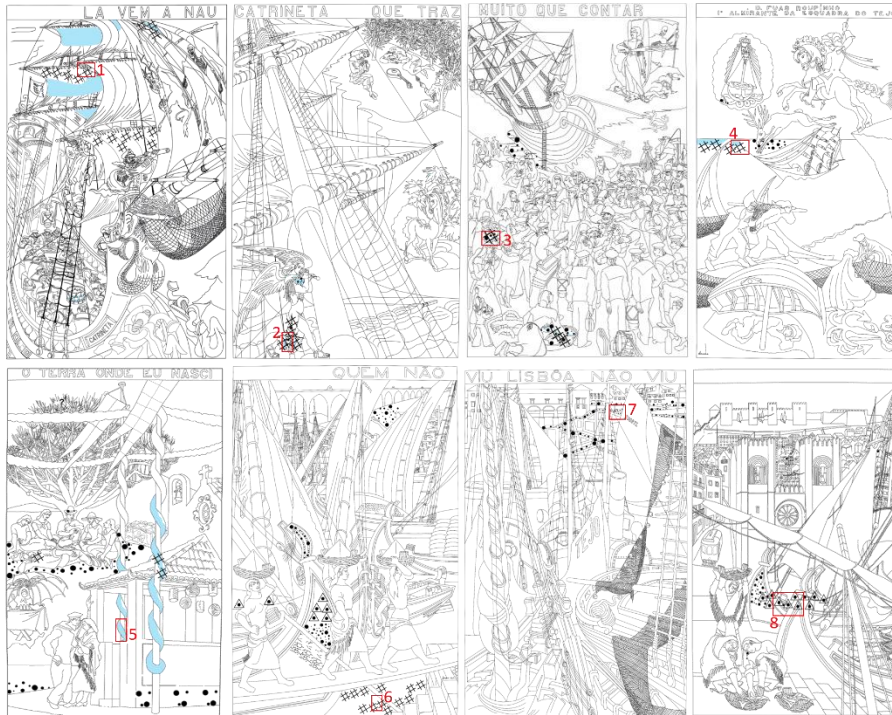
State of conservation of the green pictorial layers



Notes

The study of the state of conservation of the green paint layers was performed by visual inspection in visible and visible-Raking light. The mapping below shows the main green areas with deterioration features, focusing mainly in flaking and loss of cohesion; and other deterioration features like efflorescence. The main hypotheses that could explain the deterioration are salt formations and signs of bio-colonization. An additional hypothesis is related to a possible chromatic alteration in the green areas where the synthetic pigment PG 8 was applied in areas executed by fresco technique. However, the hypothesis cannot be confirmed without a deeper study of the painting technique.

Mapping



Loss of adhesion: loss of adhesion between layers.

Between paint layers (a1)/
Between paint layer and
intonaco (a2)

Zones at imminent risk of
loss only secured by few
points.

Loss of cohesion: material
pulverulence to the touch

Erosion: loss of mass within the
same stratum at various depths

Fissure: case of crack in which the
separation interval of the two
affected parts is not clearly visible
to the naked eye

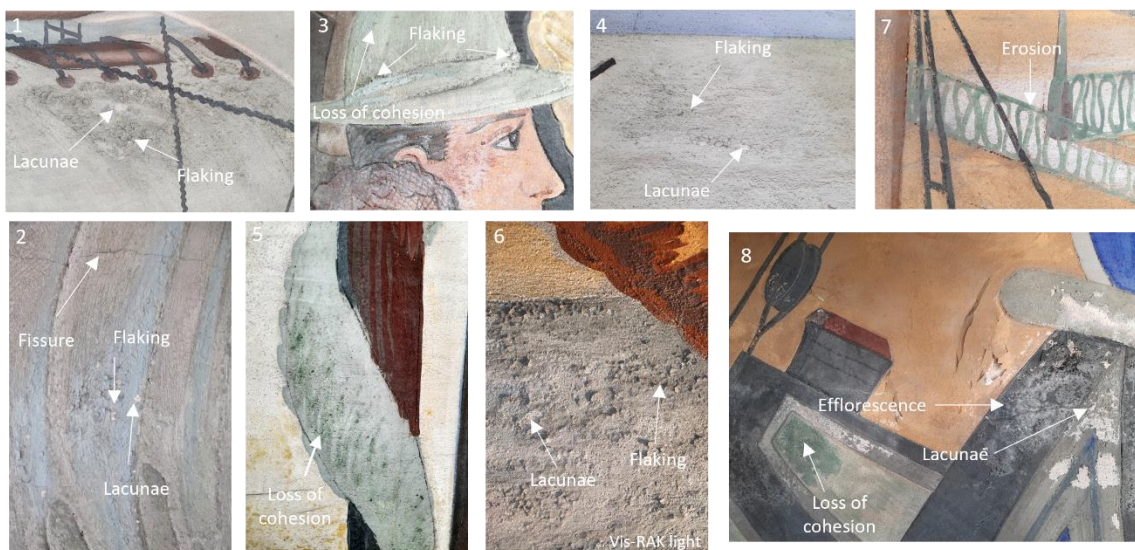
Presence of a fine
irregular
network of cracks

Salts

Efflorescence

?: area of doubts

Photographic Documentation



Appendix I

State of conservation of the green pictorial layers



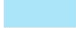
Notes


The study of the state of conservation of the green paint layers was performed by visual inspection in visible and visible-Raking light. The mapping below shows the main green areas with deterioration features, focusing mainly in flaking and loss of cohesion. Fissures are present in the green paint layers.

Mapping Panel 1



Loss of adhesion: loss of adhesion between layers.

 Between paint layers (a1)/ Between paint layer and intonaco (a2)

 Zones at imminent risk of loss only secured by few points.

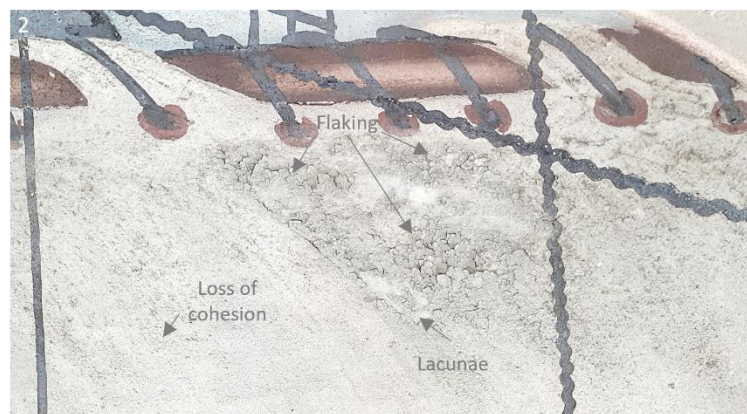
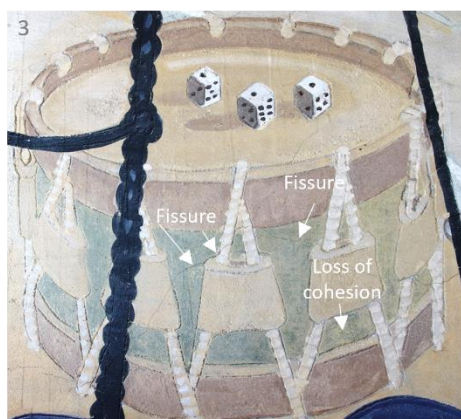
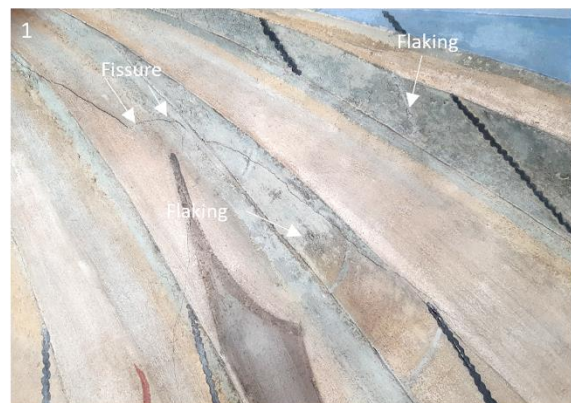
Loss of cohesion: material pulverulence to the touch



Fissure: case of crack in which the separation interval of the two affected parts is not clearly visible to the naked eye



Photographic Documentation



Appendix I

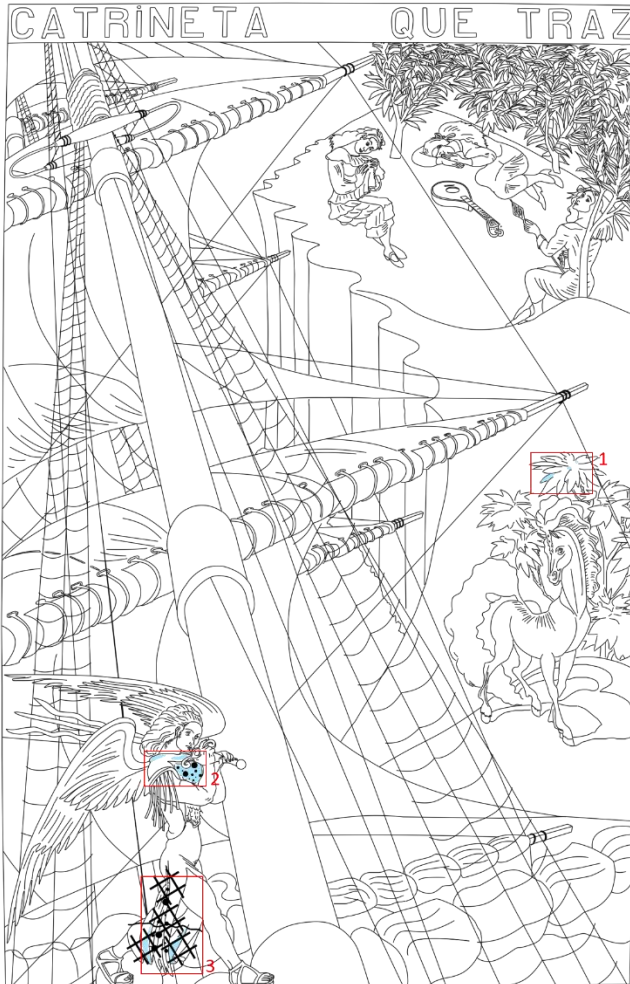
State of conservation of the green pictorial layers



Notes

The study of the state of conservation of the green paint layers was performed by visual inspection in visible and visible-Raking light. The mapping below shows the main green areas with deterioration features, focusing mainly in flaking and loss of cohesion.

Mapping Panel 2



Loss of adhesion: loss of adhesion between layers.

Between paint layers (a1)/ Between paint layer and intonaco (a2)



Zones at imminent risk of loss only secured by few points.

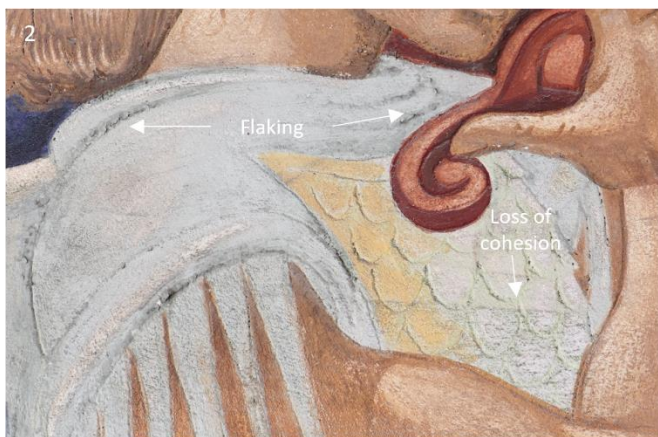
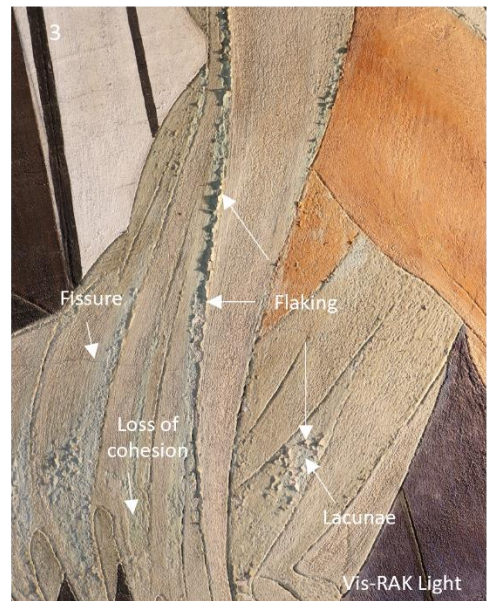
Loss of cohesion: material pulverulence to the touch



Fissure: case of crack in which the separation interval of the two affected parts is not clearly visible to the naked eye



Photographic Documentation



Appendix I

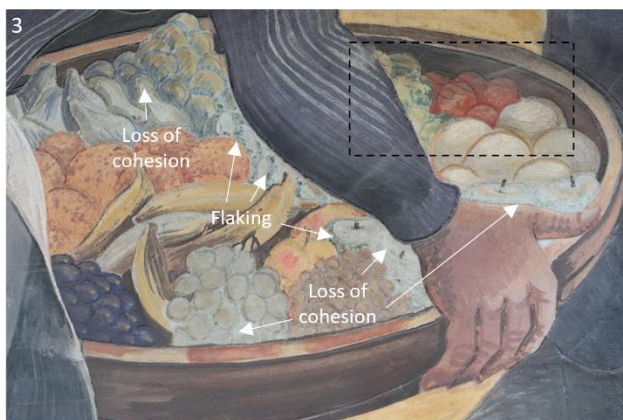
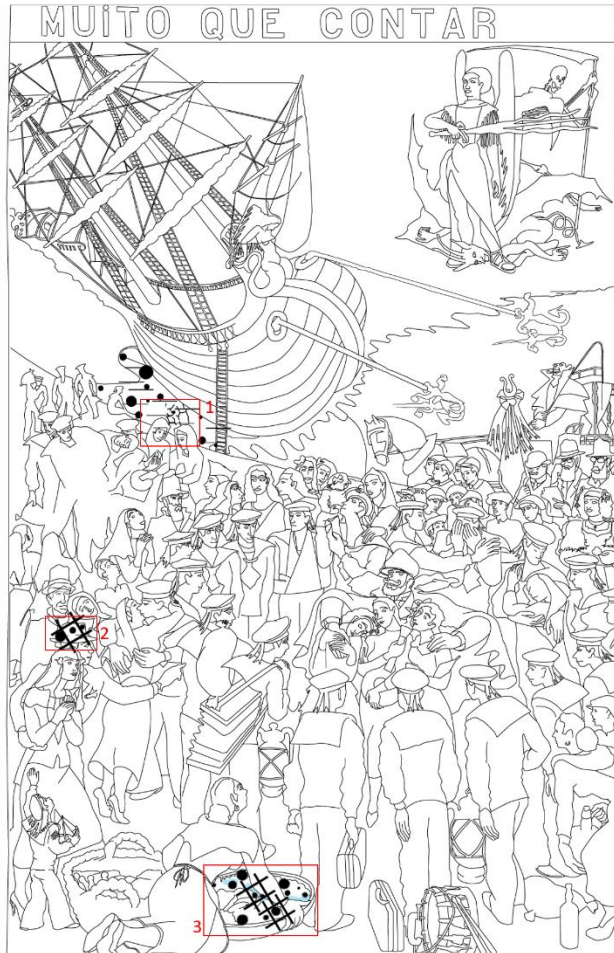
State of conservation of the green pictorial layers



Notes

The study of the state of conservation of the green paint layers was performed by visual inspection in visible and visible-Raking light. The mapping below shows the main green areas with deterioration features, focusing mainly in flaking and loss of cohesion; and the presence of fissures and erosion. The basket with fruits (Figure 3) presents the highest amount of deterioration features in the panel.

Mapping Panel 3



Loss of adhesion: loss of adhesion between layers.

Between paint layers (a1)/ Between paint layer and intonaco (a2)



Zones at imminent risk of loss only secured by few points.

Loss of cohesion: material pulverulence to the touch



Fissure: case of crack in which the separation interval of the two affected parts is not clearly visible to the naked eye

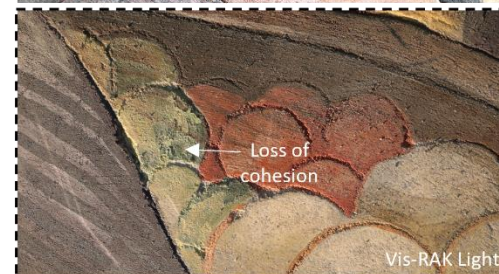
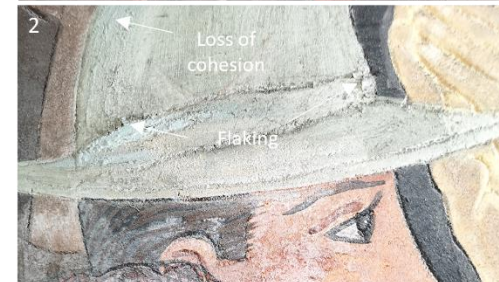


Presence of a fine irregular network of cracks

Erosion: loss of mass within the same stratum at various depths



Photographic Documentation



Appendix I

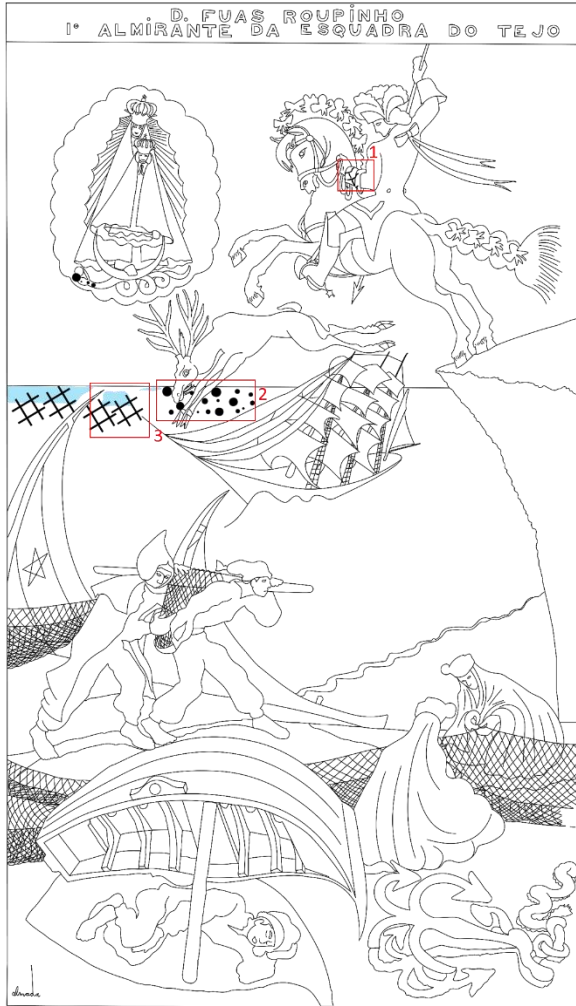
State of conservation of the
green pictorial layers



Notes

The study of the state of conservation of the green paint layers was performed by visual inspection in visible and visible-Raking light. The mapping below shows the main green areas with deterioration features, focusing mainly in flaking and loss of cohesion. Fissures are present in the green sleeve of the man.

Mapping Panel 4



Loss of adhesion: loss of adhesion between layers.

Between paint layers (a1)/ Between paint layer and intonaco (a2)



Zones at imminent risk of loss only secured by few points.

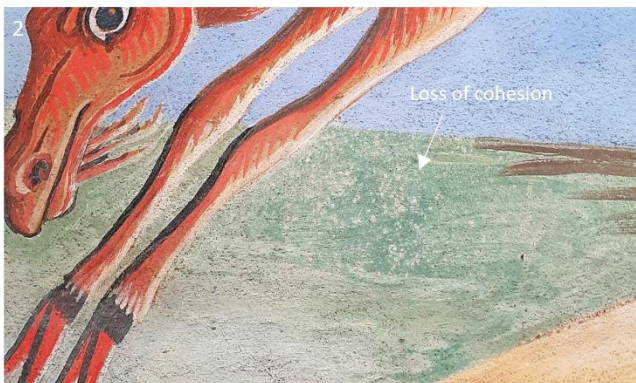
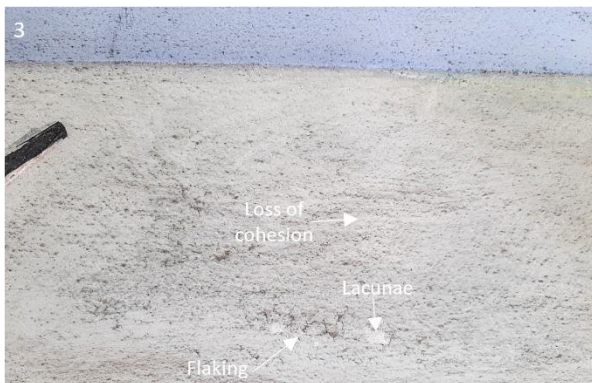
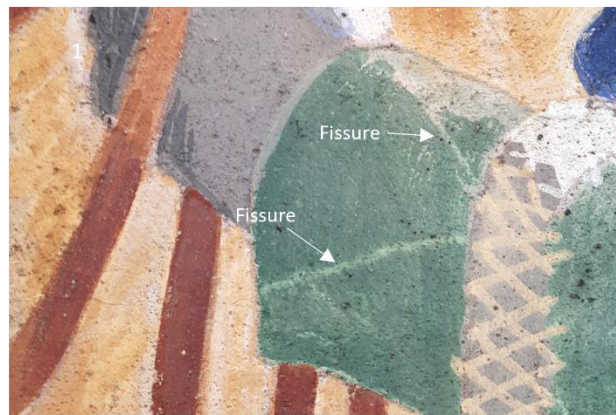
Loss of cohesion: material pulverulence to the touch



Fissure: case of crack in which the separation interval of the two affected parts is not clearly visible to the naked eye



Photographic Documentation



Appendix I

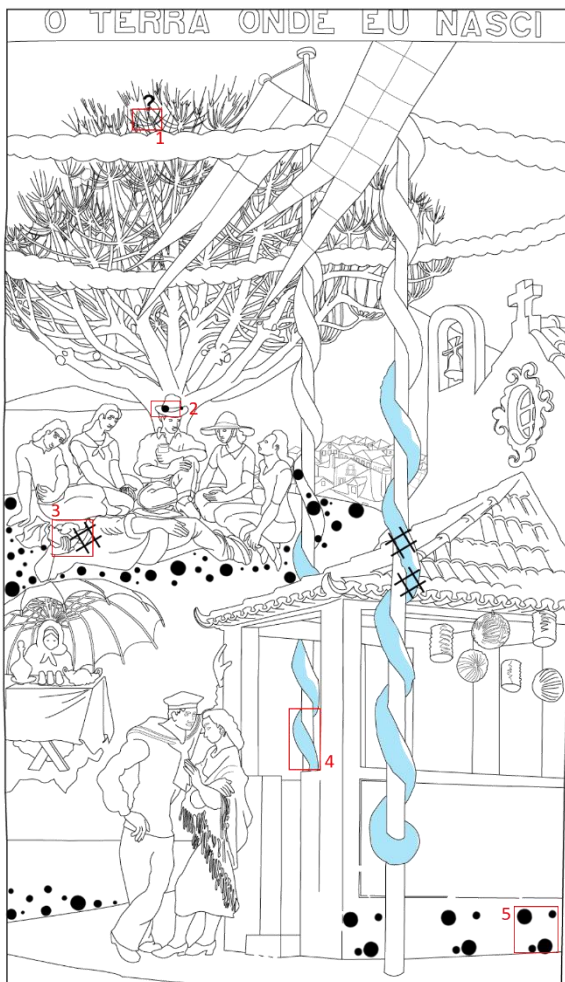
State of conservation of the
green pictorial layers



Notes

The study of the state of conservation of the green paint layers was performed by visual inspection in visible and visible-Raking light. The mapping below shows the main green areas with deterioration features, focusing mainly in flaking and loss of cohesion; There are questions concerning the deterioration features present in the tree leaves (Figure 1) marked with a question mark.

Mapping Panel 5



Loss of adhesion: loss of adhesion between layers.

Between paint layers (a1)/ Between paint layer and intonaco (a2)



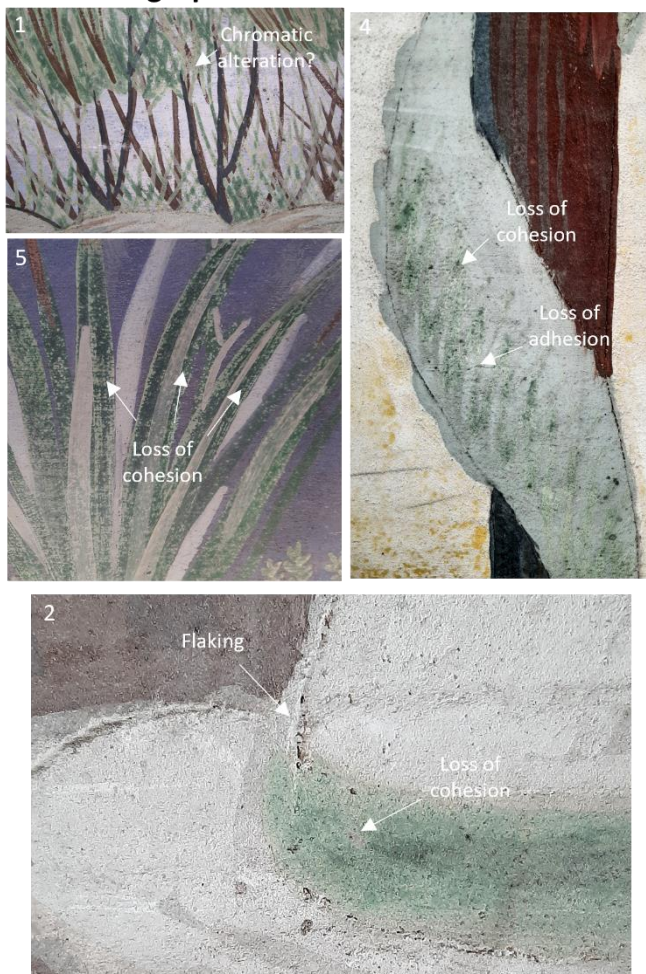
Zones at imminent risk of loss only secured by few points.

Loss of cohesion: material pulverulence to the touch



?: area of doubts

Photographic Documentation



Appendix I

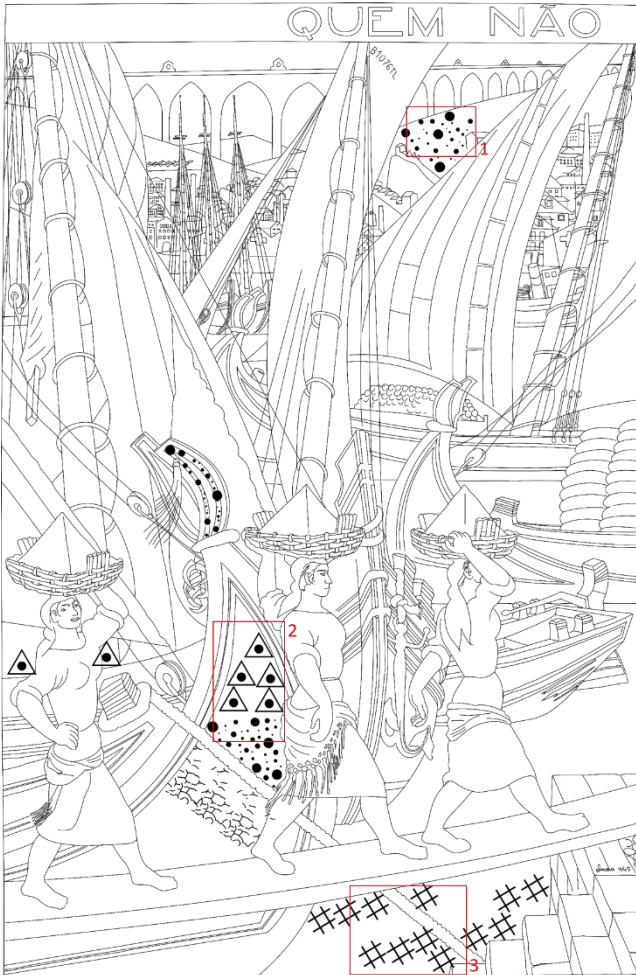
State of conservation of the green pictorial layers



Notes

The study of the state of conservation of the green paint layers was performed by visual inspection in visible and visible-Raking light. The mapping below shows the main green areas with deterioration features, focusing mainly in efflorescence, flaking, and loss of cohesion; There is an extensive area of efflorescence that horizontally crosses the mural painting. For the purpose of this project, only the green paint layers with efflorescence were signalized.

Mapping Panel 6



Loss of adhesion: loss of adhesion between layers.



Zones at imminent risk of loss only secured by few points.

Loss of cohesion: material pulverulence to the touch



Fissure: case of crack in which the separation interval of the two affected parts is not clearly visible to the naked eye



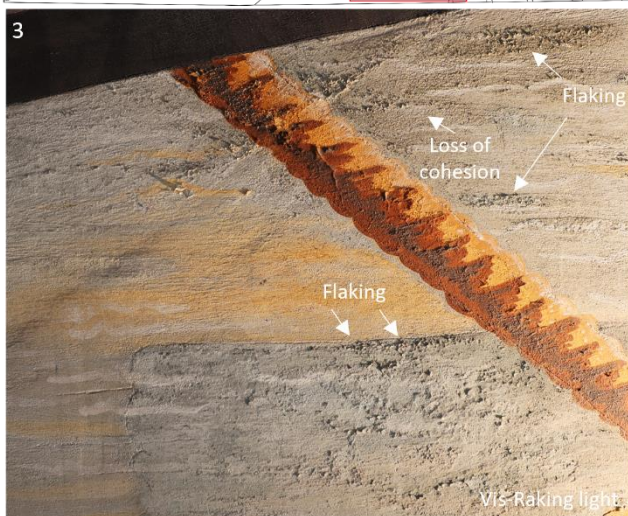
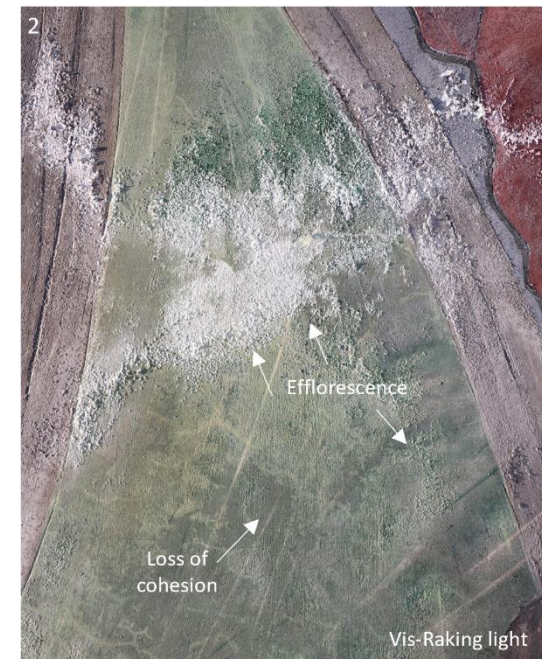
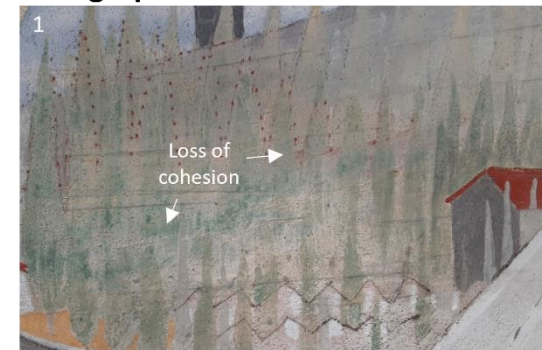
Presence of a fine irregular network of cracks

Salts



Efflorescence

Photographic Documentation



Appendix I

State of conservation of the green pictorial layers



Notes

The study of the state of conservation of the green paint layers was performed by visual inspection in visible and visible-Raking light. The mapping below shows the main green areas with deterioration features, focusing mainly loss of cohesion. There is a fissure in one of the green paint layers (Figure 1)

Mapping Panel 7



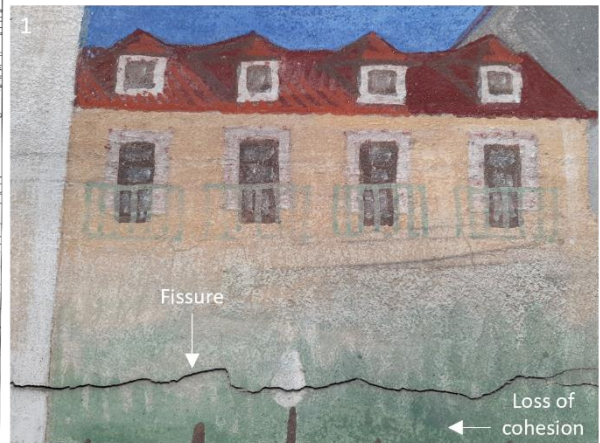
Loss of cohesion: material pulverulence to the touch



Fissure: case of crack in which the separation interval of the two affected parts is not clearly visible to the naked eye



Photographic Documentation



Appendix I

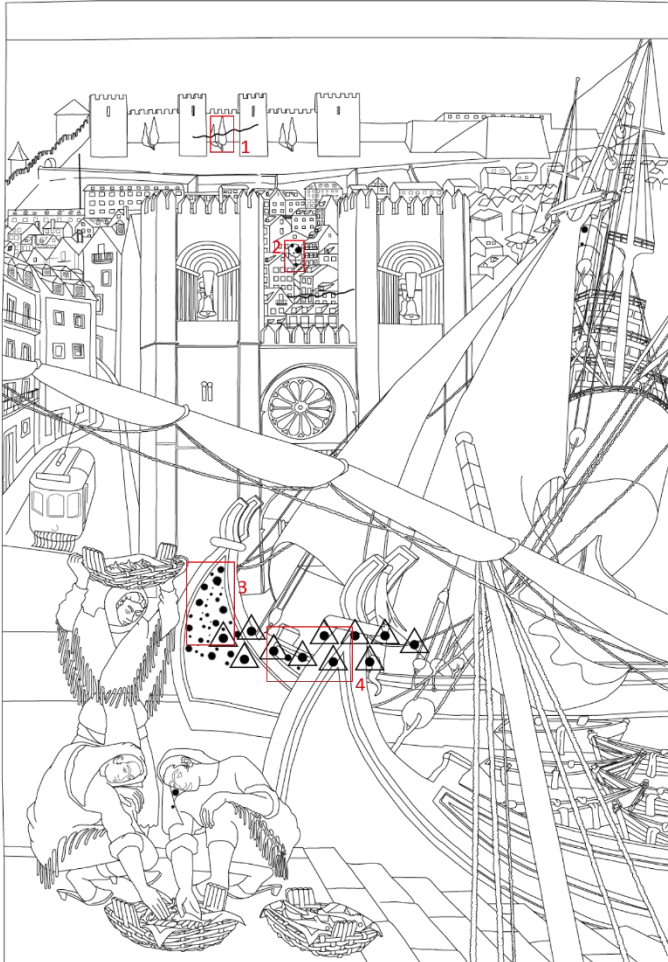
State of conservation of the
green pictorial layers



Notes

The study of the state of conservation of the green paint layers was performed by visual inspection in visible and visible-Raking light. The mapping below shows the main green areas with deterioration features, focusing mainly in efflorescence and loss of cohesion. Two fissures are identified in two green paint layers.

Mapping Panel 6



Loss of cohesion: material pulverulence to the touch



Fissure: case of crack in which the separation interval of the two affected parts is not clearly visible to the naked eye



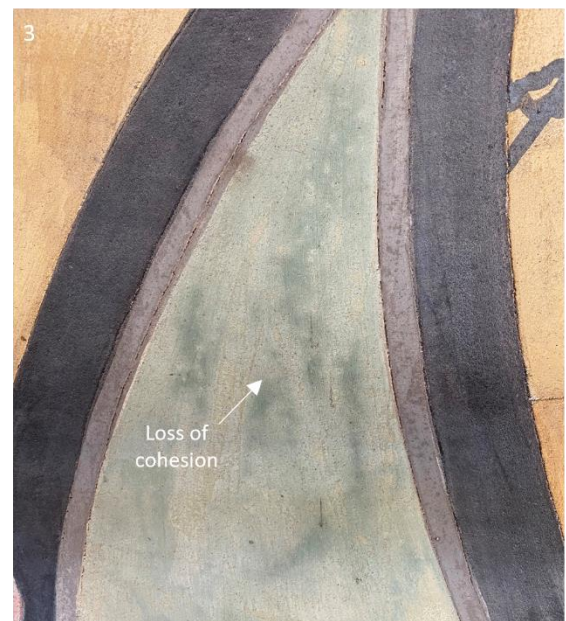
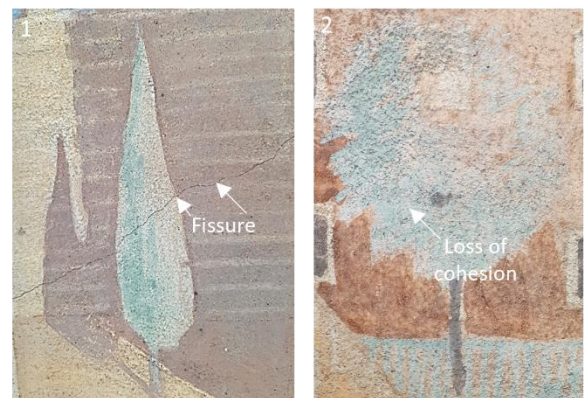
Presence of a fine irregular network of cracks

Salts



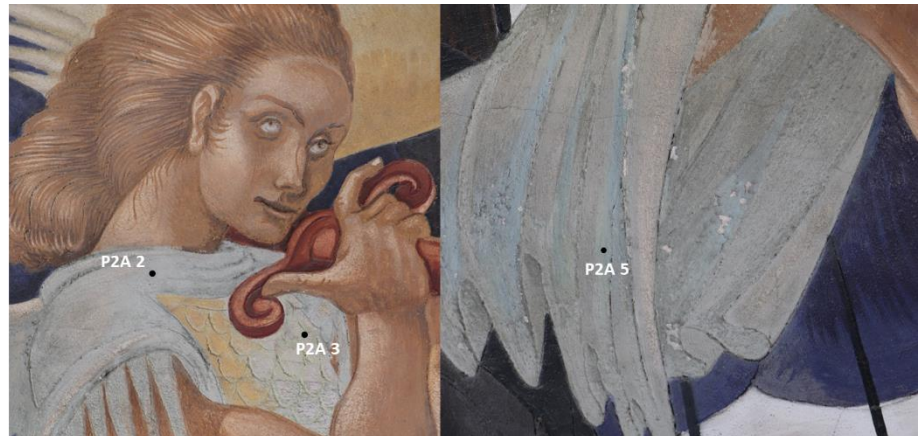
Efflorescence

Photographic Documentation



Appendix II: Punctual area location of the colorimetry/ spectrophotometry analysis

Panel 2



Panel 3

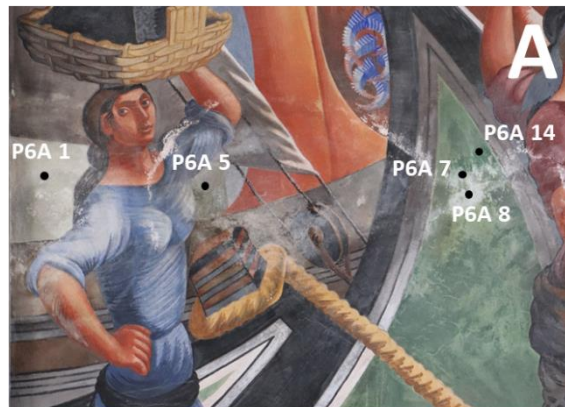




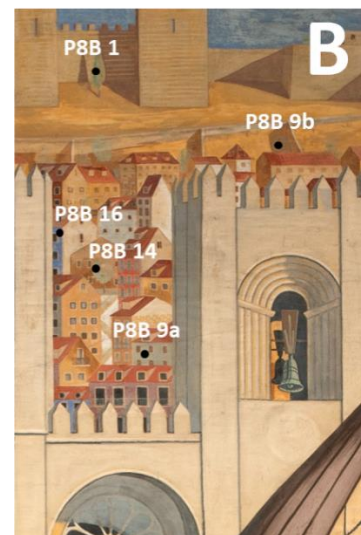
Panel 5



Panel 6

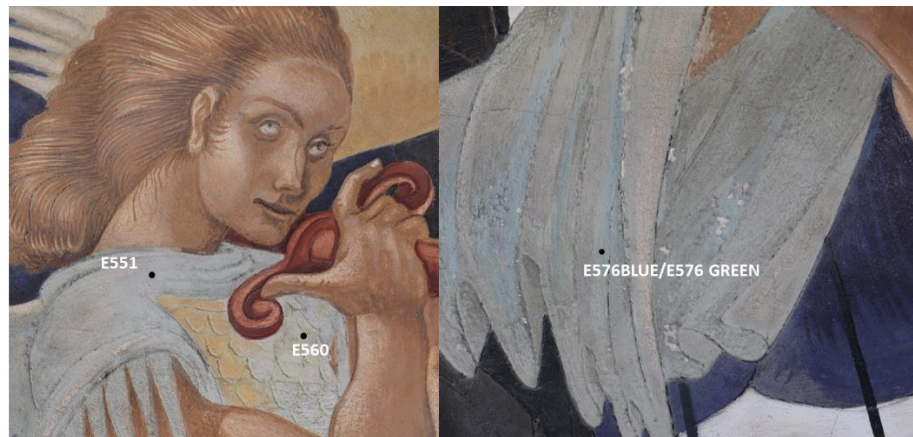


Panel 8



Appendix III: Punctual area location of the h-EDXRF analysis

Panel 2

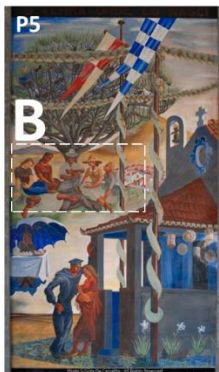


Panel 3

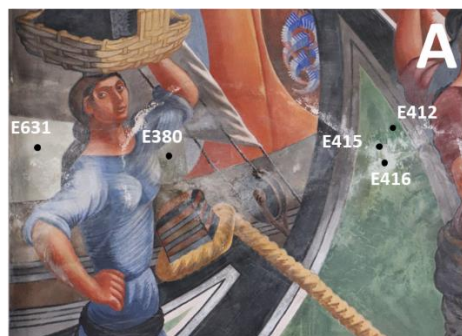




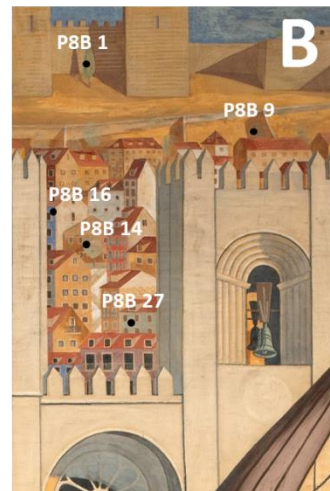
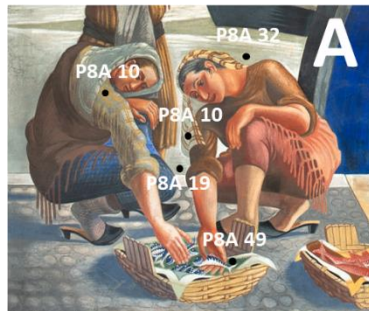
Panel 5



Panel 6




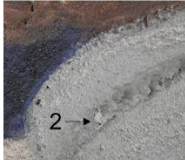


Panel 8

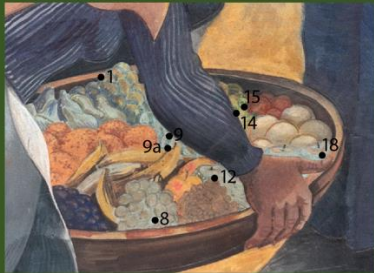
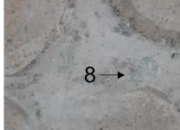





Appendix IV: Correlation colorimetry-spectrophotometry/h-EDXRF measurements

	ID Colorimetry	EDXRF
Panel 2	P2A 2	E551
	P2A 3	E560
	P2A 5	E576BLUE/ E576GREEN
Panel 3	P3C 100	P3C100
	P3C 21/21a	P3C101
	P3C 102	P3C102
	P3C 103	P3C103
	P3C 6a	P3C 15
	P3C 8	P3C55
	P3C 56	P3C56
	P3C 75	P3C75
	P3C 79	P3C79
	P3C 80	P3C80
	P3C 99	P3C99
	P3A 1	E586A / E586B
	P3A 15b	E603
	P3A 12	E605A / E605B
	P3A 8	E609A /E609B
	P3A 15	E679GREEN_A / E679GREEN_B
	P3A 8	/
	P3D 16	P3D16
	P3D 84	P3D84
Panel 5	P5B 11	(P5B) 11
	P5B 12	(P5B) 12
	P5B 34	(P5B) 34
	P5B 17b	(P5B) 40
	P5B41	(P5B) 41
	P5B 17	(P5B) 42
	P5B52	(P5B) 52
	P5B53	(P5B) 53
	P5B57	(P5B) 57
	P5B58	(P5B) 58
Panel 6	P6A 1	E361
	P6A 5	E380
	P6A 14	E412
	P6A 7	E415
	P6A 8	E416
Panel 8	P8A 10	P8A_10
	P8A 19	P8A_19
	P8A 32	P8A_32
	P8A 38	P8A_38
	P8A 27	P8A_49
	P8B 1	P8B _ 1
	P8B 14	P8B _ 14
	P8B 16	P8B _ 16
	P8B 9a	P8B _ 27
	P8B 9b	P8B _ 9

Appendix V: Microsampling location

MICROSAMPLING LOCATION – PANEL 2A	Detail	Description	Goal
 <p>Building: Shipping station of Alcântara Painting. Ref.: Guardian angel protects the "nau" Painting author: Almada Negreiros Date of the paintings: 1943-1945 Dimensions: 6.20x3.50 m Date of the microsampling: June 2020 Collector: Milene Gil</p>		Neck of the dress, flaking light greenish blue	2-Identify painting technique/pigment
		Front part of the dress (Chest) yellowish green	3-Identify painting technique/pigment
		Low part of the angel's dress, flaking light green	5-Identify painting technique/pigment



MICROSAMPLING LOCATION – PANEL 3A	Detail	Description	Goal
 <p>Building: Shipping station of Alcântara Painting. Ref.: Basket with fruits Painting author: Almada Negreiros Date of the paintings: 1943-1945 Dimensions: 6.20x3.50 m Date of the microsampling: September 2021 Collector: Milene Gil</p>		Lower grapes, eroded surface (light green)	8-Identify painting technique/pigment
		Green Apple next to the blue sleeve (flaking greyish/greenish colour)	12 -Identify painting technique/pigment
		Yellow greenish fruits, eroded surface	15-Identify painting technique/pigment
		Green Apple in the right side, eroded greyish/greenish pigment	18-Identify painting technique/pigment

MICROSAMPLING LOCATION – PANEL 3C

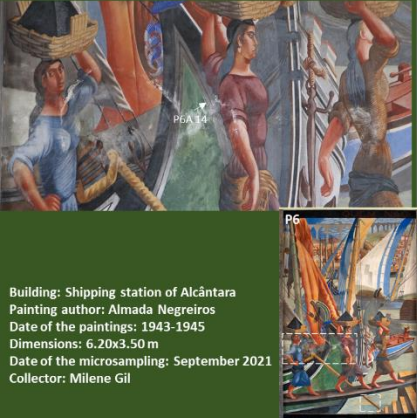
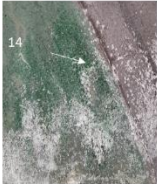
Detail	Description	Goal
	<p>6 → Hat, highlighted in dark green, secco technique?, are there salts?, what is the chromophore present?</p>	<p>6a -Identify painting technique/pigment and salts in case of presence</p>
	<p>8 → Skirt, the green pigment is stable</p>	<p>8a-Identify painting technique/pigment</p>
	<p>21 → Concertina, green lines alternated with yellow lines</p>	<p>21 and 21a -Identify painting technique/pigment</p>
	<p>22 → Green background with plaster (rendering)</p>	<p>22 -Identify painting technique/pigment</p>

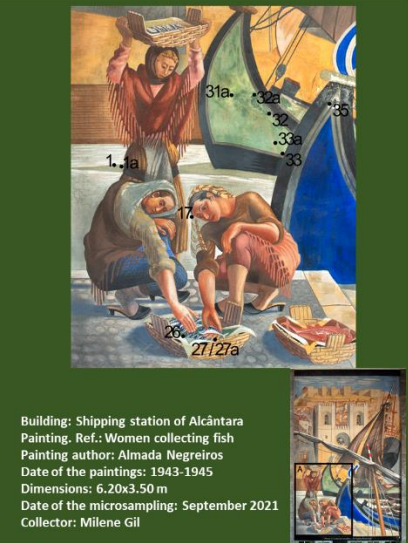
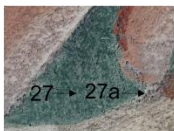
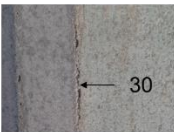
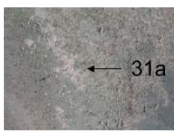
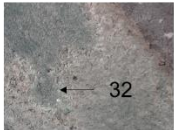
Building: Shipping station of Alcântara
Painting. Ref.: Kiss area
Painting author: Almada Negreiros
Date of the paintings: 1943-1945
Dimensions: 6.20x3.50 m
Date of the microsampling: September 2021
Collector: Milene Gil



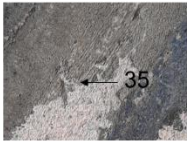
MICROSAMPLING LOCATION - PANEL 5B

Detail	Description	Goal
	<p>17 → Hat, intermediate green above light green 17a. Hat, darker green 17b. Hat, light green, is it degradation?</p>	<p>17, 17a and 17b -Identify painting technique/pigment</p>
	<p>10 → Background. Dark green with light green below.</p>	<p>10 -Identify painting technique/pigment</p>

Building: Shipping station of Alcântara
Painting. Ref.: Picnic
Painting author: Almada Negreiros
Date of the paintings: 1943-1945
Dimensions: 6.20x3.50 m
Date of the microsampling: September 2021
Collector: Milene Gil

MICROSAMPLING LOCATION - PANEL 8B	Detail	Description	Goal
 <p>Building: Shipping station of Alcântara Painting author: Almada Negreiros Date of the paintings: 1943-1945 Dimensions: 6.20x3.50 m Date of the microsampling: September 2021 Collector: Milene Gil</p>		<p>Salt efflorescence along the area of the bow ship</p>	<p>Identify chemical and mineralogical composition of the sample, as well as presence of salts. Painting technique and pigment identification</p>

MICROSAMPLING LOCATION - PANEL 8A	Detail	Description	Goal
 <p>Building: Shipping station of Alcântara Painting. Ref.: Women collecting fish Painting author: Almada Negreiros Date of the paintings: 1943-1945 Dimensions: 6.20x3.50 m Date of the microsampling: September 2021 Collector: Milene Gil</p>	   	<p>Linen in the basket, without signs of deterioration</p> <p>Ship, dark greens. Is it the original +consolidant? Or is it a retouch + consolidant?</p> <p>Ship, green in scales. Is it the original +consolidant? Or is it a retouch + consolidant?</p> <p>Ship, dark greens. Is it the original +consolidant? Or is it a retouch + consolidant?</p>	<p>27 and 27a-Identify painting technique/pigment</p> <p>31a -Identify painting technique/pigment</p> <p>32-Identify painting technique/pigment</p>

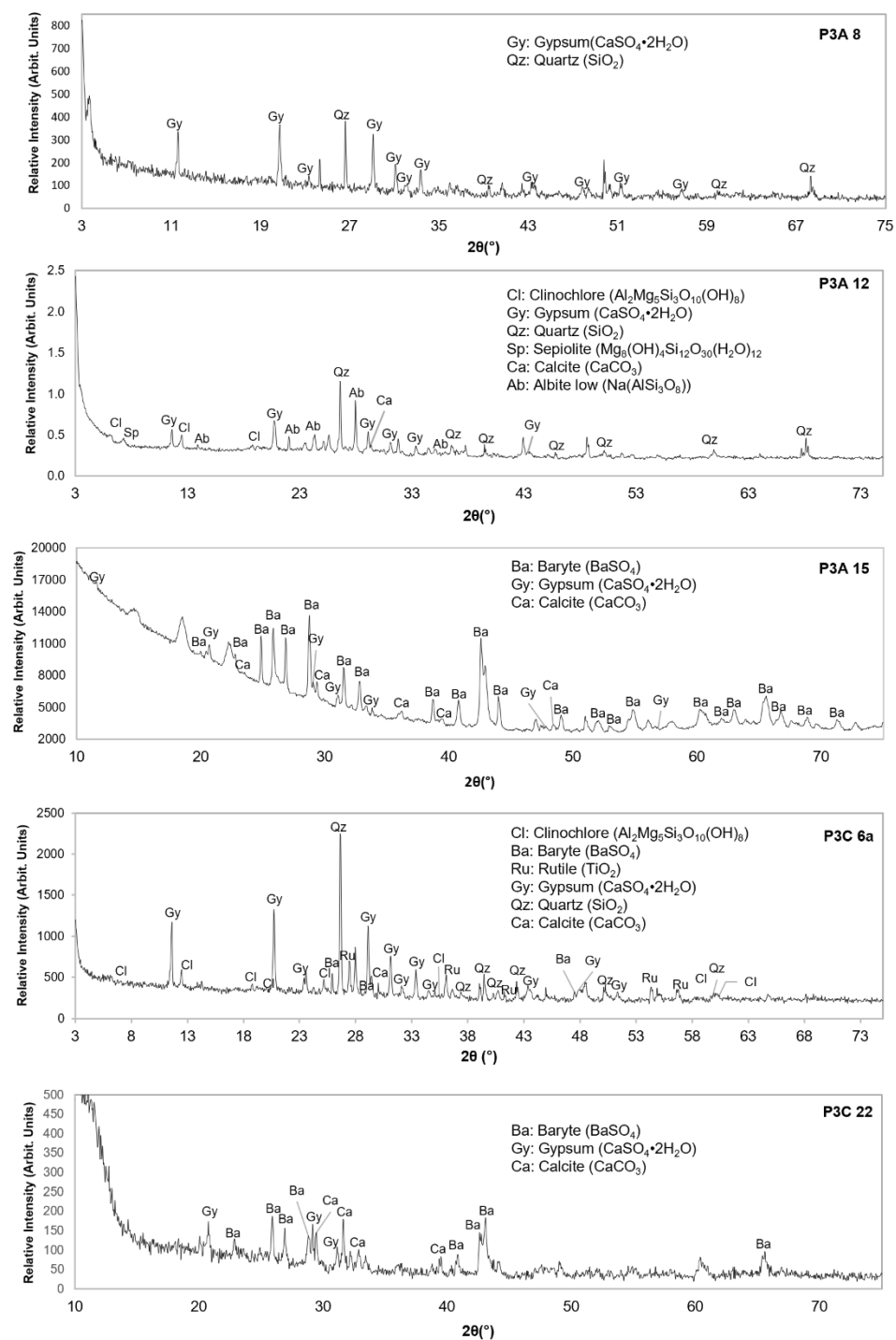
MICROSAMPLING LOCATION - PANEL 8A	Detail	Description	Goal
 <p>Building: Shipping station of Alcântara Painting. Ref.: Women collecting fish Painting author: Almada Negreiros Date of the paintings: 1943-1945 Dimensions: 6.20x3.50 m Date of the microsampling: September 2021 Collector: Milene Gil</p> 		Ship, dark greens. Is it the original +consolidant? Or is it a retouch + consolidant	32a-Identify painting technique/pigment
		Ship, green coming out	35-Identify painting technique/pigment

MICROSAMPLING LOCATION - PANEL 8B	Detail	Description	Goal
 <p>Building: Shipping station of Alcântara Painting. Ref.: Houses behind the church Painting author: Almada Negreiros Date of the paintings: 1943-1945 Dimensions: 6.20x3.50 m Date of the microsampling: September 2021 Collector: Milene Gil</p> 		Green facade	9a-Identify painting technique/pigment

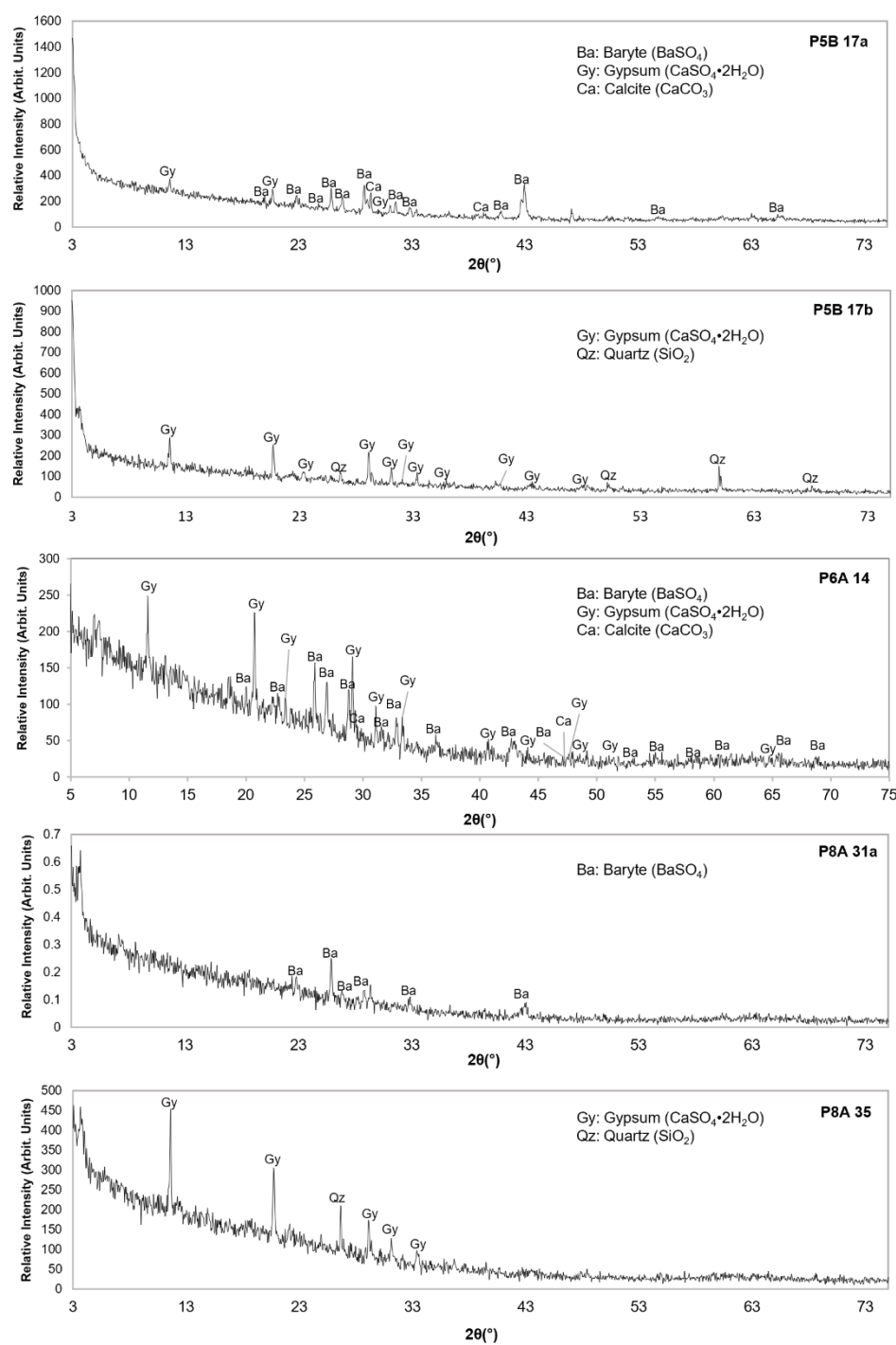
Appendix VI: Compendium of results from the samples by colorimetry, h-EDXRF, μ -XRD, and micro-Raman spectroscopy

Sample ID	CIE chromatic coordinates			h-EDXRF (in bold major elements for pigment identification)	μ -XRD	micro-Raman Spectroscopy
	L	*a	*b			
P2A 2	55.89	-0.07	7.51	Ba, Ca , Cl, Cr, Cu, Fe , K , Mn , Ni, S , Si, Sr, Ti, Zn	-	-
P2A 3	56.71	0.1	13.02	Ba, Ca , Cu, Fe, K, Mn, Ni, S , Si, Sr , Zn	-	PY 1, PG 8, baryte
P2A 5	67.99	-2.96	11.97	Ba, Ca , Cl , Cr , Cu, Fe , K, Mn, Ni, Pb , S , Si, Sr , Ti , Zn	-	-
P3A 8	55.86	0.32	7.8	Ba, Ca , Cl , Cr, Cu, Fe , K, Mn, Ni, Pb , S , Si, Sr, Ti, Zn	Gypsum, quartz	PG 1, carbon black, hematite, gypsum
P3A 12	30.95	0.19	1.45	Ba, Ca , Cl, Cr, Cu, Fe , K , Mn , Ni, S , Si, Sr, Ti, Zn	Quartz, gypsum, calcite, clinocllore, plagioclase, sepiolite	-
P3A 15	35.37	-3.45	6.53	Ba, Ca , Cl , Cr , Cu, Fe, K, Ni, Pb , S , Si, Sr , Zn	Baryte, gypsum, calcite	PG 8, hematite, baryte
P3A 18	55.4	-0.98	7.32	-	-	-
P3C 6a	61.85	-0.4	10.58	Ba, Ca , Cr, Fe , K, Mn, S, Si, Sr, Ti, Zn	Gypsum, quartz, rutile, clinocllore, calcite, baryte	-
P3C 8	55.87	-4.55	11.9	Ba, Ca , Cu, Fe, K, Ni, Pb , S , Si, Sr , Zn	-	-
P3C 21/21a	59.89	-5.48	12.81	Ba, Ca , Cr, Cu, Fe, K, Ni, S , Si, Sr , Zn	-	-
P3C 22	-	-	-	-	Calcite, baryte, gypsum	-
P5B 10	-	-	-	-	-	PG 8, baryte
P5 B 17/17a	48.15	-5.4	9.39	Ba, Ca , Cl, Cr, Cu, Fe, Mn , Ni, S , Si, Sr , Zn	Gypsum, calcite, baryte	PG 8, carbon black, gypsum
P5B 17b	63.06	-1.02	6.86	Ba, Ca , Cr , Cu, Fe , Mn , Ni, S , Si, Sr, Ti, Zn	Gypsum, quartz	.
P6A 14	41.45	-4.95	6.76	Ba, Ca , Cl, Cr, Cu, Fe, K, Ni, S , Si, Sr , Zn	Gypsum, calcite, baryte	PG 8
P8A 27/27a	45.46	-6.37	10.09	Ba , Ca , Cr, Cu, Fe, Ni, S , Si, Sr , Zn	-	-
P8A 30	-	-	-	-	-	-
P8A 31a	-	-	-	-	Baryte	PG 8, ultramarine blue, calcite, gypsum
P8A 32/32a	-	-	-	-	-	-
P8A 35	-	-	-	-	Gypsum, quartz	-
P8B 9a	65.98	-0.83	7.67	Ba, Ca , Cr , Cu, Fe , Mn , Ni, S , Si, Sr, Ti, Zn	-	-

Appendix VII: μ -XRD diffractograms of the microfragments analyzed



Appendix VII (continued)



Appendix VIII: XRPD diffractograms of selected reference pigments

